NOTE TO USERS

Page(s) not included in the original manuscript are unavailable from the author or university. The manuscript was microfilmed as received.

5, 7, 12, 28, 42, 72

This reproduction is the best copy available.

UMI®

Red blood cell derived vasodilators: determination and modulation

Juliana Garcia

A Thesis

in

The Department

of

Chemistry and Biochemistry

Presented in Partial Fulfillment of the Requierements

for the Degree of Master of Science (Chemistry) at

Concordia University

Montreal, Quebec, Canada

March 2009

Your file Votre référence
ISBN: 978-0-494-63311-3
Our file Notre référence
ISBN: 978-0-494-63311-3

Abstract

Red blood cell derived vasodilators: determination and modulation

Juliana Garcia

A luciferin-luciferase chemiluminescence method was used to quantify extracellular adenosine triphosphate (ATP) released by red blood cells (RBCs) after stimulation with nitroglycerin, a potent vasodilatory drug. Attenuation in the amount of ATP released from RBCs was observed after treatment with increasing concentrations of nitroglycerin or nitrite. However, RBCs exposed to nitroglycerin or nitrite for < 5 min released increased amounts of ATP. A mechanism of blood flow regulation through an ATP-NO/NO_2^- pathway is proposed. Nitroglycerin-derived NO_2^- is converted within RBCs to NO, which might activate ATP release. *In vivo*, ATP will stimulate endothelial nitric oxide synthase (eNOS), increasing NO production and causing vasodilation. NO could diffuse into the blood stream where it is converted to NO_2^- and taken up by downstream RBCs, further increasing their ATP production. Thus, the original RBC-derived NO_2^-/NO signal could be amplified both by the action of ATP and NO.

Nitroglycerin was also shown to act as a "suicide substrate" for RBC glyceraldehyde 3-phosphate dehydrogenase (GAPDH). GAPDH reduced nitroglycerin to glyceryl dinitrates and NO_2^- using its active-site cysteines as electrons donors. This inactivation inhibited the bioconversion of nitroglycerin to NO_2^- and caused an attenuation of the drug's effect. The dehydrogenase activity of GAPDH was also suppressed, thereby limiting the production of ATP and propagation of the vasodilation signal.

The extracellular profile of ATP-derived ADP, AMP and adenosine was additionally studied by LC-UV. Preliminary ESI mass spectrometric analysis of epoxyeicosatrienoic acids and prostacyclin, RBC vasodilators derived from arachidonic acid, was explored.

Acknowledgments

I would like to express my gratitude to Dr. Ann M. English for her advice, patience and guidance as my supervisor during my Masters degree.

Also I would like to thank my committee members Dr. Rober Bushel and Dr. Pat Forgione, for their helpful ideas. Very special thanks to Dr. Cameron Skinner for his kindness, willingness to help and unconditional support.

Many thanks to all my colleagues who passed through Dr. English's laboratory: Dr. Mengwei Ye, Dr. Michelle Chretien, Biao Shen, Julie Laterreur, Xiao Gao, Renée Kennedy, Dr. Amedea Seabra, and special thanks to Bing Li, for her support and understanding trough the tough times.

Special thanks also to Stella Muthuri, Michel Boisvert, and Dr. Ernesto Moran, who became dearest friends during my time at Concordia University.

To my family, for being the constant in this long journey, gracias.

To Arlen, there are not enough ways to thank you for being my best friend, head psychologist, life coach, vocational advisor, motivational speaker, source of inspiration, granola shaman, English teacher, proofreader and world's best cook. You are my rock and my reason.

Table of contents

List of Figures

List of Schemes

List of Tables

List of Abreviations

$6KPGF_{1\alpha}$	6-keto prostaglandin $F_{1\alpha}$
AA	Arachidonic acid
ACN	Acetonitrile
Acyl-CoA	Acyl coenzime A
ALDH1	Aldehyde dehydrogenase 1
ALDH2	Aldehyde dehydrogenase 2
COX-1	Cycloxygenase 1
COX-2	Cycloxygenase 2
$cPLA_2$	Cyclic phospholipases A_2
CYP450	Cytochrome P450
$D4\text{-}6KPGF_{1\alpha}$	Deuterated6-keto prostaglandin $F_{1\alpha}$
deoxyHb	Deoxyhemoglobin
DHET	Dihydroxyeicosatrienoic acid
DTT	Dithiothreitol
EDHF	Endothelium-derived hyperpolarizing factor
EDRF	Endothelium-derived relaxing factor
EDTA	Ethylenediaminetetraacetic acid
EEA	Epoxyeicosanoic acid
EET	Epoxyeicosatrienoic acid
ELISA	Enzyme-linked immunosorbent assay
eNOS	Endothelial nitric oxide synthase

E-NPP	ecto-nucleotide pyrophosphatase/phosphodiesterase
E-NTPDase-1	Ecto-nucleoside triphosphate diphosphohydrolase-1
E-NTPDase-2	Ecto-nucleoside triphosphate diphosphohydrolase-2
E-NTPDase-3	Ecto-nucleoside triphosphate diphosphohydrolase-3
E_{ox}	Oxidized enzyme
E_{red}	Reduced enzyme
ESI	Electrospray ionization
FeII(heme)	Ferrous heme
FeIII(heme)	Ferric heme
g	g force
G protein	Guanine nucleotide-binding protein
GAPDH	Glyceraldehyde-3-phosphate dehydrogenase
GC	Guanylate cyclase
GDN	Glyceryl dinitrate
GSH	Glutathione
GSSG	Glutathione dimer
GST	Glutathione S-transferase
Hb	Hemoglobin
Hct	Hematocrit
LH_2	*D*(-)luciferin
LH_2-AMP	*D*(-)luciferin adenylate
metHb	Methemoglobin
mPGES-1	Prostaglandin-E_2 synthase-1

NOS	Nitric oxide synthase
OxL	Oxyluciferin
OxL*	Excited oxyluciferin
PCR	Polymerase chain reaction
PGI_2	Prostacyclin
PGK	Phosphoglycerate kinase
PKA	Protein kinase A
PLC	Phospholipase C
PSS	Physiological salt solution
RBC	Red blood cell
RIA	Radioimmunoassay
RSNO	*S*-nitrosothiol
SEM	Standard deviation of the mean
TA	Tridecanoic acid
TCEP	Tris(2-carboxyethyl)phosphine

1. General Introduction

1.1. Red blood cells and vasodilation

The regulation of vascular tone and blood flow is a complex process driven mainly by local regulatory mechanisms at the blood vessel wall. An important regulatory system in localized vasodilation is the molecular crosstalk between red blood cells (RBCs) and endothelial cells in the microvasculature (1). It is well-established that the endothelium produces and releases a number of vasodilatory factors including the endothelial-derived relaxing factor (EDRF) that is nitric oxide (NO), adenosine, prostaglandins and the endothelium-derived hyperpolarizing factor (EDHF) (2).

RBCs are responsible for the transport and delivery of oxygen to meet the metabolic demands of tissues. O_2 gradients act as the main regulator of blood flow in the microvasculature (3-6). Recent research has shown that RBCs are also responsible for the release of blood flow regulators including adenosine triphosphate (ATP) under physiological stress (7-9). Pharmacological agents that treat cardiovascular diseases in which vasodilation is compromised, such as myocardial ischemia (angina), modify the normal patterns of this local regulation of blood flow. A focus of this thesis is the export of ATP and others vasodilators from isolated human RBCs. The results obtained contribute to our understanding of the role of RBCs in the localized regulation of blood flow in the microvasculature.

1.1.1. Red blood cell properties

Mammalian RBCs are small, flexible, biconcave discs consisting of a plasma membrane and a few associated proteins (10). RBCs are produced and matured in the bone marrow, and are known as reticulocytes prior to being released into the blood stream. In humans, RBCs are the smallest cells with an average diameter of 8 μm and a life span of 120 days (1). Mature RBCs lack nuclei, mitochondria, and other specialized organelles, so they are unable to synthesize proteins. Hemoglobin (Hb), at an intracellular concentration of 5 mM, is the major component of RBCs. Its primary role is the transport of O_2 from the lungs to the muscles and the transport of CO_2 from the muscles to the lungs to be exhaled. Historically, RBCs had been characterized as "dead" cells, or mere Hb-filled receptacles with the sole function of O_2 transport. However, recent research has shown that RBCs carry out more than O_2 transport; they are actively involved in controlling the dilation of blood vessels. Identified mechanisms by which RBCs participate in vasodilation require O_2-regulated binding and bioactivation of NO by Hb and ATP release (10-14).

1.1.2. Nitric oxide and vasodilation

In 1998 Furchgott, Ignarro and Murad were awarded the Nobel Prize in Medicine "*for their discoveries concerning nitric oxide as a signaling molecule in the cardiovascular system*" (15). They identified NO as the endothelium-derived relaxing

factor (EDRF), a potent vasodilator formed on the hydrolysis of *L*-arginine to *L*-citrulline mediated by the enzymatic action of nitric oxide synthase (NOS) in the presence of oxygen (2) (Figure 1.1). In the vasculature, endothelial nitric oxide syntahse (eNOS) is the isoform responsible for the production of NO that triggers the signaling cascade resulting in smooth muscle relaxation (Figure 1.2).

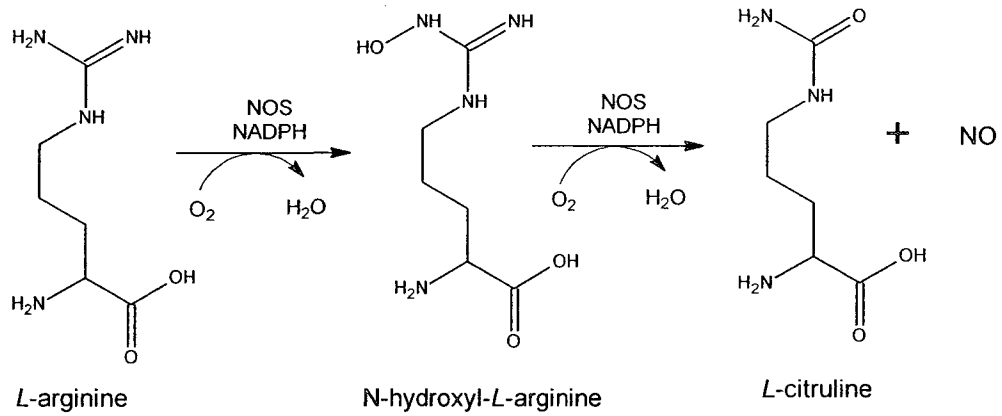

Figure 1.1 Enzymatic nitric oxide formation. Oxidation of *L*-arginine to *L*-citrulline with formation of NO by nitric oxide synthase (NOS). Adapted from (16).

NO has a short half-life (5 s) under physiological conditions (17). Possible mechanisms of NO scavenging in blood are its oxidation by O_2 to generate nitrite (NO_2^-), which is catalyzed by ceruloplasmin (18), and its reactions with Hb (19, 20). These mechanisms act to control vascular tone by reducing the smooth muscle exposure to NO, as proposed by Stamler and co-workers (21). Currently, some research groups consider nitrite to be the major storage pool of NO vasoactivity in blood (13, 22).

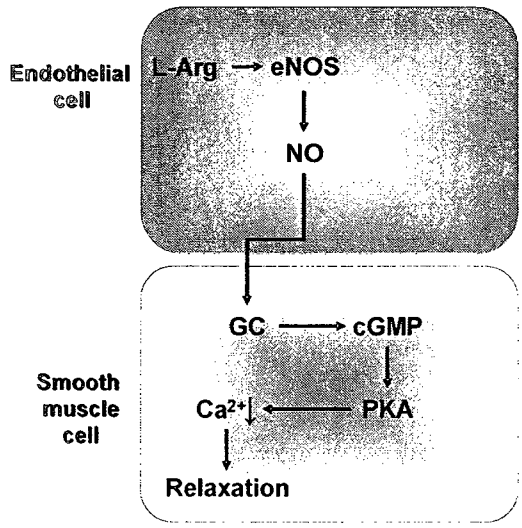

Figure 1.2 Signaling cascade originated by the formation of NO. NO, synthesized from L-arginine in the endothelium by eNOS activity, stimulates guanylate cyclase (GC) leading to increased cyclic guanosine monophosphate (cGMP) levels. These activate protein kinase A (PKA), which results in smooth muscle relaxation by reducing the intracellular calcium concentration. Adapted from (2).

1.1.3. Nitrite in vasodilation

Nitrite salts were used in antiquity by different cultures mainly as a food preservative (23). In the early 1800s, industrial exploitation of sodium nitrite focused on the manufacture of dyes, pharmaceuticals, anticorrosives and meat preservatives. Its physiological and biological relevance became more evident around 1860, when studies on the reactivity of nitrite with Hb were described by Hermann (24).

Diet represents the principal source of nitrite in mammals. In the gastric system, nitrite (NO_2^-) is generated by the reduction of nitrate, which is abundant in vegetables and drinking water (23). Nitrite is accumulated in saliva and partially reduced to NO and

oxygenase-1 (25). Gladwin and coworkers demonstrated that nitrite infusion into the human forearm increases blood flow, and they hypothesize that vasodilation is mediated through the reduction of nitrite to NO by deoxyHb (13). They also proposed that nitrite is the largest storage pool of NO in the blood stream (13). However, no evidence exists that nitrite donors activate NO release from RBCs. Moreover, Li and co-workers recently showed that NO production from nitrite occurs mainly in tissues and not in blood (26), suggesting that a molecular messenger other than NO is responsible for RBC-derived vasoactivity.

1.1.4 Epoxieicosatrienoic acids

Epoxyeicosatrienoic acids (EETs) are cytochrome P450 metabolites of arachidonic acid with an important role in the mediation of vasodilation in muscle tissue. Four structural isomers are physiologically available, and 11,12-EET and 14,15-EET are the most abundant (Figure 1.4). 11,12-EET is suggested to be the endothelial-derived hyperpolarization factor (EDHF) (27-29) responsible for modulation of relaxation of vascular smooth muscle. EETs are involved in other signaling cascades that control inflammation and in regulating cell proliferation and migration processes (30).

Both RBCs (Figure 1.5) (31) and endothelial cells (32) produce and release EETs. These messengers cause vasodilation by activation of calcium-dependent phosphate channels, reducing the intracellular calcium concentration in smooth muscle and hyperpolarizing the cell (Figure 1.6).

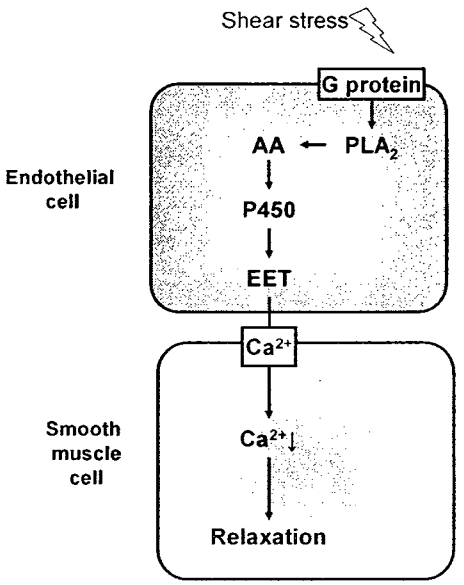

Figure 1.6 EET-derived vasoactivity. Shear stress and reduced oxygen levels activate membrane G-proteins which stimulate phospholipase A2 (PLA_2), causing the release of arachidonic acid (AA) from membrane phospholipids. The epoxigenase action of cytochrome P450 converts AA to EETs, which are released from RBCs and endothelial cells and activate calcium channels in the membrane of smooth muscle cells, reducing calcium influx and hyperpolarizing the cell. Adapted from (2).

1.1.5 Prostaglandins

The endothelium is the major source of prostaglandins in the vasculature (2). These are a family of molecules derived from arachidonic acid (AA) *via* the action of cyclooxygenases (COX-1 and COX-2). Prostaglandins are involved mainly in inflammatory processes and cardiovascular tone control. Prostaglandin I_2 (PGI_2), which is also known as prostacyclin (Figure 1.7a), is involved in the regulation of muscle blood flow. Prostacyclin causes vasorelaxation predominantly *via* the adenylyl cyclase/cyclic-AMP transduction system (34) (Figure 1.7b).

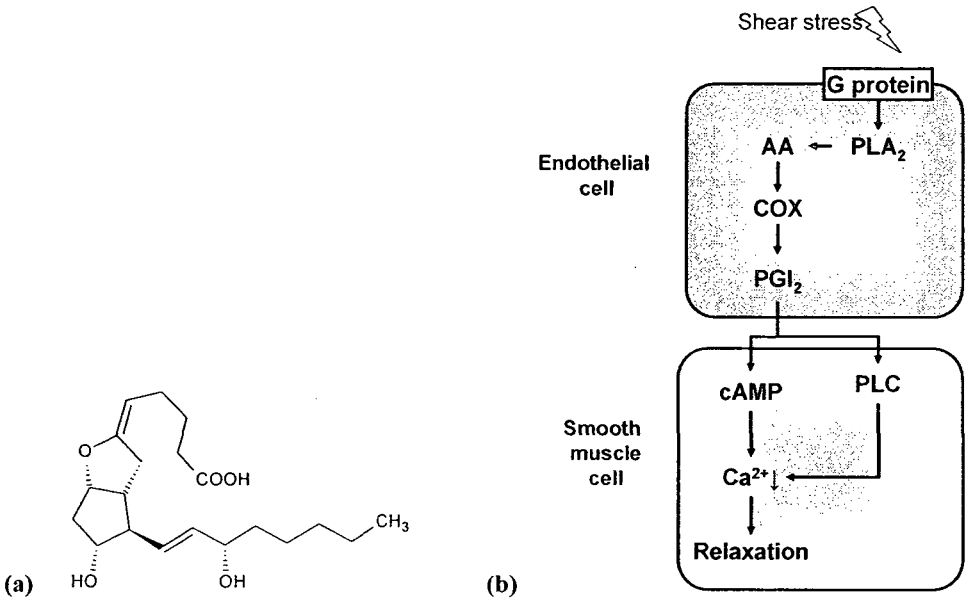

Figure 1.7 (a) Structure of prostacyclin. (b) PGI_2-derived vasoactivity. Shear stress and reduced O_2 levels activate membrane G-proteins which in turn activate phospholipase A2 (PLA_2), resulting in the transformation of membrane phospholipids into arachidonic acid (AA). The action of COX on AA generates PGI_2, which increases the levels of cyclic adenosine monophosphate (cAMP) and decreases phospholipase C (PLC) activity. The net result is a reduction in intracellular calcium which leads to smooth muscle relaxation. Adapted from (2).

1.1.6 Adenosine triphosphate

ATP is one of the most ubiquitous molecules in nature. It participates in many neurotransmission metabolic pathways as the *energy currency* of the cell and acts as the chemical energy storage for intracellular processes (35). ATP is also involved in signaling by targeting membrane purinergic receptors (36). Structurally, the molecule is composed of an adenosine unit, a purine nucleoside formed by adenine and ribose, covalently bond to three inorganic phosphate groups (Figure 1.8):

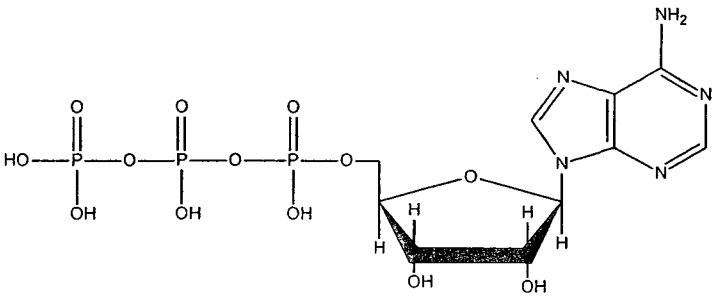

Figure 1.8 Structure of adenosine triphosphate (ATP)

RBCs are known to release ATP at low pH or low oxygen concentration and in response to mechanical deformation (8, 9, 37) (Figure 1.9). This release of ATP is believed to act as a response to high oxygen demand in the microvasculature and provides evidence for RBC control over vascular tone (14, 38). ATP is known to exert a very powerful vasodilatory response in skeletal muscle, lung, and brain (39-42), although the mechanism of action is a matter of much debate. It has been demonstrated that ATP is the RBC link to NO synthesis in rabbit lung (43).

RBC-derived ATP activates the NO signaling cascade in endothelial cells by yielding adenosine and stimulates the membrane heterotrimeric guanine nucleotide-binding (G) protein, which promotes EET and PGI_2 production (Figure 1.9).

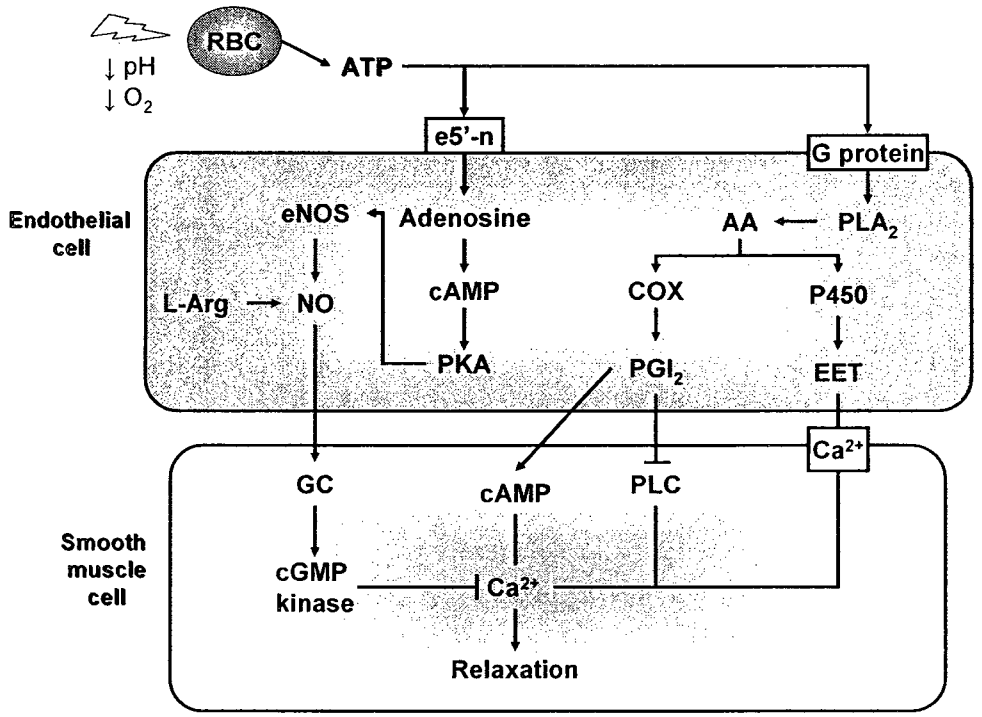

Figure 1.9 RBC-derived ATP increases production of vasodilators in endothelial cells. Shear stress, reduced oxygen levels and low pH cause the release of ATP from the RBC. ATP is converted by ecto-5'-nucleotidase (e5'-n) into adenosine, a potent vasodilator that acts through the NO signaling cascade. Other mechanisms are the activation of the PGI_2 and EET signaling cascades by activating membrane heterotrimeric guanine nucleotide-binding (G) protein, which then activates PLA2 stimulating the production of arachidonic acids from membrane phospholipids. Adapted from (2).

1.1.7 Glyceraldehyde 3-phosphate dehydrogenase

One of the major metabolic sources of ATP in mammalian cells is glycolysis. The glycolytic pathway is central in energy metabolism, providing a significant portion of the cell's energy requirements by converting glucose to pyruvate. This is accompanied by the generation of two moles of ATP (35), as shown in Reaction 1.1.

1.2 Nitroglycerin

The Heart Disease and Stroke 2008 Update Statistics compiled by the American Heart Association lists ischemic heart disease as one of the main causes of death in North America (49). Since 1879, the standard treatment for angina, the most common symptom of this condition, has been the administration of nitroglycerin (50) (Figure 1.11). Angina is the chest pain experienced by patients with ischemic conditions due to the lack of oxygen supply to the heart and the inability to increase coronary blood flow. Nitroglycerin acts as a potent vasodilator, causing a rapid increase in myocardial oxygen supply and relief of pain associated with angina.

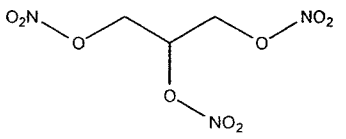

Figure 1.11 Nitroglycerin structure

1.2.1 Pharmacology and pharmacokinetics

The metabolism of nitroglycerin leads to the formation of NO (51), which can exert an intense vasodilatory response (Section 1.1.2). The mechanism by which nitroglycerin yields NO is still not entirely understood (Figure 1.12) but there is strong evidence for an enzyme-dependent process. To date many enzyme candidates have been proposed (Section 1.2.2).

Nitroglycerin can be administered through several routes: sublingual, buccal, oral, transdermal, and intravenous. Patches, sprays, and rapidly dissolving tablets are widely available comercially. Doses of 0.2-0.8 mg can be administered orally with 5 minute intervals between doses until pain disappearance. Patches containing 5.0 mg are designed to release small doses over 24 hours. Physiological effects are experienced within 3 to 5 minutes of nitroglycerin adminstration.

Nitroglycerin undergoes rapid clearance by the liver, lungs and blood, and most denitrated metabolites are excreted *via* the kidney (50). Metabolic half-lives in whole blood of 3-5 minutes, in plasma ~52 minutes and ~3 minutes in RBCs have been reported (52). These values suggest that most of the metabolic processing of nitroglycerin in whole blood is performed by RBCs.

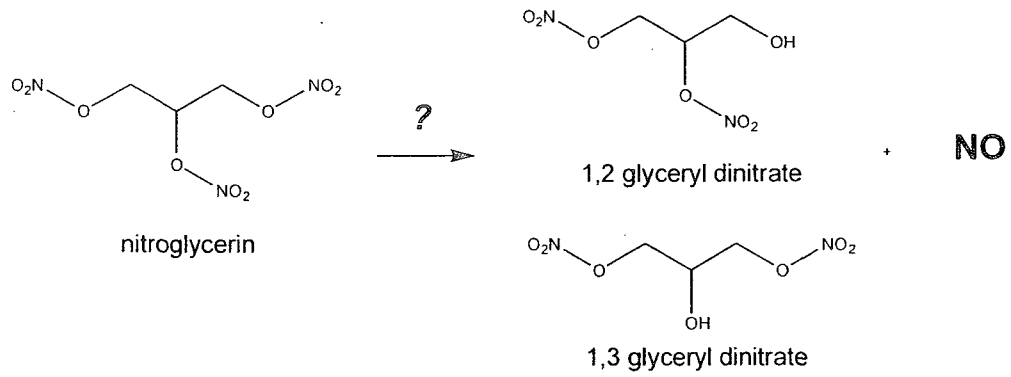

Figure 1.12 Nitric oxide derived from nitroglycerin. Activation processes and mediators are still under debate. Both the 1,2- and 1,3-glyceryl dinitrate byproducts possess some vasodilatory activity but less than nitroglycerin (53).

1.2.2 Bioactivation

The vasodilatory potential of nitroglycerin and related organic nitrates is related to their ability to yield NO (50). Few nonenzymatic mechanisms have been reported for nitroglycerin bioactvation. Notably, Ignarro and Gruetter proposed $-NO_2$ transfer from nitroglycerin to cysteine that yields NO (54).

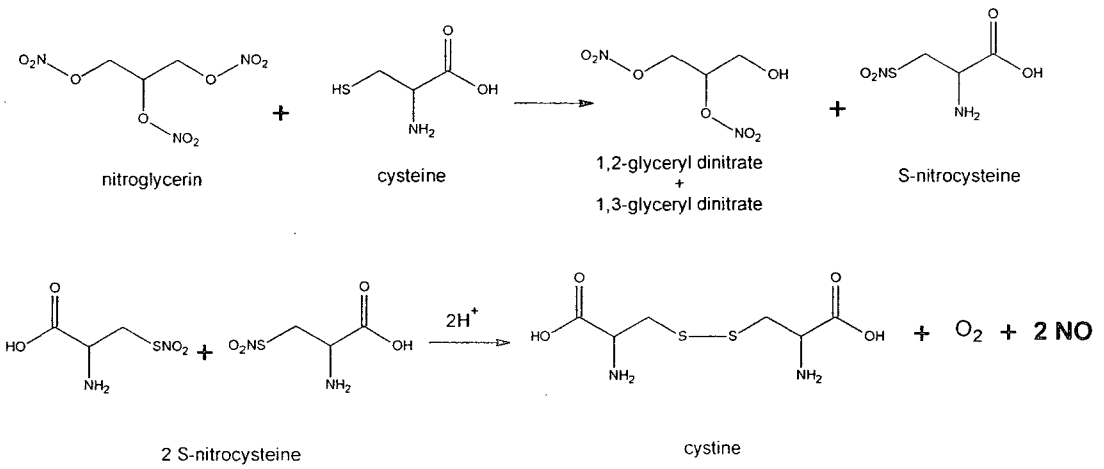

Figure 1.13 Bioactivation of nitroglycerin by cysteine. Nitroglycerin ($RONO_2$) reacts with cysteine (RSH) to generate 1,2- or 1,3-glyceryl dinitrate and S-nitrocysteine. Two S-nitrocysteine molecules react to form cystine and NO. Adapted from (54).

Enzymatic bioactivation of nitroglycerin by many candidate enzymes has been proposed and there is still much debate about their relative efficiencies. These candidates are discussed in the following sections.

1.2.2.1 Glutathione S-transferases

Glutathione S-transferases (GSTs) are a family of cytosolic and mitochondrial proteins with different isoforms. Detoxification of endogenous compounds is one of their many functions and GSTs were among the earliest candidates postulated as nitroglycerin bioactivators (55, 56). Bioactivation of nitroglycerin (RNO_2) by GST requires 2 molecules of glutathione (GSH) with the formation of nitrous acid (HNO_2) (pK_a = 3.4) (57) as shown in Reactions 1.2 and 1.3.

$$\mathbf{GSH + RONO_2 \rightarrow [GS\text{-}NO_2] + ROH} \qquad \mathbf{(1.2)}$$

$$\mathbf{[GS\text{-}NO_2] + GSH \rightarrow GSSG + HNO_2} \qquad \mathbf{(1.3)}$$

$$\mathbf{2HNO_2 \rightarrow NO + H_2O + NO_2} \qquad \mathbf{(1.4)}$$

Disproportionation of nitrous acid in an aqueous environment (Reaction 1.4) (57) leads to the formation of NO and NO_2, which could induce a vasodilatory response in vascular tissue. Research by Kurz and coworkers found a linear correlation between GST activity and NO_2^- production when using nitroglycerin as a substrate for the enzyme (58). Reaction 1.2 involves $-NO_2$ transfer to a thiol as in Figure 1.13. However reaction of a free thiol and a nitrothiol yields HNO_2 as an intermediate (Reaction 1.3) vs the direct NO generation proposed in Figure 1.13 for reaction of two nitrothiols.

1.2.2.2 Hemoglobin

Bioconversion of nitroglycerin in the vascular system has been extensively discussed since this process has been suggested to be both endothelial-dependent (59) and independent (50). At the same time, it has been reported that nitroglycerin is relatively stable in plasma and it is poorly metabolized by human serum albumin (60). Importantly, in plasma, nitroglycerin has a half-life (~52 min) that surpasses the time frame (3-5 min) in which physiological effects are experienced (52). Thus, RBC-associated proteins are suitable candidates for nitroglycerin bioactivation in whole blood.

As mentioned in Section 1.1.1, Hb is the most abundant protein in RBCs. Its main function is the transport of O_2 and CO_2 to and from tissues. RBCs are known to concentrate nitrite in the vasculature, and the nitrite reductase activity of deoxyHb has been proposed to give rise to NO vasoactivity in these cells (20). The conversion of deoxyHb to methemoglobin (metHb) *via* reaction with NO_2^- suggests the potential role of deoxyHb as a nitroglycerin activator. Bennett and coworkers spectrometrically followed the interaction of deoxyHb and deoxymyoglobin with nitroglycerin and showed that it led to the preferential formation of 1,2-glyceryl dinitrate and nitrite (61). They proposed heme-mediated reductive denitrosation with a 2:1 stoichiometry:

$$\mathbf{2\ Fe^{II}(heme) + RONO_2 + H^+ \rightarrow\ 2\ Fe^{III}(heme) + ROH + NO_2^-} \qquad (1.5)$$

1.2.2.3 Cytochromes P450

Cytochromes P450 (CYP450) are a superfamily of hemoproteins involved in electron transfer, steroid biosynthesis, and xenobiotic metabolism (62). The most common reaction catalyzed by this enzyme family is the monooxygenation of organic substrates. Most CYP450 are found in hepatic cells, and are considered the front-line defense against drugs and toxins artificially introduced to the cell. This is why CYP450s were considered as potential nitroglycerin activators. Servant and co-workers found evidence for nitroglycerin biotransformation by hepatic CYP450 since they detected the nitrosyl-heme CYP450-Fe(II)-NO complex spectroscopically (63). Later, McDonald and Bennett showed that CYP450 transforms nitroglycerin to glyceryl dinitrate derivates, with a preference for the 1,3- isomer (64). Isoforms of CYP450 in human heart blood vessels showed the ability to convert isosorbide dinitrate, an organic nitrate related to nitroglycerin, to NO (65). Associated with CYP450, cytocrome P450 reductase (CPR) has also been suggested as an important player in the bioactivation mechanisms of organic nitrates (66). The CPR-CYP450 nitroglycerin activation complex involves the two enzymes in different stages. Initially CPR reduces nitroglycerin ($RONO_2$) to an organic nitrite (RONO), following by quick hydrolysis to HNO_2 in a thiol-free environment. The nitrite reductase activity of CYP450 then catalyzes the conversion of HNO_2 to NO. If thiol groups are available, either NO or nitrosothiols (R'SNO) can be formed (Figure 1.14) (66).

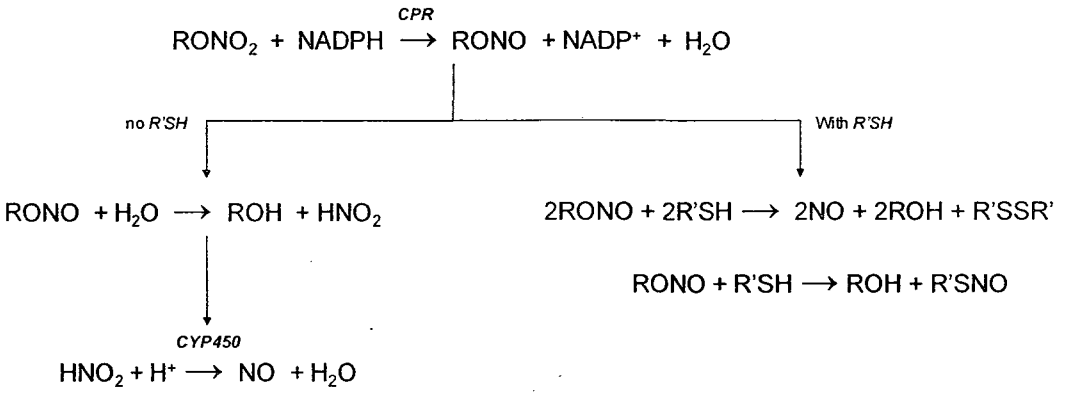

Figure 1.14 Nitroglycerin bioactivation by CPR-CYP450. Nitroglycerin ($RONO_2$) is reduced to an orgnic nitrite (RONO) that hydrolyzes to nitrous acid. The latter is catalytically converted to NO by CYP450. In the presence of thiols, RONO yields either NO or nitrosothiols (R'SNO). Adapted from (66).

1.2.2.4 Xanthine oxidase

Xanthine oxidase is a molybdoflavoprotein abundant in certain mammalian cells, and it has been implicated in nitrate to nitrite reduction (67, 68). In addition to molybdenum and FAD, it contains two iron-sulphur redox centres. It has been reported that xanthine oxidase can catalyze the reductive denitrosation of organic nitrates to yield NO_2^- under anaerobic conditions (69, 70). A xanthine oxidase-mediated mechanism for nitroglycerin and isosorbide dinitrate bioactivation was proposed by Li and coworkers, and involves initial oxygen transfer from the substrate ($RONO_2$) to the reduced enzyme (E_{red}). Subsequent reaction of RONO with R'SH gives R'SNO (Reactions 1.6 – 1.7) (71), which can donate NO.

$$E_{red} + RONO_2 + 2H^+ \rightarrow R\text{-}O\text{-}NO + H_2O + E_{ox} \quad (1.6)$$

$$R\text{-}O\text{-}NO + R'SH \rightarrow R\text{-}OH + R'SNO \quad (1.7)$$

1.2.2.5 Mitochondrial aldehyde dehydrogenase (ALDH2)

ALDH2 is a homotetramer (56.4 kDa per subunit) responsible for the conversion of acetaldehyde to acetic acid (72), which is important in alcohol metabolism. There are two major aldehyde dehydrogenase isozymes: cytosolic (ALDH1) and mitochondrial (ALDH2). In ~50% of the Asian population ALDH2 is not present, this being a possible cause of high rates of alcohol intoxication and low alcohol dependence present in this population (72). In 2002, Chen *et al.* identified ALDH2 as a major enzyme responsible for nitroglycerin bioactivation. They demonstrated both *in vitro* and *in vivo* that the nitrate reductase activity of ALDH2 specifically catalyzes the formation of 1,2-glyceryl dinitrate and nitrite from nitroglycerin, leading to relaxation of vascular smooth muscle (73). The overall reaction proposed for nitroglycerin activation by ALDH2 is shown in Figure 1.15.

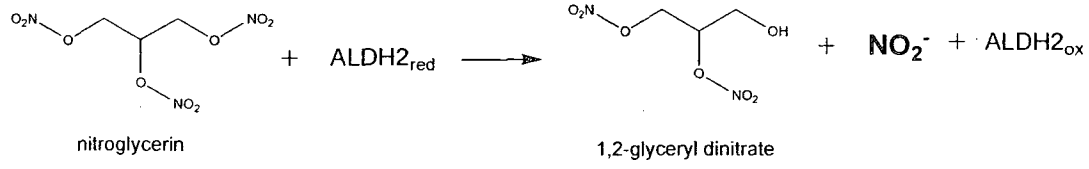

Figure 1.15 Biocativation of nitroglycerin by mitochondrial aldehyde dehydrogenase. Nitroglycerin is activated by the reduced form of mitochondrial aldehyde dehydrogenase ($ALDH2_{red}$), causing its oxidation ($ALDH2_{ox}$) and generating 1,2-glyceryl dinitrate and NO_2^-. Adapted from (59).

Human ALDH2 possesses three consecutive cysteine residues in its sequence, active-site Cys302 and adjacent Cys301 and Cys303. Two of these cysteines form an intramolecular disulfide bond on reductive denitrosation of nitroglycerin with NO_2^- release, as shown in Scheme 1.1. The intramolecular disulfide bond in ALDH2 has been characterized by mass spectrometry (74), and causes inactivation of the enzyme by oxidazing the active-site Cys302. Inactivation of ALDH2 has been proposed for the development of nitrate tolerance in patients under nitroglycerin treatment (59), which will be discussed in Section 1.2.3.

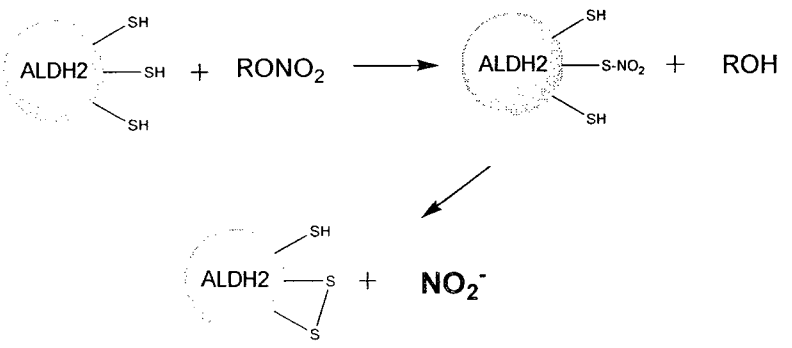

Scheme 1.1 Nitroglycerin bioactivation by ALDH2. The transfer of $-NO_2$ from nitroglycerin to one of the thiols of ALDH2 produces glyceryl dinitrate (ROH) and a Cys-NO_2 moiety that reacts with an adjacent free thiol. This results in a disulfide bond formation (S-S) and release of NO_2^-. Adapted from (59).

1.2.2.6 Glyceraldehyde-3-phosphate dehydrogenase

Structural homology between ALDH2 and glyceraldehyde-3-phosphate dehydrogenase (GAPDH) suggests that the latter could be involved in nitroglycerin

bioactivation in the vasculature. In addition to dehydrogenase activity, GAPDH and ALDH2 share the possession of multiple free cysteine residues. The GAPDH monomer has four cysteines: active-site Cys149 and neighboring Cys153, as well as Cys244 and Cys281. The architecture of the active site suggests that nitroglycerin could interact with GAPDH in a similar manner as it does with ALDH2 (Scheme 1.1).

As discussed in Section 1.1.6, GAPDH is a key enzyme in the glycolytic pathway. It catalyzes the conversion of glyceraldehydes-3-phosphate to D-glycerate-1,3-bisphosphate, and the latter donates a phosphate group to adenosine diphosphate (ADP) yielding ATP in a reaction catalyzed by phosphoglycerate kinase (PGK) (Figure 1.16) (35). GAPDH is highly concentrated in RBCs which exhibit high glycolytic metabolism (47). Inhibition of GAPDH would result in a substantial decrease in ATP production which may affect ATP release from the RBCs. Diminished ATP-mediated stimulation of endothelial nitric oxide synthase (eNOS) would in turn suppress relaxation of the smooth muscle due to decreased EDRF/NO production (Figure 1.9). Thus, inhibition of GAPDH by nitroglycerin could contribute to nitrate tolerance by two mechanisms as discussed further in Chapter 4 of this thesis.

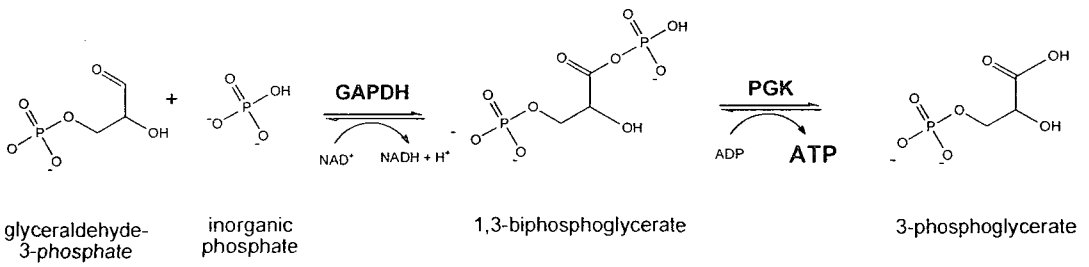

Figure 1.16 Role of GAPDH in glycolysis and ATP production. (35).

Table 1.1 summarizes the published catalytic parameters in enzymatic nitroglycerin bioactivation.

Table 1.1 Catalytic parameters and products reported in enzymatic bioactivation of nitroglycerin

Enzyme	K_m	V_{max}	NO_x products	1,2-/1,3-glyceryl dinitrate	Ref.
GST aortic μ (pI 8.3)	1.1 mM	-	HNO_2	-	(75)
GST μ	2.5 mM	-	NO_2	-	(75)
GST I	0.3 mM	-	NO	-	(75)
deoxyHb	-	-	NO_2^-	11:1	(61)
deoxyMb	-	-	NO_2^-	3:1	(61)
CYP450	-	-	NO	1:5	(64)
Xanthine oxidase	-	-	RSNO	-	
ALDH2	11.98 μM	3.03 nmol/min per mg	NO_2^-	5:1	(73)

1.2.3 Nitrate tolerance

Despite the efficacy of nitroglycerin in the treatment of ischemia, its chronic effects are rapidly blunted. This phenomenon is known as *nitrate tolerance*. Tolerance is not related to the pharmacokinetics of the drug, since this remains unaltered during chronic nitroglycerin exposure (76). Thus, factors such as reduced absorption, accelerated metabolism or excretion of nitrates and related metabolites are unlikely to play a role in the development of tolerance.

Loss of vascular bioactivation of nitroglycerin seems to play an important role in the development of nitrate tolerance. The classical mechanism proposed by Needleman points to the decreased availability of sulfhydryl groups (77). The Needleman hypothesis suggests a "vascular nitrate receptor" that contains –SH groups that interact with organic nitrates to release nitrite and induce vasodilation. This hypothesis has evolved to include inhibitory mechanisms in which disulfide bonds are formed in the active sites of enzymes, such as ALDH2 (Scheme 1.1) and GAPDH. Research aiming to restore the vasodilation effects of nitroglycerin by reducing the disulfide bond in ALDH2 has strengthened this hypothesis by demonstrating that enzymatic activity is recovered upon treatment with different reductants (59). For clinical applications, the use of reducing agents such as dithiothreitol (DTT) or TCEP is not viable, therefore regeneration of the nitroglycerin-induced vasodilatory effect must await the recovery of the free sulfhydryl groups by the reductase activity of thioredoxins (78, 79), glutaredoxins (80) and lipoic acid (81), or the synthesis of new enzymes with unaltered –SH functions (82). The latter could explain why drug free periods of more than eight hours allow tolerant patients to regain nitrite reactivity to a new dose of nitroglycerin (83).

The presence of oxidative stress in the vasculature has also been suggested as a possible cause of nitrate tolerance (84). Exposure to nitroglycerin increases the activity or the expression of angiotensin II, a vasoconstrictor oligopeptide, which elevates vascular production of the superoxide anion ($O_2^{\cdot-}$) leading to enhanced degradation of circulating nitric oxide to a less potent vasodilator ($ONOO^-$) (82).

Nitrite-induced counter regulation is another phenomenon that has been linked to the development of nitreate tolerance, mostly in chronic exposure to nitroglycerin. An

example is the case of industrial munitions workers who developed ischemic heart conditions after retirement and their symptoms were relieved by treatment with nitroglycerin and/or return to industrial exposure (85). Additionally, alterations of metabolic or enzymatic activities have been proposed as an alternate explanation for nitrate tolerance and cross tolerance (80, 86). Increases in hormonal vasoactive agents such as catecholamine and rennin are not consistently reported with the development of tolerance. However, changes in the expression of mRNA of several genes present in blood vessels upon nitroglycerin infusion have been described in the past (87).

1.3 Scope and outline of thesis

The work performed for this thesis focused on the characterization of the effects of different vasodilators, both endogenous and exogenous, on RBCs and the possible vasodilatory chemical signaling originating from these cells. The results contribute to the elucidation of the role of RBCs in the regulation of blood flow at the microvascular level.

Chapter 2 presents an adaptation of the well documented luciferin-luciferase chemiluminescence assay in microplate-reader format for the measurement of ATP released from human RBCs. Also, the use of HPLC to survey the ribonucleotide profile arising from RBCs was evaluated.

In **Chapter 3**, the effects of nitroglycerin and nitrite on ATP release from human RBCs are compared. The changes in the ATP levels induced by time of exposure to these compounds as well as the effects of varying their concentrations at a fixed time are presented. ATP levels were measured by the chemiluminescent method described in

Chapter 2. Based on the results obtained, a novel mechanism is proposed to explain the role of RBC-derived ATP in the propagation of a vasodilation signal.

An extended version of this chapter, with additional work performed by the other co-authors, was submitted on February 28, 2009 for publication to Nature Medicine as a letter under the title "*Nitrite and nitroglycerin induce rapid release of the vasodilator ATP from erythrocytes: Evidence for a NO_2^-/ATP feedback signaling pathway in blood-flow regulation*", authors: Juliana I. Garcia, Amedea B. Seabra, Renée Kennedy, and Ann M. English.

Chapter 4 describes the effects of nitroglycerin on the glycolytic activity of the enzyme, glyceraldehyde-3-phosphate dehydrogenase (GAPDH). GAPDH activity was measured spectrophotometrically and the possible relevance of results to reversible nitrate tolerance is discussed.

Chapter 5 presents preliminary results on the development of a method for the detection and quantitation in blood plasma of the arachidonic-acid derived vasodilators, epoxyeicosatrienoic acids (EETs) and prostacyclin (PGI_2). Overall conclusions and suggestions for future studies are presented in **Chapter 6.**

2. Measurement of human RBC extracellular ATP

2.1 Introduction

The most commonly used methods for ATP determination in blood are chromatography and the luciferin-luciferase bioluminescence assay. Chromatographic methods are more often used on blood plasma, lysed cells and treated or extracted samples, since co-elution and interference from other substances are common in more complex systems. The luciferin-luciferase assay is the method used for real time ATP estimation, such as the measurement of release rates from cells (88). It is also more convenient and commonly used on untreated samples.

The term "bioluminescence" was defined by Newton Harvey in 1916 to describe the naturally occurring phenomenon in which living organisms emit 'cold' light (luminescence) (89). Bioluminescence is present in many organisms in nature, and it has been extensively studied in bacteria, crustacea and fireflies (Figure 2.1). In 1885, the physiologist Raphael Dubois described the reaction that generated this light emission by producing a luminescent solution when dissolving ground up abdomens of the *Pyrophores* beetle in cold water (90). Dubois called luciferin and luciferase the two interacting substances responsible for the luminescent effect. Subsequently, Harvey demonstrated the occurrence of this same reaction on the tail of fireflies (91). Almost thirty years later, McElroy reported the dependency of this reaction on the presence of ATP (92) and Mg^{2+} (93).

(OxL) (Reactions 2.1 – 2.3). The luciferin-luciferase reaction has the highest known quantum yield of any bioluminescence reaction, with a quantum yield of ~1 (96), indicating that nearly one photon of light is emitted for every luciferin molecule oxidized.

$$E + LH_2 + ATP + Mg^{2+} \rightarrow E{\bullet}LH_2\text{-}AMP + PPi + Mg^{2+} \quad (2.1)$$

$$E{\bullet}LH_2\text{-}AMP + O_2 \rightarrow E{\bullet}OxL^* + AMP + CO_2 \quad (2.2)$$

$$E{\bullet}OxL^* \rightarrow E{\bullet}OxL + h\upsilon \quad (2.3)$$

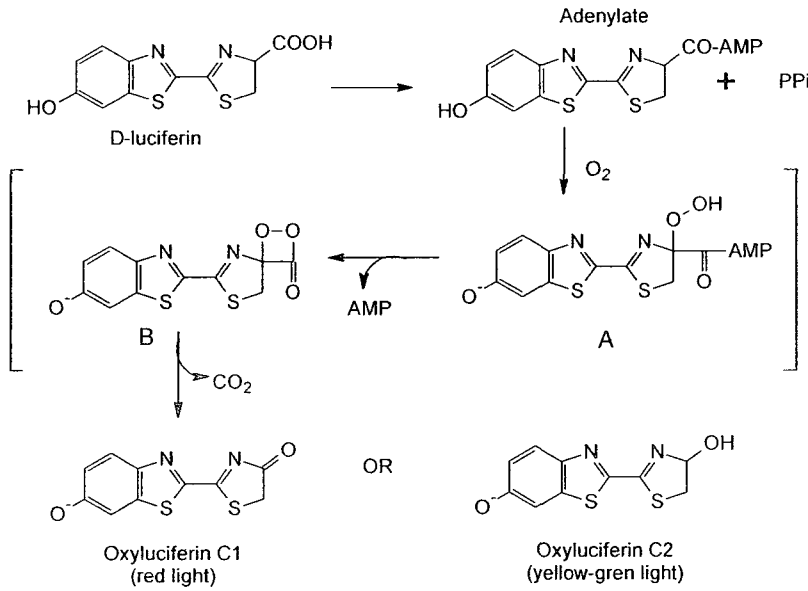

Figure 2.3 Mechanism of bioluminescent oxidation of firefly luciferin catalyzed by firefly luciferase. Most likely D-luciferin binds as the dianion to luciferase. In the presence of ATP and Mg^{2+}, luciferin is converted to an adenylate, yielding pyrophosphate (PPi). Oxygenation of the adenylate in the presence of air generates the peroxide intermediate A. This is converted to the dioxietanone intermediate B after releasing AMP. The decomposition of intermediate B produces an excited state of oxyluciferin C1 (monoanion) or dianion C2. To reach the ground state C1 emits red light (λ_{max} 615 nm), and C2 emits yellow-green light (λ_{max} 560 nm). Adapted from (94, 95).

Firefly luciferase is composed of a single 62 kDa polypeptide of 550 amino acids and is active in the monomeric form. The crystalline form of firefly luciferase was reported by Green and McElroy in 1956 (97). Later studies on the crystal structure of the enzyme led to the characterization of the active site when a highly conserved sequence was found near the C-terminal of three families of related enzymes: firefly luciferase, acyl-CoA ligases and peptide synthetases (98).

Firefly luciferin crystallizes as microscopic needles when purified and exhibits fluorescence. The enzyme shows maximum absorption at 560 nm in acidic and 615 nm in basic solutions (94) (Figure 2.4). A molar extinction coefficient of 18,200 $cm^{-1}M^{-1}$ was determined at 328 nm (99).

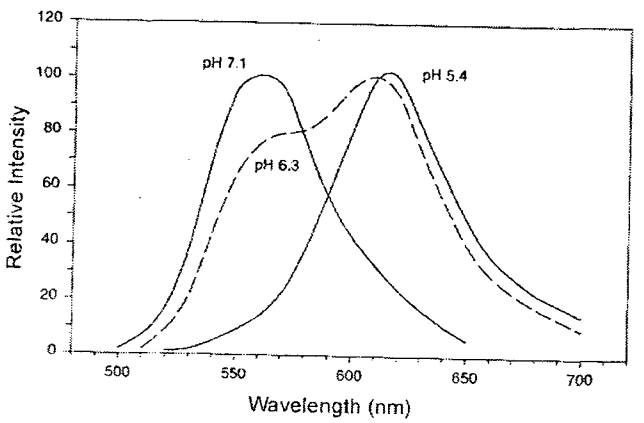

Figure 2.4 pH-dependent spectrophotometrical changes of firefly luciferin. The common yellow-green luminescence of luciferin at pH 7.1 changes to red in acidic media (pH 5.4). Adapted from (100).

The luciferin-luciferase bioluminescence assay has been widely studied and applied (8, 37, 101-103). The goal here was to adapt the method to our experimental needs and to bench-mark the parameters of re-suspended RBCs for the experiments

presented in this thesis. Linearity of the calibration curve and limit of detection of the method were determined. Also, the total extracellular ribonucleotide profile arising from RBCs was examined by HPLC.

2.2 Materials and methods

2.2.1 Materials

Blood was collected in standard 4-mL Vacutainer® heparinized tubes (BD, Franklin Lakes, NJ). KCl, $MgCl_2$ methanol (HPLC grade) were purchased from Fisher Scientific (Pittsburgh, PA). $CaCl_2$ and $MgSO_4$ were purchased from ACP Chemicals (Montreal, QC). NaCl, tris(hydroxymethyl)aminomethane and dextrose were purchased from Bioshop (Burlington, ON). Sucrose was purchased from Anachemia (Lachine, QC). Distilled water was purified in a Milli-Q Simplicity 185, Millipore (Billerica, MA), and Ultrafree®-0.5 centrifugal filter Units, 10 kDa cut-off ultrafiltration membranes were purchased from the same supplier. Bovine serum albumin, ATP, firefly lantern extract, HEPES, EGTA, KH_2PO_4, $K_2HPO_4{\cdot}3H_2O$ and $NaNO_2$ were purchased from Sigma-Aldrich (St. Louis, MO). White 96-well plates and UV/Vis transparent lids were purchased from Corning (Corning, NY). Nitrogen gas (ultra high purity) was purchased from Praxair (Danbury, CT). HPLC analyses were carried out with an 1100 Agilent HPLC system using a Hypersil ODS C18RP column (Agilent Technologies, Santa Clara, CA). Physiological salt solution (PSS) was prepared using the following materials: in M,

0.0047 KCl, 0.0020 $CaCl_2$, 0.0012 $MgSO_4$, 0.1405 NaCl, 0.0210 tris(hydroxymethyl)aminomethane, 0.0111 *D*-glucose with 0.5% *w/v* bovine serum albumin, pH adjusted to 7.4. Sucrose buffer was prepared as follows: in M, 0.321 sucrose, 0.032 HEPES, 0.003 EGTA, 0.006 $MgCl_2$, pH adjusted to 7.4.

2.2.2 Preparation of red blood cells

All procedures involving the collection of human blood samples were in accordance with the Concordia University Ethics Guidelines. After their informed written consent was obtained, blood was collected from healthy female volunteers (aged between 20-35 years) by venipuncture into the heparinized tubes. Within two hours of collection, the blood was centrifuged at 5,000 rpm at 4 °C for 10 min. The plasma was collected by aspiration and stored at -80 °C. The buffy coat was also collected by aspiration and discarded. Packed RBCs were resuspended and washed three times in PSS.

2.2.3 Measurement of ATP by chemiluminescence

From a stock solution of 2.5 mM ATP in PSS, ATP standards ranging from 10 nM to 39.1 μM ATP were prepared in PSS. The luciferin-luciferase assay solution used to measure ATP by chemiluminescence was prepared by dissolving 13.3 mg of crushed firefly extract in 10.0 mL of Milli-Q water. Chemiluminescence proportional to the ATP

in the sample was measured using a Wallac Victor$_2$ 1420 multilabel plate reader (PerkinElmer, Waltham MA). Background emission of 100 µL of the luciferin-luciferase assay solution in a white 96-well plate was recorded, and immediately following mixing with 100 µL of ATP standard, the emission was measured. Following background correction, double-log plots of emission versus [ATP] yielded a linear standard curve over 5 nM - 20 µM. To measure sample ATP levels, 100 µL of RBCs at different Hct values were added to 100 µL of the blanked assay solution, the light emission was recorded, and ATP concentrations were determined using the ATP standard curve.

2.2.4 Chromatographic determination of ATP and its metabolites

ATP and metabolites were identified using an 1100 Agilent HPLC consisting of a quaternary gradient pump, a variable wavelength detector and a solvent degasser. Separation was achieved with a Hypersil (5-µm particles) ODS C18RP column (100×4.6 mm). Separation of ATP and its metabolites was performed as described previously by Coolen *et al.* (104). Briefly, a gradient of 50 mM phosphate buffer (pH 6.0) (solvent A) and 100% methanol (solvent B) at a flow rate of 0.6 mL/min was used as the mobile phase. The analytes were eluted using the following linear gradient: 100% A over 2 min; 100-87.5 % A over 10 min, 87.5% A for 12 min; 87.5–100% A over 17 min and 100% A over 19 min for re-equilibration of the column prior to the next sample injection. RBCs were prepared as described in Section 2.2.2, resuspended at 10% Hct in sucrose buffer at 4 °C for 2 h, centrifuged at 5,000 rpm at 4 °C for 5 min, and 200 µL of supernatant was

loaded into a preconditioned Ultrafree®-0.5 cell with a 10-kDa cut-off ultrafiltration membrane (Millipore, Billerica, MA). The sample was centrifuged at 12,000 × g at 4 °C for 10 min. The ultrafiltrate (50 µL) was diluted into 200 µL of mobile phase A and 25 µL of this sample was injected into a sample vial for HPLC analysis. The HPLC autosampler temperature was set at 4 °C, and the column was kept at 20 °C.

2.3 Results and discussion

2.3.1 Chemiluminescence

Since the luciferin-luciferase reaction is affected by the presence of oxygen (94), chemiluminescence was measured in 96-well plates covered with a UV/Vis transparent lid. This also served to avoid biological contamination of the plate reader. Calibration curves were generated by plotting the logarithm of the chemiluminescence intensities (I) vs the logarithm of the ATP concentration of the standards. All measurements were performed using the luciferin-luciferase assay solution (Section 2.2.3). Acceptable linearity and reproducibility were obtained for the calibration curve averaged over 15 independent measurements of ATP standards in the range of 9.54 nM to 39.1 µM. The equation obtained was $\log I = 0.81 (\pm 0.06) \log[ATP] + 8.6 (\pm 0.4)$ with a correlation coefficient $R^2 = 0.9982 (\pm 0.0047)$. Deviation from the average is expressed as ± standard variation.

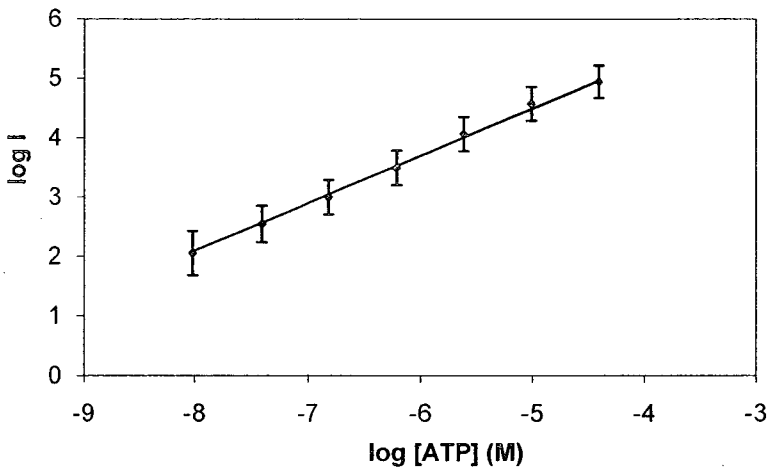

Figure 2.5 ATP calibration curve. Logarithm of chemiluminescent intensity (I) vs logarithm of ATP concentration in the range 9.54 nM – 39.1 μM. Least square analysis reveals linear behavior [log I = 0.81 (± 0.06) log[ATP] + 8.6 (± 0.4)] and a correlation coefficient R^2 of 0.9982 (± 0.0047) (± standard deviation). The ATP standards (100 μL) in PSS at the concentrations indicated in the figure were mixed with 100 μL of luciferin-luciferase assay solution (Section 2.2.3). Chemiluminescence intensities were recorded at 22 °C. Each data point represents the average of 15 independent measurements.

2.3.1.1 Interferences

The effect of nitroglycerin on the luciferin-luciferase ATP assay was investigated to determine if the drug altered the luminescent signal. ATP standard solutions were divided into two aliquots, one was mixed with assay solution and the second with assay solution plus 33.3 μM nitroglycerin. The results shown in Figure 2.6 confirm that the ATP standards with or without nitroglycerin fall on the same line. Thus, nitroglycerin does not interfere with the assay and the difference in the slopes of the calibration curve is within the standard deviation (Figure 2.5).

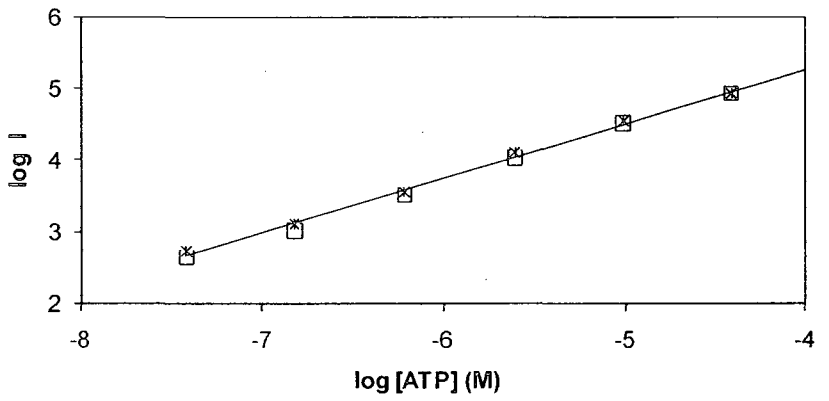

Figure 2.6 ATP calibration curve in the presence and absence of nitroglycerin. Logarithm of chemiluminescence intensity (I) vs logarithm of ATP concentration in the range 38.2 nM – 39.1 μM least square analysis reveals linear behavior both in the presence (*: y = 0.7793x + 8.388) and absence (□: y = 0.7553x + 8.2923) of 3.33 mM of nitroglycerin, with corresponding correlation co-efficients R^2 of 0.9978 and 0.9975. See Figure 2.5 for experimental conditions.

2.3.2 Effect of Hct on chemiluminescence intensity

To determine a suitable RBC concentration for the extracellular ATP assay, the profile of light intensities at different Hct values was tested following mixing with the assay solution. Spence *et al.* used 7% Hct (8, 37, 105) in their flow-through system. For our experiments, RBC concentrations varying from 5-24% Hct were mixed with luciferin-luciferase assay solution to study the ATP signal. The results shown in Figure 2.7 indicate no relationship between the measured ATP concentration and Hct, suggesting saturation of the signal. The standard curves in Figures 2.5 and 2.6 reveal that the light intensity is directly proportional to the ATP concentration up to ~40 μM. The extracellular ATP concentrations in Figure 2.7 are outside this range.

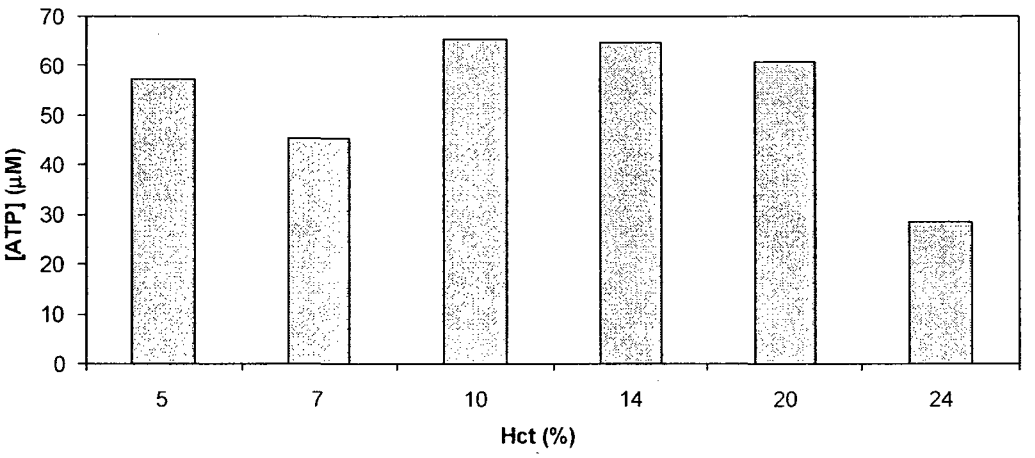

Figure 2.7 Measured extracellular ATP vs Hct. The ATP concentration was determined from the light intensities using the calibration curve in Figure 2.5. RBCs at 5-24% Hct (100 μL) were mixed with 100 μL of assay solution. The lack of correlation between ATP concentration and Hct suggests signal saturation.

Thus, lower Hcts were assessed. The light emitted from solutions varying from 0-3.5% Hct was measured and the results (Figure 2.8) indicate a linear correlation up to 1% Hct. Linearity is lost above 1% Hct, indicating that the signal saturates at relatively low ATP concentration using a plate reader. A value of 1% Hct was chosen for all subsequent measurements of extracellular ATP, since it yields a high signal response within the linear range of the assay.

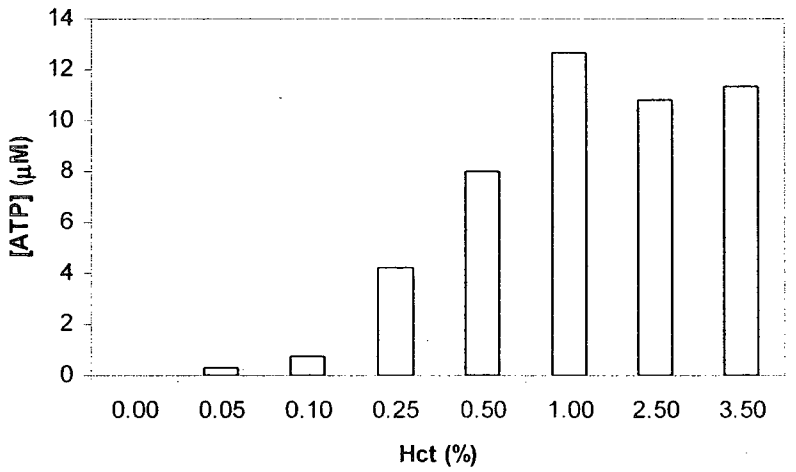

Figure 2.8 Measured extracellular ATP at low Hct. The ATP concentration was determined from the light intensities using the calibration curve in Figure 2.5. RBCs at 0-3.5% Hct (100 μL) were mixed with 100 μL of assay solution. A linear correlation between ATP concentration and Hct is observed between 0 and 1% Hct.

2.3.3 HPLC determination of extracellular ATP and its metabolites

Since ATP is readily metabolized to ADP, AMP and other metabolites, the presence of extracellular ATP and its metabolites was investigated by HPLC using methodology and chromatograms published by Coolen *et al.* for whole blood (104). A HPLC-UV (254 nm) calibration curve for ATP concentrations in the range examined by chemiluminescence (9.54 nM - 39.1 μM), was prepared by plotting the area under the ATP peak observed at 4 min. A linear correlation was observed (Figure 2.9) with a correlation co-efficient R^2 of 0.9944.

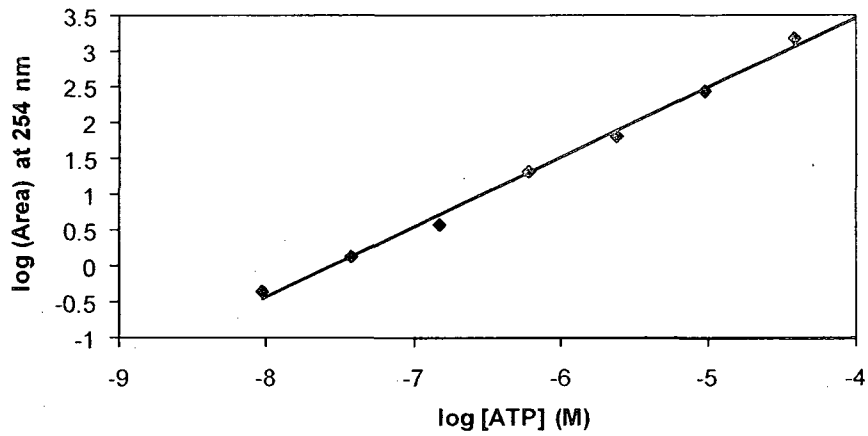

Figure 2.9 HPLC-UV (254 nm) calibration curve for ATP. Plot of peak area at 254 nm vs ATP concentration. Linear correlation with the equation y = 0.977x + 7.388 and correlation coefficient R^2 = 0.994. The y-axis corresponds to the area under the ATP peak at 4 min in the HPLC/UV chromatogram. ATP standards (9.54 nM – 39.1 µM) prepared in 50 mM phosphate buffer (pH 6.0) were injected and eluted from a 100×4.6mm C_{18} column as described in Section 2.2.4.

Chromatographic analysis of the extracellular medium revealed the ribonucleotide profile. The detected levels of adenosine monophosphate (AMP) were ~18-fold higher than those of ATP (~0.3 µM) (Figure 2.10). Coolen *et al.* reported that the ribonucleotide profile depends on the anticoagulant used in the blood-collection tubes. Overall, lower levels of ATP are detected when blood is collected in Li-heparin compared with EDTA-coated tubes. EDTA chelates Ca^{2+} which inactivates ATP-degrading enzymes (106). Therefore, there is a slower rate of ribonucleotide degradation in EDTA vs Li-heparin-coated tubes (104, 106).

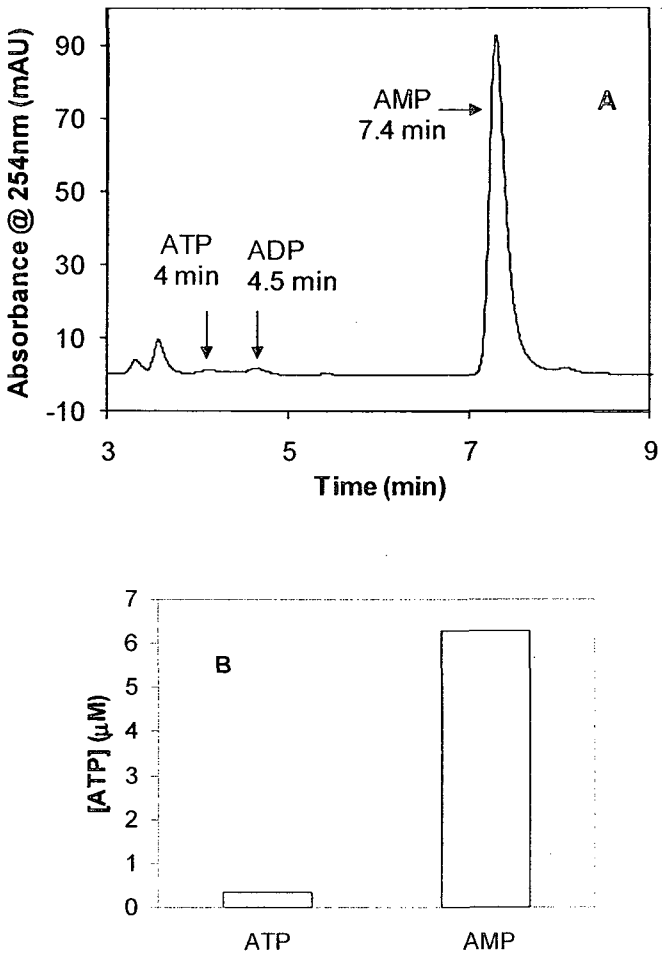

Figure 2.10 HPLC-UV (254 nm) analysis of extracellular RBC-derived ribonucleotides. (A) Chromatographic profile of RBC-derived ribonucleotides from blood drawn in heparinized tubes. **(B)** AMP levels (~6 μM) are ~18-times higher than ATP levels (0.3 μM). RBCs prepared as described in Section 2.2.2, were resuspended at 10% Hct in sucrose buffer at 4 °C for 2 h, 200 μL of supernatant was concentrated to 50 μL using a 10-kDa cut-off ultrafiltration membrane and a 1:4 dilution of the ultrafiltrate in 50 mM phosphate buffer (pH 6.0) was injected and eluted from a 100×4.6mm C_{18} column as described in Section 2.2.4. Peaks at 3.5 and 3.7 min in **(A)** were not identified.

The ribonucleotide profiles examined here from blood collected in Li-heparin and EDTA-coated tubes showed no marked difference in AMP/ATP ratio (Figure 2.11).

However, Coolen *et al.* also reported that ATP is largely converted to AMP in RBCs within 30 min of blood collection (104), consistent with the results in Figure 2.11.

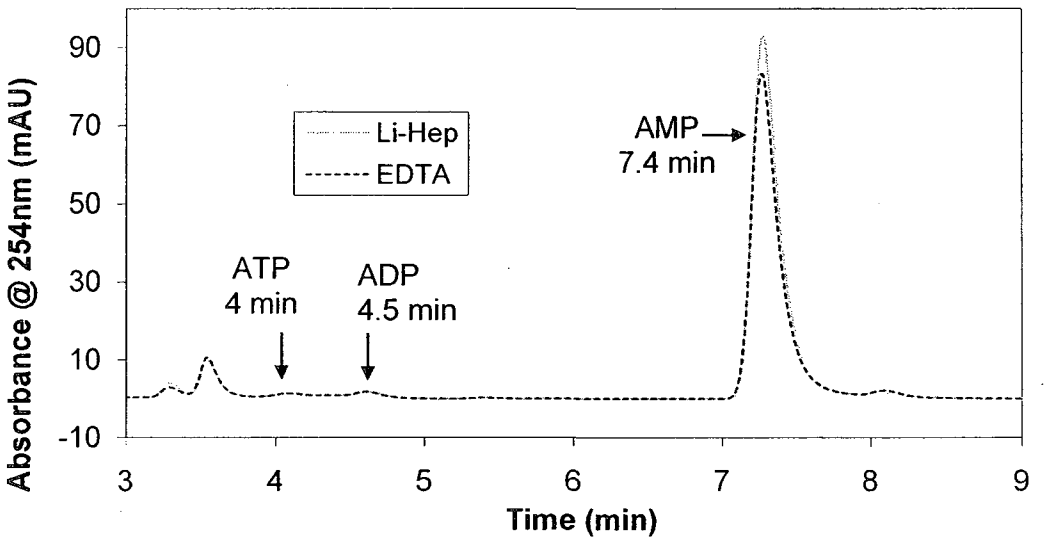

Figure 2.11 HPLC-UV (254 nm) analysis of extracellular RBC-derived ribonucleotides from blood collected in Li-Heparin and EDTA-coated tubes. RBCs were treated as described in the legend of Figure 2.10. The extracellular medium was examined 2 h after blood collection. This experiment was carried out only once.

ATP is converted to AMP *via* different mechanisms. Under physiological conditions, ATP is directly converted to AMP *via* ecto-nucleotide pyrophosphatase/ phosphodiesterase (E-NPP) and, to a lesser extent, ecto-nucleoside triphosphate diphosphohydrolase-1 (E-NTPDase-1) (Figure 2.12). These are ubiquitous enzymes found in RBCs (107, 108) and a variety of tissues in mammals, including brain (109), glial (110) and hepatic cells (111). Some soluble ecto-nucleotidases can also be found in plasma (108).

2.4 Conclusions

A chemiluminescent assay to measure extracellular ATP in RBC suspensions at low Hct was developed. Suitable RBC and luciferin-luciferase concentrations were established to obtain high instrument response without signal saturation. This method could be extended to the analysis of pharmacologically treated RBCs in order to determine the effects of drugs on the release of ATP or other chemical signals arising from these cells.

The HPLC-UV method presented revealed that AMP is the major extracellular ribonucleotide detected in RBC suspensions. It is hypothesized that the ATP released from hypoxic RBCs is rapidly metabolized to AMP by the enzymes shown in Figure 2.12. Hence the release of AMP from RBCs should also be evaluated. The HPLC approach used here for the detection of ribonucleotides could be employed to study the role of nucleases in the regulation of ATP levels in blood and plasma.

3. Effects of nitroglycerin and nitrite on ATP release from human red blood cells

3.1 Introduction

Recent research has considerably modified our understanding of the relative importance of central versus local regulation of blood flow. There is now compelling evidence that the endothelium plays an active role in the regulation of the microcirculation (9, 29, 34, 112). Importantly, in endothelial-mediated vasodilation is the formation and release of NO, which is also known as EDRF (endothelium-derived relaxing factor) (113, 114). Stimulation with adenosine triphosphate (ATP) released from red blood cells (RBCs) (115), and other regulators (116) results in increased NO production and release from endothelial cells. NO uptake by adjacent smooth muscle cells leads to relaxation *via* the well-documented NO/cGMP pathway (117, 118), and the outcome is enhanced blood flow.

Increased muscle metabolism, as occurs during exercise, triggers "ascending vasodilation" to augment blood flow to the active muscles (115). The capillaries, arterioles, and venules contribute to the enhanced blood flow in a coordinated manner but mechanisms by which the vasodilatory signal is propagated remains to be fully elucidated (3, 119). O_2 gradients are the principal regulators of blood flow in the microvasculature (3-6). Decreases in blood O_2 content result in increases in blood flow and *vice versa* (120). Thus, signal transduction pathways that induce vasodilation must exist between

tissues and the microvasculature. As stated recently by Singel and Stamler, "...a general principle of physiology holds that cells precisely regulate their primary function. For RBCs this primary function is the delivery of O_2 to tissues" (120). Since O_2 delivery is determined primarily by blood flow rather than by O_2 saturation of hemoglobin (120, 121), RBCs should be capable of triggering blood vessel dilation to regulate blood flow. The current consensus view is that this involves O_2^- and hemoglobin-linked NO production and release from RBCs (21, 122, 123). While mechanisms of NO production inside RBCs, such as the nitrite reductase activity of deoxyhemoglobin, have been well documented (20, 124, 125), there are conflicting theories as to the mechanism by which NO or an NO-derived vasodilator is released into the circulation (11, 123, 126, 127). In fact, to the best of our knowledge, the efflux of NO (or any NO_X) from RBCs has not been demonstrated *in vivo* or *in vitro* whereas NO (or EDRF) release from the endothelium has been convincingly demonstrated by a number of groups (112, 113, 128-130).

In contrast to the lack of evidence for NO release, ATP export from RBCs as a response to stimuli including hypoxia, structural deformation, and chemical agonists has been widely documented (7, 8). Moreover, the generation of NO in the endothelium is stimulated by RBC-derived ATP (9, 43). The vasodilatory power of NO is exploited pharmacologically in the treatment of cardiovascular diseases, such as *angina pectoris*, since nitro drugs including nitroglycerin are believed to act *via* the production of NO *in vivo* (50). The mechanism of nitroglycerin bioactivation has been a matter of much debate (54, 58, 61, 63, 70, 73, 131) but the current view is that this anti-anginal and anti-ischemic prodrug is reduced by thiols to release NO_2^- (77, 132), which is considered to be

an important store of NO vasoactivity in blood and tissues (133) Since nitroglycerin is rapidly taken up by RBCs in whole blood (52, 134), we speculated as to its effects on ATP release from these cells. In this work, we report our findings following the exposure of freshly isolated human RBCs to pharmacological concentrations of nitroglycerin and physiological NO_2^- concentrations. Our results reveal that nitroglycerin-derived NO_2^- promotes ATP release from RBCs thereby contributing to the therapeutic efficacy of the drug. Furthermore, since NO is generated by the nitrite reductase activity of deoxyhemoglobin (20, 125),

$$\mathbf{NO_2^- + 2deoxyHb + 2H^+ \rightarrow HbFe^{II}NO + metHb + H_2O} \qquad \mathbf{(3.1)}$$

we propose that enhanced NO production in RBCs leads to changes that stimulates ATP export, and that the nucleotide is a mediator of NO vasoactivity. Our findings constitute the first report of vasodilator release from RBCs following stimulation by an endogenous NO donor (NO_2^-) as well as the seminal observation that nitroglycerin modulates levels of an endogenous vasodilator (ATP). The far-reaching implications of ATP involvement in the transduction of the NO signal between RBCs and the endothelium are discussed.

3.2 Materials and methods

3.2.1 Materials

Blood collections were done in 4-mL Vacutainer® heparinized tubes (BD, Franklin Lakes, NJ). KCl, $MgCl_2$, Fisherbrand 3.0 mL disposable cuvets and ethanol were purchased from Fisher Scientific (Pittsburgh, PA). $CaCl_2$ and $MgSO_4$ were purchased from ACP Chemicals (Montreal, QC). NaCl, tris(hydroxymethyl)aminomethane and dextrose were purchased from Bioshop (Burlington, ON). Sucrose was purchased from Anachemia (Lachine, QC). Bovine serum albumin, ATP, firefly lantern extract, HEPES, EGTA, $NaNO_2$ and propylene glycol were purchased from Sigma-Aldrich (St. Louis, MO). Distilled water was purified in a Milli-Q Simplicity 185, Millipore (Billerica, MA). White 96-well plates were purchased from Corning (Corning, NY). Nitrogen gas was purchased from Praxair (Danbury, CT). Nitroglycerin as Nitroject® was purchased from Omega Ltd. (Montreal, QC). Physiological salt solution (PSS) at pH 7.4 was prepared from (in mM): 4.7 KCl, 2 $CaCl_2$, 1.2 $MgSO_4$, 140.5 NaCl, 21 tris(hydroxymethyl)aminomethane, 11 dextrose with 0.5% *w/v* bovine serum albumin); and sucrose buffer at pH 7.4 from (in mM): 321 sucrose, 32 HEPES, 3 EGTA, 6 $MgCl_2$). The buffer pHs were adjusted to 7.4 by adding aqueous solution of sodium hydroxide (NaOH) or hydrochloric acid (HCl).

3.2.2 Preparation of red blood cells

All procedures involving the collection of human blood samples were in accordance with the Concordia University Ethics Guidelines. After their informed written consent was obtained, blood was collected from healthy female volunteers (aged between 20-35 years) by venipuncture into the heparinized tubes. Within 2-4 h of collection, the blood was centrifuged at 5000 rpm at 4 °C for 10 min. The plasma was collected by aspiration and stored at -80 °C. The buffy coat was also collected by aspiration and discarded. Packed RBCs were resuspended and washed three times in PSS.

3.2.3 Measurement of ATP

From a stock solution of 2.5 mM ATP in PSS, ATP standards ranging from 10 nM to 40 μM ATP were prepared in PSS. The luciferin-luciferase assay solution used to measure ATP by chemiluminescence was prepared by dissolving 13.3 mg of crushed firefly extract in 10.0 mL of Milli-Q water. Chemiluminescence proportional to the ATP in the sample was measured using a Wallac $Victor_2$ 1420 multilabel plate reader (PerkinElmer, Waltham, MA). Background emission of 100 μL of the luciferin-luciferase assay solution in a white 96-well plate was recorded, and immediately after 100 μL of each ATP standard was added and the chemiluminescence intensity was measured. Following background correction, double log plots of intensity I vs [ATP] yielded a linear standard curve over 10 nM- 40 μM. To measure sample ATP levels, 100 μL of

RBCs at different Hct values were added to 100 μL of the blanked luciferin-luciferase assay solution, the light intensity was recorded, and ATP concentrations were determined using the ATP standard curve. To prepare anoxic RBCs, a 1.5-mL solution of cells at 1% Hct was sealed in a 5-mL vial with a crimpable aluminum seal. Nitrogen gas was bubbled over the surface of the solution at 5 psi for 15 min, and the ATP concentration of a 100 μL aliquot of the hypoxic RBCs was measured as described above.

3.2.4 Exposure of RBCs to nitroglycerin

From a commercial stock solution of 5 mg/mL (22 mM) nitroglycerin, 100 μL dilutions (0.05 – 2.0 mM) were prepared in 5% *w/v* aqueous dextrose (278 mM D-glucose). Packed RBCs (20 μL) were mixed with 20 μL of each nitroglycerin dilution and 260 μL of sucrose buffer. RBCs at 7% Hct where incubated at 37 °C for 1 h in a water bath without shaking, centrifuged at 5000 rpm at room temperature for 45 s, the supernatants were removed, RBCs at 1% Hct were suspended in PSS, 100 μL were mixed with 100 μL of luciferin-luciferase assay solution and concentrations of extracellular ATP were measured as described in Section 3.2.3. A control sample prepared with 20 μL drug vehicle only (30% v/v ethanol, 30% v/v propylene glycol and 40% v/v water) was treated and analyzed in the same manner.

To probe the effects of preincubation time on ATP release, packed RBCs were diluted to 2% Hct in sucrose buffer containing 10 μM nitroglycerin at 37 °C. Aliquots of 1 mL were removed from the mixture over 0–60 min, immediately centrifuged at 5,000

rpm at room temperature for 45 s, the supernatants were removed, solutions at 1% Hct were prepared in PSS, and concentrations of extracellular ATP were measured as described above.

3.2.5 Exposure of RBCs to nitrite

$NaNO_2$ stock solutions (0.5, 2.5, 5.0, 10.0, 25.0 and 50.0 μM) were prepared in 5% *w/v* aqueous dextrose (278 mM D-glucose). Packed RBCs (20 μL) were mixed with 260 μL of sucrose buffer and with 20 μL of each stock $NaNO_2$ solutions, leading to the following nitrite concentrations (nM) during the incubation: 33, 167, 333, 667, 1667, 3333. The samples were treated and analyzed as described in Section 3.2.3. The effects of incubation time on extracellular ATP were also examined by incubating 200 μL of packed RBCs with 200 μL of $NaNO_2$ (final concentration of 2% Hct and 100 nM $NaNO_2$) in 9.6 mL of sucrose buffer at 37 °C. Aliquots of 1 mL were removed over 0–60 min, centrifuged, and analyzed for ATP release as described in Section 3.2.3.

3.2.6 Statistical methods

Statistical significance between experimental runs was determined with Student's *t*-test. P values ≤ 0.05 were considered statistically significant. Results are reported as ± SEM.

3.3 Results

3.3.1 Hypoxia-induced release of ATP

To validate our method, the well-documented increases in ATP release from RBCs in response to hypoxia (37, 135) was first examined. Prior exposure of RBCs to N_2 for 15 min increased the extracellular ATP concentration by 1.6-fold compared to RBCs maintained in vials exposed to air (Figure 3.1). This increase in ATP under anoxic conditions is less than that observed by Faris and coworkers (37), but they measured prompt changes in ATP within 15 min of exposure to N_2. Figure 3.2A shows the variation in ATP release from RBCs from six healthy, age-matched, volunteers. An average ATP increase of 13±4 nM was observed, where the error reflects both biological and assay variability. Interestingly, volunteers #3–5, whose RBCs released higher concentrations of ATP, were also actively involved in exercise training. Measurements on the blood from volunteer #1 at 4 h and 26 h after collection revealed that the amount of ATP exported decreases as cells age, which may reflect a decrease in total RBC ATP with time following blood collection (136).

The average extracellular ATP reported in the present work (26±4 nM) can be compared with the data reported by Meyer *et al.* (105), who measured extracellular ATP from cells at 7% Hct. When normalized to 1% Hct, the equivalent of 37±8 nM extracellular ATP was reported (n=7), which is comparable to our average value (n = 6). This agreement is noteworthy given that our experimental approaches are different:

Meyer *et al.* (105) used a flow-through set up containing 7% Hct whereas our measurements were made following mixing 100 µL of cells at 1% Hct with 100 µL of luciferin-luciferase assay solution in a static plate-reader as outlined in Section 3.2.2. Furthermore, the breakdown of released ATP by ATPases renders the assay time sensitive (Section 2.4.4). We, like previous workers in the field (37, 103), used heparin-containing tubes. Although less ATP breakdown should occur in EDTA tubes due to Ca^{2+} chelation, which inactivates ATPases (104), no difference was noted here using the experimental procedure outlined in Figure 2.11.

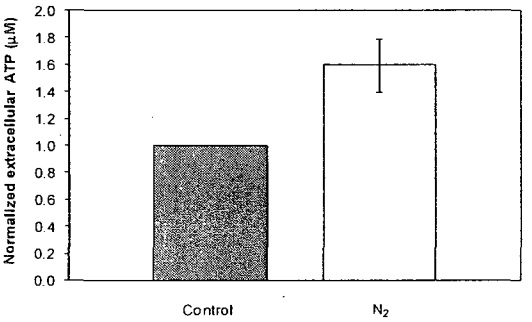

Figure 3.1 Hypoxia-induced ATP release from fresh human RBCs. Cells from the venous blood of four healthy volunteers were treated as described in Section 3.2.2. The extracellular ATP from the RBCs at 1% Hct in PSS from cells stored in a vial at 22 °C under air (control, filled bar) and under nitrogen for 15 min (N_2, open bar). The ATP concentration was determined in triplicate by a luciferin-luciferase chemiluminescence assay at 2 h after blood collection. The error bars represent the standard error of the mean (±SEM), which reflects the variation in ATP release from the RBCs of the four volunteers as well the assay variability.

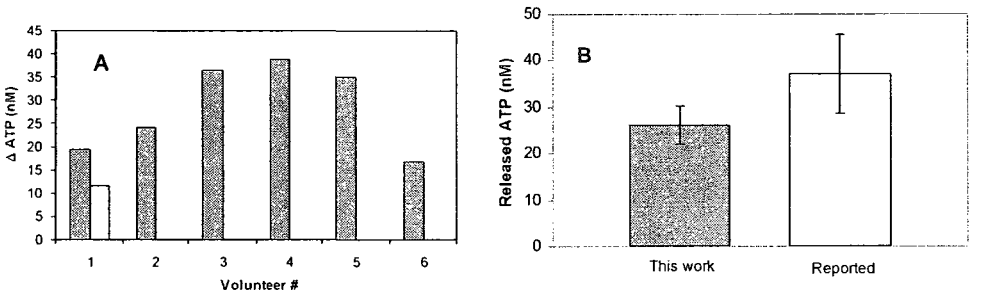

Figure 3.2 Hypoxia-induced increase in extracellular ATP. (A) ATP in PSS containing fresh human RBCs from the venous blood of six volunteers was measured as described in the legend of Figure 3.1 at 4 h (filled bar) or 26 h (open bar) following blood collection. (B) Comparison of average values for ATP release from (A) and those reported from cells in PSS at room temperature by Meyer *et al.* (105).

3.3.2 Effects of preincubation with nitroglycerin at various concentrations on extracellular ATP

Fresh RBCs from venous blood were first incubated with varying concentrations of nitroglycerin. As Figure 3.3A shows, 60-min preincubation of cells with nitroglycerin inhibits ATP release in a dose-dependent manner. The extracellular ATP concentration is reduced by 35% and 42% in the presence of 33 μM and 133 μM nitroglycerin, respectively. Since nitroglycerin is metabolized to nitrite, RBCs were exposed to 3.3-133 μM $NaNO_2$ but a foul odor was detected and immediate and dramatic darkening of the cells was observed. The latter is likely due to extensive formation of methemoglobin, which is dark brown in color (137), *via* two pathways: Reaction 3.1 and the scavenging of the NO produced by oxyhemoglobin to generate nitrate (NO_3^-) as well as methemoglobin. Clearly, the slow release of NO_2^- is critical in the therapeutic efficacy of

the drug. Considering that physiological NO_2^- levels are in the nanomolar to low micromolar range (138), we next investigated the effects preincubation with of 33-3333 nM $NaNO_2$ on ATP release from RBCs. As Figure 3.3B reveals, this lower level of NO_2^- results in extracellular ATP levels similar to those seen at the higher nitroglycerin concentrations; for example, 60 min after exposure to 167 nM and 667 nM NO_2^-, the extracellular ATP concentration dropped by 18% and 36%, respectively. We attribute the comparable efficacy of nanomolar NO_2^- and micromolar nitroglycerin as inhibitors of ATP release to the relatively slow metabolism of the prodrug. Assuming that NO_2^- (or NO derived from NO_2^-) is the effective inhibitor of ATP release, then only ~0.5% of nitroglycerin is metabolized to NO_2^- within the RBC over 60 min since a 80-fold lower NO_2^- concentration produces a similar effect as nitroglycerin (e.g., 133 μM nitroglycerin vs. 1667 nM NO_2^- attenuates ATP levels by ~50% whereas 6.7 μM nitroglycerin vs. 167 nM NO_2^- cause ~20% attenuation, Figure 3.3). The effects of both nitroglycerin and NO_2^- also appear to be saturateable (Figure 3.3), which combined with their similar attention of ATP release, suggest that NO_2^- (or NO) may actually contribute to "nitrate tolerance" as discussed below. Extracellular ATP was measured here immediately following transfer of cells from the preincubates with NO_2^- or nitroglycerin (Sections 3.2.3 and 3.2.4). However, ATP is not expected to accumulate with time in the RBC suspension, due to the action of RBC ATPases (104, 106).

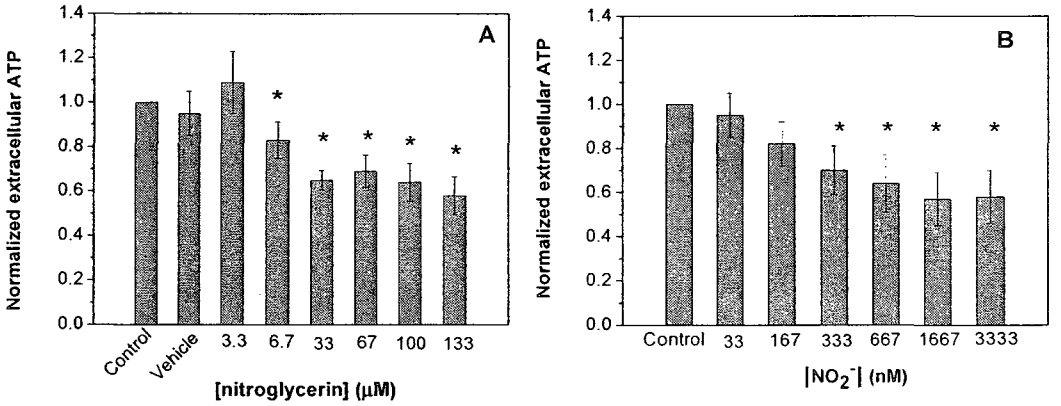

Figure 3.3 Variation in extracellular ATP following 60 min preincubation of intact human RBCs at 7% Hct with nitroglycerin and NO_2^-. Effects of (**A**) nitroglycerin and (**B**) NO_2^- concentrations on the extracellular ATP levels displayed as normalized averages for cells from five (A) and three (b) volunteers where the control values (no stimulant) were normalized to 1.0 for each volunteer. The error bars denote the standard error of the mean (± s.e.m.) and represent assay variability. Approximately 2 h after blood collection, control, vehicle, and sample cells were diluted to 7% Hct in sucrose buffer only (control), in sucrose buffer with 7% v/v drug vehicle (30% v/v ethanol, 30% v/v propylene glycol and 40% v/v water), and in sucrose buffer with stimulant, respectively, and preincubated at 37 °C for 60 min. Following RBCs resuspension at 1% Hct in PSS, and addition of an equal volume of assay solution, the extracellular ATP concentrations were determined by a luciferin-luciferase chemiluminescence assay (see Section 3.2.2). *: *P* values, determined using Student's *t*-test, are given for $P \leq 0.05$

3.3.3 Extracellular ATP vs nitroglycerin and nitrite preincubation time

Since both nitroglycerin (54, 139) and nitrite (122, 134) are known to induce vasodilation within minutes, we next examined release at different times after cells were preincubated with a pharmacologically relevant concentration of the drug. As Figure 3.4A shows, a 150% increase in ATP concentration is observed after 30 s preincubation with 10 μM nitroglycerin. The ATP level stabilized to the control value within 15 min preincubation, and remained at 34% of the control value after 30 and 60 min

preincubation. On exposure to 100 nM $NaNO_2$ (Figure 3.4B) an immediate 100% increase in extracellular ATP concentration was followed by a profile similar to that observed for nitroglycerin (Figure 3.4B). The 30-s or so slower nitroglycerin-induced spike in ATP efflux from RBCs is attributed to the time required for bioactivation of the prodrug by these cells to yield NO_2^-. Bioactivation is obviously not necessary in the case of $NaNO_2$.

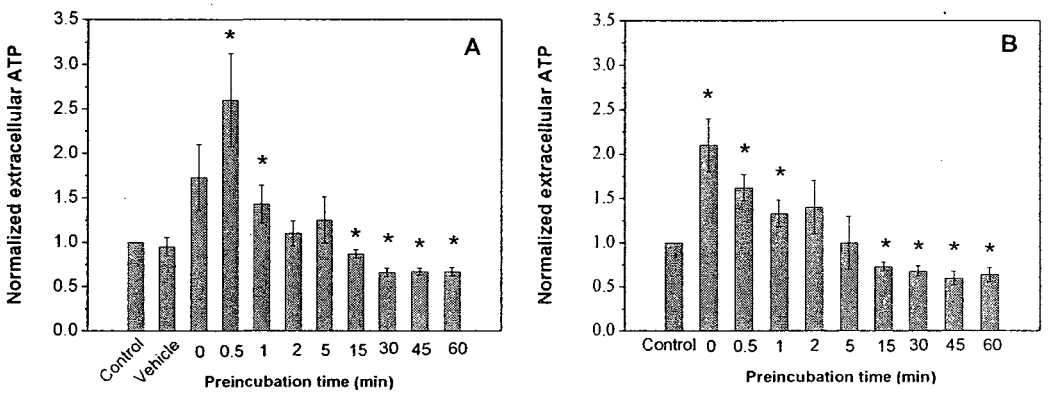

Figure 3.4 Variation in extracellular ATP following 0-60 min preincubation of intact human RBCs at 2% Hct with nitroglycerin and NO_2^-. Preincubation at 37 °C in sucrose buffer containing (**A**) 10 μM nitroglycerin and (**B**) 100 nM $NaNO_2$. Results are displayed as averages (means ± s.e.m.) for cells from five volunteers where the control values (no stimulant) were normalized to 1.0 for each volunteer. See legend of Figure 3.2 for experimental details. *: *P* values, determined using Student's *t*-test, are given for $P \leq 0.05$.

We also investigated whether a spike in ATP release would be observed each time a bolus of nitroglycerin or $NaNO_2$ was added to the cells. Preincubation a second time with 10 μM nitroglycerin of cell previously preincubated for 60 min with nitroglycerin resulted in negligible change in the ATP concentration (data not shown). Likewise, preincubation with 100 nM $NaNO_2$ did not alter the ATP level. The same results were observed for the cells in Figure 3.4B, which were first preincubated with 100 nM $NaNO_2$

rinsed in PSS and then preincubated with $NaNO_2$ or nitroglycerin after 60 min. Since the extracellular ATP levels did not change, the cells appear to have lost their responsiveness to the NO donors, which may contribute to the nitrate tolerance observed in patients on nitrates as discussed further below.

3.4 Discussion

As transducers of tissue ischemia, RBCs play a pivotal role in triggering increased blood flow in the microcirculation (6, 119, 120). In this work, we report that preincubation of freshly isolated human RBCs with pharmacological concentrations of nitroglycerin results in an initial spike in ATP efflux. Within 15 min of preincubation, the amount of extracellular ATP detected from nitroglycerin-exposed cells was the same as that from control cells but dropped to 34% below the control after 30 min (Figure 3.4A). The effects of physiological concentrations of NO_2^- mirror those of nitroglycerin but the ATP spike was within the mixing time (Figure 3.4B). Since NO_2^- is a metabolite of nitroglycerin (3, 58, 73), the combined results in Figure 3.4 indicate that nitroglycerin-derived NO_2^- stimulates ATP release from human RBCs. We propose that this key finding is a contributory factor in the therapeutic effects of nitroglycerin. The prodrug is metabolized by RBCs to provide a controlled release of NO_2^- which stimulates ATP export. This constitutes the *first* report of vasodilator release following RBC stimulation by an endogenous (NO_2^-) or a pharmacological NO donor (nitroglycerin). Since NO_2^- is reduced to NO in RBCs (Reaction 3.1) (122), we further propose that RBC-derived ATP is a regulator of NO-mediated vasoactivity in the circulation.

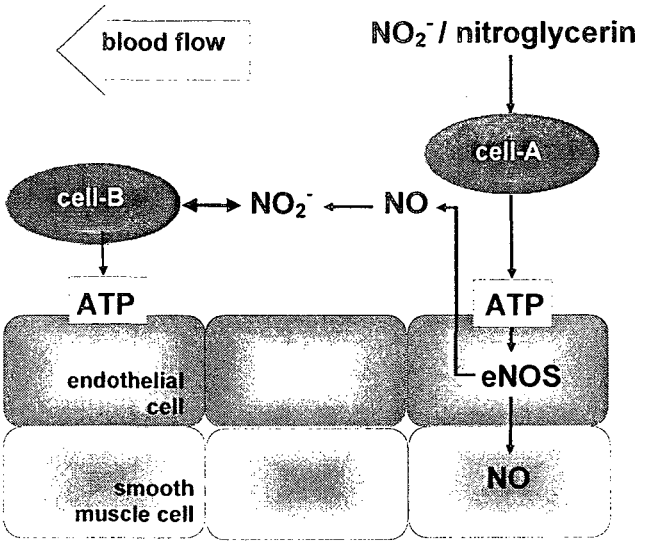

Figure 3.5 Proposed chemical physiology of blood flow regulation by ATP and NO/NO_2^- pathways RBC (cell-A) stimulated by nitroglycerin or its vasoactive metabolite, NO_2^-, causes a rapid increase in ATP efflux. Since NO_2^- is converted to NO within RBCs, the latter may be the direct effector of enhanced ATP release. In an intact blood vessel, ATP will bind to purinergic receptors on the endothelium and stimulate endothelial nitric oxide synthase (eNOS) (140) thereby increasing levels of NO/EDRF that exert relaxation of smooth muscle cells, causing vasodilation. NO also diffuses to the vascular lumen where it is converted to NO_2^- by the action of ceruloplasmin (18), and taken up by downstream RBCs (cell-B), which further increases their ATP production. Thus, the original RBC-derived NO_2^-/NO signal is amplified both by the action of ATP on the endothelium and by the NO/EDRF released into the lumen, which gives rise to a positive feedforward mechanism and propagated vasodilation. The signal is shut-off by attenuating ATP release from RBCs after a certain period of exposure to elevated NO_2^-, suggesting that NO_2^-/NO can also inhibit ATP release.

Our seminal findings and their implications in vasodilation are summarized in Figure 3.5. NO/EDRF released from the endothelium not only diffuses to the vascular smooth muscle cells, but is also released into the vascular lumen where it is converted to NO_2^-, and plasma NO_2^- levels are considered an index of eNOS activity (141). RBCs take up NO_2^-, which may directly, or following its reduction to NO (Reaction 3.1), give rise to a

spike in ATP release by an as yet unknown signaling pathway that may involve the heterotrimeric G protein, G_i (142). Since RBC-derived ATP is an agonist for NO/EDRF production by the endothelium (143), RBC NO_2^- uptake from the lumen and RBC ATP release into the lumen will occur in intact blood vessels. Since RBCs are in transit, downstream cells (B in Figure 3.5) will also be exposed to higher NO_2^- levels, which will serve to propagate a vasodilatory signal.

The model in Figure 3.5 is compatible with the chemical stability of the signaling molecules involved. ATP and NO_2^- are relatively stable species that can survive in the vascular lumen whereas NO reacts readily with O_2 and O_2^- (144, 145). Thus, while NO may endure direct transfer from the endothelium to the adjacent vascular smooth muscle, is it less likely to survive export from RBCs and indirect delivery to smooth muscle cells. Our model not only would ensure that the unstable NO/EDRF message reaches the smooth muscle, it also provides mechanisms for propagated vasodilation: RBC-derived ATP amplifies the vasodilatory signal from the endothelium, and reuptake from the lumen by downstream RBCs of the NO/EDRF-derived NO_2^- (Figure 3.5) would result in a positive forward mechanism.

However, despite its efficiency as an anti-anginal, anti-ischemic prodrug, the vasodilatory response to nitroglycerin diminishes with continuous use, giving rise to nitrate tolerance (146). Many hypotheses have been developed to explain the mechanism by which tolerance is developed, including decreased activation of the NO/cGMP signaling pathway, reduced bioconversion of nitrates to NO, and enhanced production of superoxide anions that destroy NO (50). Here we have shown that there is attenuation in the extracellular ATP released from RBCs preincubated with nitroglycerin or NO_2^- for 30

min or less (Figure 3.5). Also the cells do not respond to a second preincubation with the NO donor. Both NO-donors activate an initial rapid spike in ATP efflux followed by a drop-off (Figure 3.4) and loss of responsiveness. We hypothesize that ATP release is attenuated following exposure of RBCs to relatively high levels of nitroglycerin or NO_2^- *via* a negative feedback mechanism, which would be essential to prevent over dilation of blood vessels. This mechanism is also likely to contribute to nitrate tolerance.

Since NO_2^- is converted within RBCs to NO *via* Reaction 3.1, the data in Figure 3.4 are also consistent with the report that decreased ATP was observed in the medium 20 min after incubation of RBCs with 0.1 mM spermine NONOate, which spontaneously releases NO (147). ATP levels following shorter exposure times to the NO donor were not reported (147), but we speculate that NO may be the causative agent in ATP release and that attenuation of ATP efflux may be due to "NO tolerance". Alternatively, NO is oxidized to NO_2^-, and overstimulation with NO_2^- leads to "NO-tolerance". Regardless of the NO_x involved, the proposed NO_x-induced vasodilation mechanism shown in Figure 3.5 would eventually lead to hypotension. Thus, it is clearly essential for survival that a negative feedback mechanism exist. We suggest that NO_x contributes to this negative feedback on stimulation with high NO_x levels, and that NO_x tolerance may be a more appropriate description for nitrate tolerance.

4. Effects of nitroglycerin on glyceraldehyde-3-phospahate dehydrogenase activity

4.1 Introduction

The role of GAPDH in the bioactivation of nitroglycerin has been introduced previously in Section 1.2.2.6. GAPDH is a tetramer of molecular weight 144,000 Da that plays a key role in glycolysis by catalyzing the NAD-mediated oxidative phosphorylation of glyceraldehydes-3-phsphate to D-1,3-byphosphoglycerate (Figure 4.1) (148). The enzyme consists of four identical noncovalently bonded polypeptide chains (36,000 Da) each accommodating one molecule of NAD^+ as coenzyme (149). The enzyme is used for the determination of D-glyceraldehyde-3-phosphate, NAD^+, inorganic phosphate (Pi), ATP, 1,3-byphosphoglycerate and phosphoglycerate kinase activity (150).

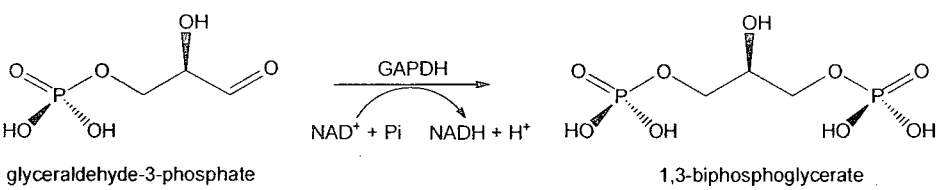

Figure 4.1 Glyceraldehyde-3-phosphate conversion to 1,3-biphosphoglycerate. GAPDH's catalytic role in this reaction is NAD^+ dependent. The absorbance change at 340 nm on NAD^+ reduction to NADH was used in this project for the spectrophotometric determination of GAPDH activity.

In vitro studies in our lab have shown that nitroglycerin, like glyceraldehyde-3-phosphate (G3P), acts as a substrate for the GAPDH (M. Antonic *et al.*, unpublished results). GAPDH catalyzes the reduction of nitroglycerin to 1,2- and 1,3-glycerol dinitrate (GDN) and nitrite (Reaction 4.1). The nitrite produced could be then further reduced in RBCs by deoxyHb to NO (Reaction 3.1). This mechanism represents a possible pathway for nitroglycerin bioactivation in the blood stream, resulting in the desired vasodilatory response induced by nitric oxide.

$$\text{Nitroglycerin} \xrightarrow{\text{GAPDH}} \text{1,2-GDN} + \text{1,3-GDN} + NO_2^- \qquad (4.1)$$

Our previous research also demonstrated that nitroglycerin inhibits GAPDH glycolytic activity. This inhibition would not only affect the bioconversion of nitroglycerin to NO but, since GAPDH plays an important catalytic role in glycolysis, the production of ATP in the RBC would be attenuated. The importance of ATP in vasodilation was discussed in Chapter 3.

Preliminary research in our laboratory with rat RBCs and purified GAPDH from rabbit muscle (R. Kennedy, unpublished data) set the basic parameters for the assessment of GAPDH activity in lysed human RBCs. As shown in Figure 4.2, the glycolytic activity of GAPDH from lysed rat RBCs follows a similar profile to purified GAPDH from rabbit muscle and can be measured using the same experimental protocol.

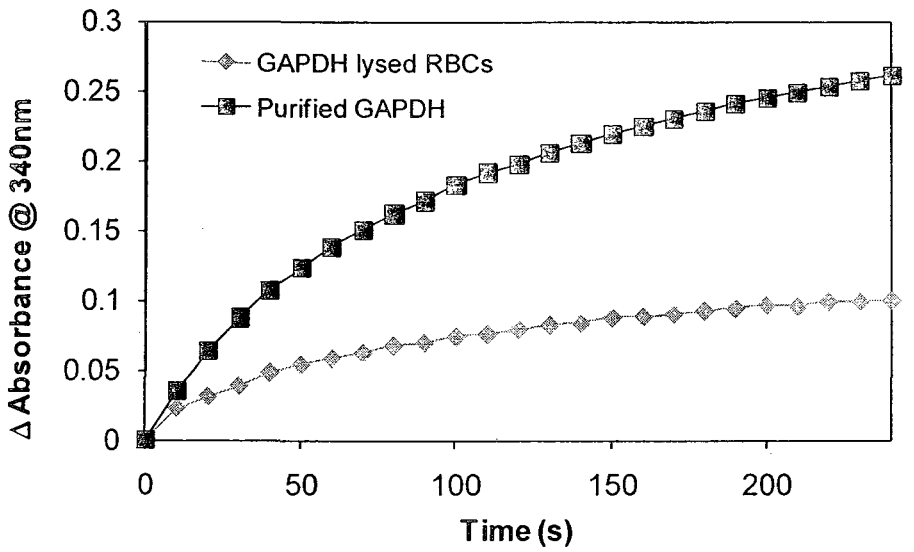

Figure 4.2 Glycolytic activities of purified GAPDH (from rabbit muscle) and GAPDH from RBC lysate. Glycolytic activity of 1 μM GAPDH purified from rabbit muscle and 233 μL of rat RBCs lysate was measured. Assay with purified GAPDH was performed in sodium pyrophosphate buffer adjusted to pH 8.5 at 22 °C. Assay for GAPDH in cell lysate was performed in sucrose buffer adjusted to pH 7.4 at room temperature. In both cases 0.4 M potassium arsenate was used as substrate. Reduction of NAD^+ to NADH was monitored at 340 nm for 4 min using a Beckman DU-650 spectrometer. Absorbance values are adjusted so that $A_0 = 0$ at $t = 0$ s. Adapted from R. Kennedy, unpublished data.

The concentration-dependent effect of nitroglycerin on GAPDH's glycolytic activity was also assessed in previous work. Experimental observations showed that the activity of GAPDH from lysed rat RBCs diminished with increasing concentration of nitroglycerin (Figure 4.3), indicating inactivation of the enzyme in the lysate.

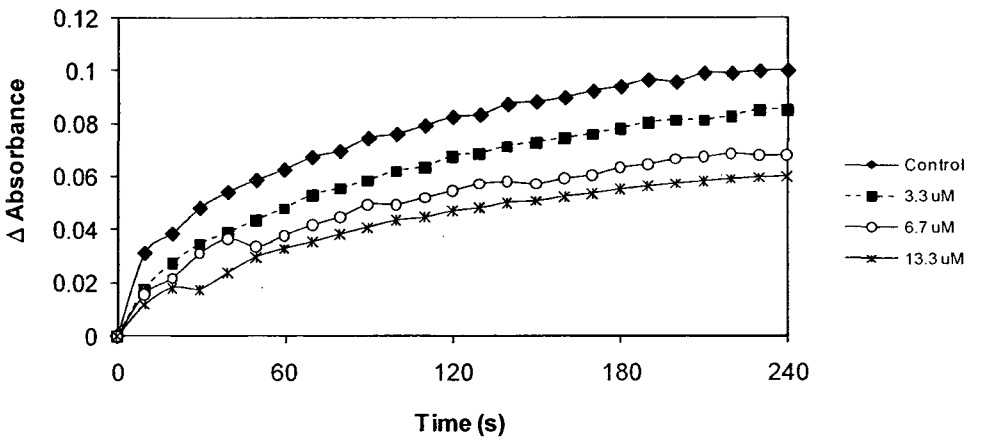

Figure 4.3 Effect of nitroglycerin on the glycolytic activity of GAPDH from rat RBC lysate. Lysed rat RBCs were incubated for 1 h at 37 °C with the nitroglycerin concentrations indicated in the presence of 0.01 M glyceraldehyde-3-phosphate, 0.01 M NAD^+ and 0.4 M potassium arsenate in sucrose buffer at pH 7.4. Reduction of NAD^+ to NADH was monitored at 340 nm for 4 min using a Beckman DU-650 spectrometer. Absorbance values were adjusted so that $A_0 = 0$ at $t = 0$ s. Adapted from R. Kennedy, unpublished data.

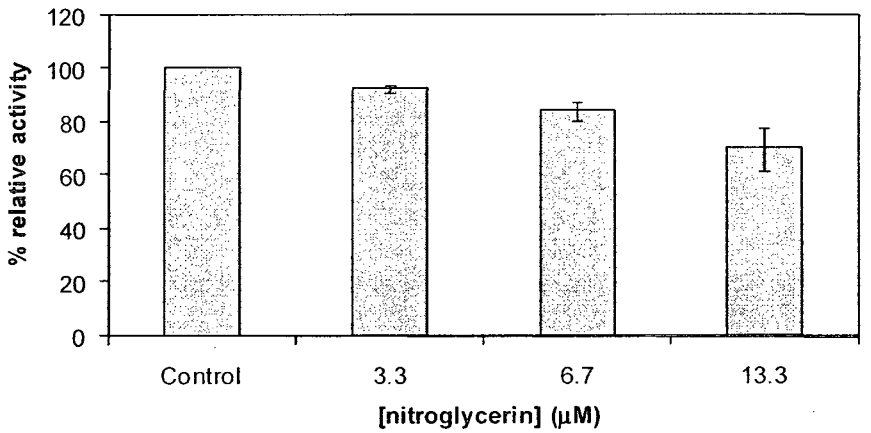

Figure 4.4 Bar graph of the effect of nitroglycerin on the glycolytic activity of GAPDH from rat RBCs. Lysed rat RBCs were incubated for 1 h at 37 °C with the nitroglycerin concentrations indicated in the presence of 0.01 M glyceraldehyde-3-phosphate, 0.01 M NAD^+ and 0.4 M potassium arsenate in sucrose buffer at pH 7.4. Reduction of NAD^+ to NADH was monitored at 340 nm for 4 min using a Beckman DU-650 spectrometer. Activities are given relative to the control (no nitroglycerin) at $t = 0$ s. Adapted from R. Kennedy, unpublished data.

In this chapter the focus is on describing the effects of nitroglycerin on GAPDH glycolytic activity in human RBCs. In order to fulfill these goals, a method based on the role of GAPDH in arsenate reduction (151) was adapted to measure GAPDH activity in intact and lysed RBCs (Figure 4.5). These spectrophotometric assays may help determine the role of erythrocytic GAPDH in nitrate tolerance.

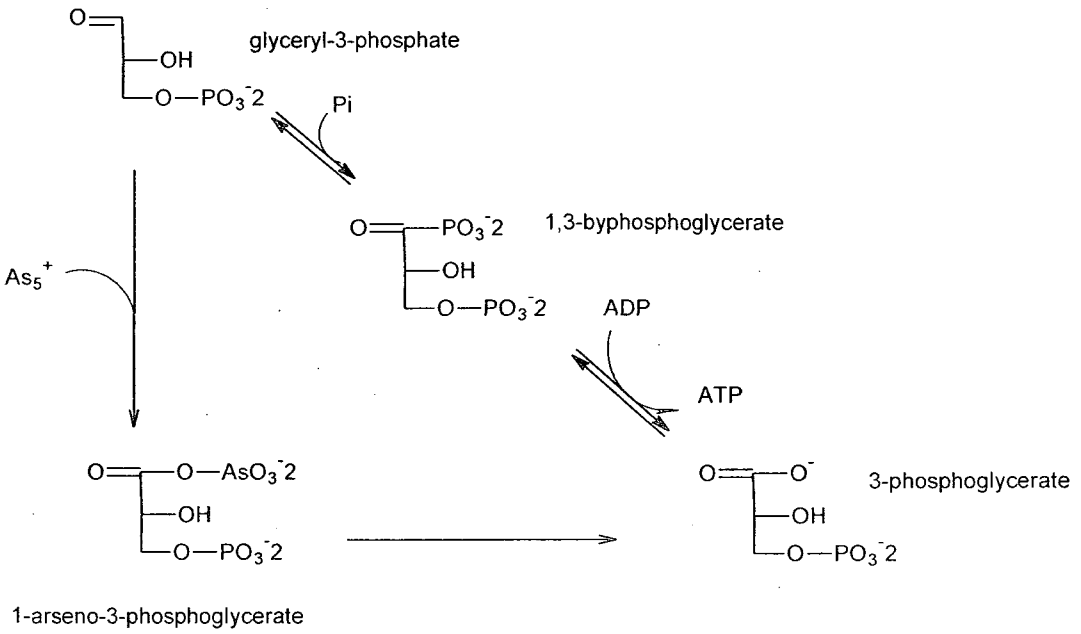

Figure 4.5 Arsenate vs phosphate in the conversion of glyceryl-3-phosphate by GAPDH. For this work potassium arsenate is used instead of inorganic phosphate (Pi) as a GAPDH substrate to inhibit the reverse reaction. As^{5+} has the same oxidation state and shares many chemical properties with inorganic phosphate (P^{5+}) and can substitute for Pi in ATP production. When using arsenate as a substrate, GAPDH produces 1-arseno-3-phosphoglycerate rather than 1,3-bisphosphoglycerate. 1-arseno-3-phosphoglycerate hydrolyzes spontaneously, so that ATP continues to be produced. Adapted from (152).

4.2 Materials and methods

4.2.1 Materials

Distilled water purified in a Milli-Q Simplicity 185, Millipore (Billerica, MA) was used to prepare all aqueous solutions. D,L-glyceraldehyde-3-phosphate, β-nicotinamide adenine dinucleotide, sodium pyrophosphate, potassium arsenate, HEPES, EGTA and bovine serum albumin were purchased from Sigma-Aldrich (St. Louis, MO). $CaCl_2$ and $MgSO_4$ were purchased from ACP Chemicals (Montreal, QC). $MgCl_2$ and KCl were obtained from Fisher Scientific (Pittsburgh, PA). NaCl, tris(hydroxymethyl)aminomethane and dextrose were purchased from Bioshop (Burlington, ON). Sucrose and tris-HCl was purchased from Anachemia (Lachine, QC). Nitrogen gas was purchased from Praxair (Danbury, CT). Nitroglycerin as Nitroject® was purchased from Omega Ltd. (Montreal, QC) and human blood was collectied in 4-mL Vacutainer® heparinized tubes (BD, Franklin Lakes, NJ). All spectral measurements were carried out using an Agilent 8453 UV-Visible diode-array spectrophotometer (Agilent Technologies, Santa Clara, CA).

4.2.2 RBCs incubation with nitroglycerin

Packed RBCs were obtained from human blood following the procedure described in Section 2.2.2. Next, 20 μL of intact RBCs at 7% Hct were preincubated with

an equal volume of nitroglycerin of varying concentration (0 - 6.7 μM) in 260 μL of sucrose buffer (pH 7.4, prepared as described in Section 2.2.1) at 37 °C in a water bath for 1 h. After preincubation, samples were centrifuged at 5,000x*g* at 4 °C for 45 s, the supernatant was removed and discarded, and the packed RBCs were retained for the GAPDH activity assay.

4.2.3 Assay of RBC GAPDH activity

The packed RBCs from Section 4.2.2 were resuspended in 33 volumes of ice-cold sodium saline, centrifuged, and the supernatant was removed. The cells were osmotically lysed at 1% Hct by adding 99 volumes of ice-cold water and sonicating for 5 min. Solids that may interfere with spectrophotometric analysis were removed by centrifugation at 5,000 *g* at 4 °C for 45 s, the supernatant was conserved and the pellet discarded. In a 1.5-mL Fisherbrand disposable cuvette, 700 μL of sucrose buffer, 16.7 μL of 0.01 M NAD^+, 16.7 μL of 0.01 M glyceraldehyde-3-phosphate and 16.7 μL of 0.4 M potassium arsenate were mixed to give the final concentrations listed in Figure 4.6. This solution was incubated at 22 °C for 5 min and then used to blank the spectrophotometer at 340 nm. The assay was initiated by adding 233 μL of RBC lysate (control or incubated with nitroglycerin) and the absorbance increase due to the reduction of NAD^+ to NADH ($\Delta\varepsilon_{340}$ = 6,220 $M^{-1}cm^{-1}$) was recorded every 10 s for 4 min.

4.3 Results

4.3.1 Effect of nitroglycerin on glycolytic activity of GAPDH in human RBC lysates

GAPDH activity in the lysed RBC samples was assessed by spectrophotometrically monitoring NADH production, which directly relates to the activity of the enzyme (Figure 4.1). As seen in Figure 4.1, one mol of NADH is required per mol of substrate turned over by GAPDH.

The inhibitory effect of nitroglycerin on GAPDH from human RBCs was demonstrated using cumulative dose-response curves (Figure 4.6). As can be seen from Figure 4.6B the initial rates of GAPDH glycolytic activity decreased with increases of nitroglycerin concentration.

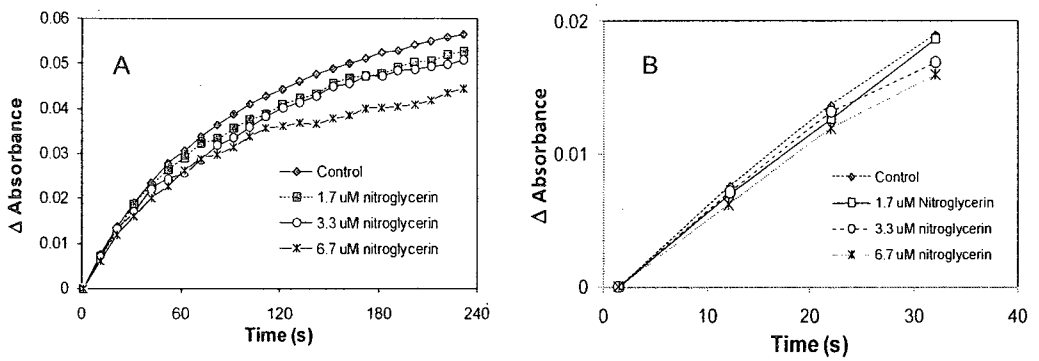

Figure 4.6 Effects of nitroglycerin on glycolytic activity of GAPDH from human RBC lysate. (A) Activity of RBC GAPDH over 240 s. **(B)** Initial rates (0-30 s). Human RBCs at 7% Hct were incubated for 1 h at 37 °C with 0.0 (control), 1.7, 3.3 and 6.7 μM nitroglycerin. RBC lysates were prepared from cells at 1% Hct in the presence of 0.01 mM glyceraldehyde-3-phosphate, 0.01 mM NAD^+ and 0.4 mM potassium arsenate in sucrose buffer at pH 7.4 at 25 °C. Reduction of NAD^+ to NADH was monitored at 340 nm in a 1-cm cuvette and the initial absorbance (due to the presence of Hb in the lysate) was subtracted from each value.

Normalization of the control to 100% activity at 240 s revealed GAPDH activity decreases of 6.4, 10.0, and 21.1% when a lysate of RBCs at 1% Hct was preincubated with 1.7, 3.3, and 6.7 μM nitroglycerin, respectively (Figure 4.7). These values are similar to those found in our lab for rat RBCs lysates (Figure 4.4).

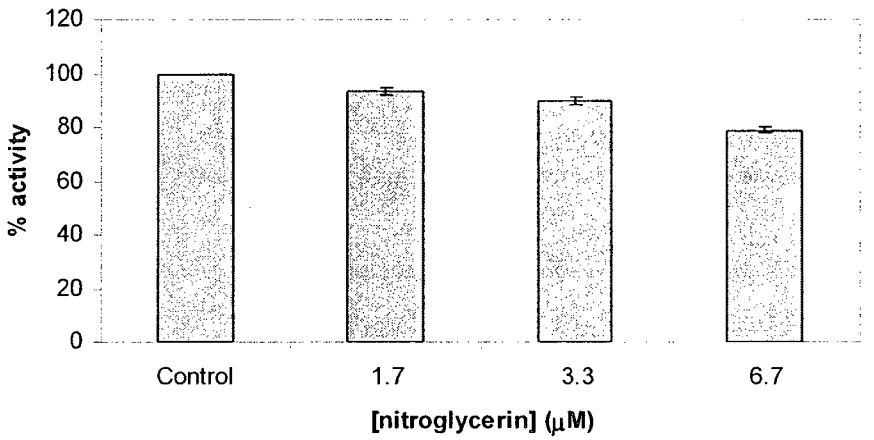

Figure 4.7 Bar graph of the nitroglycerin effect on the glycolytic activity of GAPDH from human RBCs. Activities are given relative to the control (no nitroglycerin) at t = 0 s. The experimental details are given in the legend of Figure 4.6.

4.4 Discussion

Activity assays for nitroglycerin-treated human RBC lysates showed that the drug exerts a concentration-dependent inhibitory effect on GAPDH. This confirms the previous finding in our group (M. Antonic *et al.*, unpublished results) that nitroglycerin is a "suicide substrate" of GAPDH *in vitro*. GAPDH acts as a bioactivator of nitroglycerin by reducing it to nitrite and glyceryl dinitrites using active-site Cys149 and Cys153 as electron donors (Section 1.2.2.6). This results in the formation of a disulfide bond

between the two cysteines, inactivating the enzyme. RBC GAPDH inactivation could contribute to nitrate tolerance. Chronic exposure to nitroglycerin would decrease the amount of active GAPDH in the cells available to activate the drug, thereby blunting the effects of the drug. Compounding this effect would be the reduction in RBC ATP production and possibly a reduction in extracellular ATP as seen in Figures 3.5 and 3.4.

Previous research in our lab has demonstrated that the disulfide bond in GAPDH can be reconverted to free cysteines by tris(2-carboxyethyl)phosphine (TCEP), a disulfide reducing agent (Scheme 4.1), suggesting reversible inactivation of the enzyme *in vivo*. This is also consistent with the evolution of nitrate tolerance. Upon temporary withdrawal from nitroglycerin treatment (e.g., 12-hour "drug holiday") the pharmacological effects of the drug can be experienced again. Reactivation of GAPDH *in vivo* would be carried out by the action of one or more disulfide reductase systems present in cells. These systems would recover the enzymatic activity of GAPDH by reducing the disulfide bond formed between the active-site Cys149 and Cys 153.

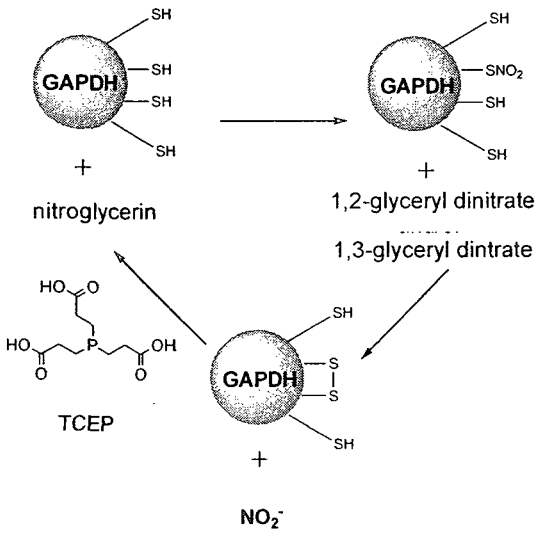

Scheme 4.1 Proposed mechanism of nitroglycerin bioactivation by GAPDH. GAPDH catalyzes the transfer of NO_2 from nitroglycerin to Cys149 at its active site. This transfer is accompanied by the formation of 1,2- and/or 1,3-glyceryl dinitrates. Neighboring Cys153 nucleophilically attacks the thionitrate group forming an intramolecular disulfide bond and releasing NO_2^-. The disulfide bond is reduced to the original free thiol functionalities by the reducing agent TCEP (tris(2-carboxyethyl)phosphine) or another disulfide-reducing system. This mechanism is based on that proposed for ALDH2 in Scheme 1.1 (59).

The study of the vasodilator concentrations in the blood stream could help elucidate the localized mechanisms of blood-flow regulation and the synergism between these chemical messengers. In this chapter, the development of analytical methodology for detection and quantitation of EETs and PGI_2 in human plasma is presented. Specifically, the stability of EETs as well as the optimization of their analysis by mass spectrometry are established and $6KPGF_{1\alpha}$ was confirmed as a stable biomarker for PGI_2.

5.1.1 Epoxyeicostrienoic acids (EETs)

EETs are cytochrome P450 metabolites of arachidonic acid that mediate muscle vasodilation. The most abundant isoforms are 11,12-EET and 14,15-EET, and they are also known to be involved in many metabolic processes including cell proliferation and migration (153). Additionally, it has been suggested that 11,12-EET could be the endothelial-derived hyperpolarization factor (EDHF) (28). EETs exert strong vasodilatory effects in a wide variety of tissues such as brain, intestines (159), kidney (160), heart and coronary arteries (154, 161, 162), and blood vessels (155, 156).

Many methods have been reported for the detection and quantitation of EETs (33, 163, 164). However, only a few methods have been developed for blood plasma since its complexity as a matrix makes the quantitative analysis of EETs challenging. A sequential extraction method for vasodilation-related metabolites in interstitial fluid was developed in our lab (164). Jiang *et al.* showed that detection and quantitation of EETs in plasma

can be performed by ESI-MS/MS (155) and an adaptation of this method is presented here.

5.1.2 Prostacyclin (PGI_2)

PGI_2 is a member of the prostaglandin family. Physiologically classified as hormones, these fatty acid derivates play important roles in vasodilation, coagulation and inflammatory processes (34). Prostaglandins are produced from arachidonic acid by cycloxygenase (COX) enzymatic conversion (Figure 5.2).

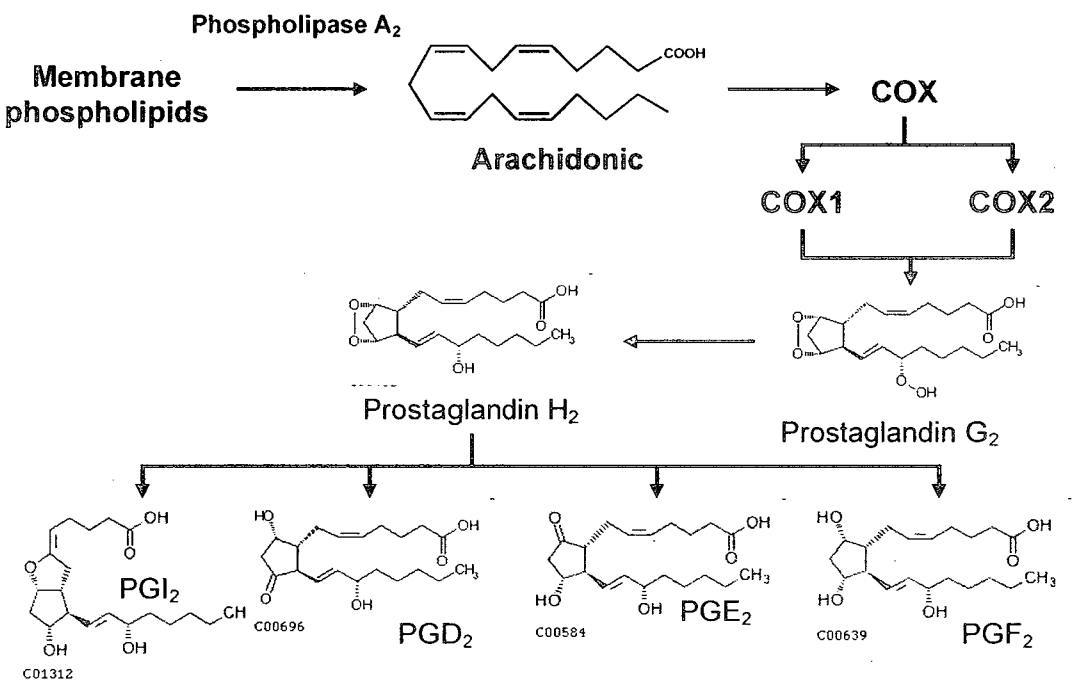

Figure 5.2 Metabolic pathways of prostaglandins production. Membrane phospholipids are converted to arachidonic acid (AA) by phospholipase A_2. AA is a substrate of both isoforms COX and it is converted to Prostaglandin G_2. Dehydroxilation of prostaglandin G_2 generates prostaglandin H_2, the precursor of all functional prostaglandins (PGI_2, PGD_2, PGE_2 and PGF_2). Adapted from (165).

Numerous methodologies have been proposed for the analysis of these substances in complex matrixes. Gelpí *et al.* highlighted the applications of liquid chromatography with radioimmunoassay (HPLC-RIA) for analysis of eicosanoids (166). This methodology involves the inoculation of viable vectors with radio labeled antigens, with the limitations of animal breeding and handling and the special conditions in which radioactive substances have to be manipulated. Daret *et al.* propose the analysis of analyzed monohydroxylated fatty acids and eicosanoids by gas chromatography with a mass spectrometry detector (GC-MS). This methodology involves the derivatization of the fatty acid-like molecules to volatile methyl esters to be suitable for GC analysis (167). Dickinson *et al.* present a very fast and efficient method for the overall study of many arachidonic acid derivates (168). This method was adapted to our research for the detection and quantitation of PGI_2 which posses a short half-life both *in vivo* and *in vitro*, ranging from 30 seconds to a few minutes (169). It is stable in basic buffers ($pH \geq 8$) but is rapidly hydrolyzed through a non-enzymatic mechanism to 6-keto prostaglandin $F_{1\alpha}$ ($6KPGF_{1\alpha}$) in neutral or acidic solutions (Figure 5.3). This inactive and stable end product can be used as a biomarker of PGI_2 (170).

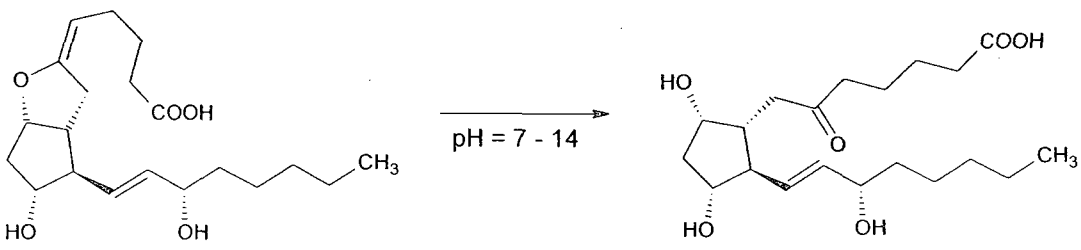

prostaglandin I_2 (PGI_2)

6-keto prostaglandin $F_{1\alpha}$ ($6KPGF_{1\alpha}$)

Figure 5.3 Hydrolysis of prostaglandin I_2 to 6-keto prostaglandin $F_{1\alpha}$. Adapted from (169).

5.2 Materials and methods

5.2.1 Materials

11,12-epoxy-(5*Z*,8*Z*,14*Z*)-eicosatrienoic acid (11,12-EET), 14(*R*),15(*S*)-epoxy-(5*Z*,8*Z*,11*Z*)-eicosatrienoic acid (14,15-EET), triphenylphosphine (TPP), magnesium chloride and bovine serum albumin (BSA) were purchased from Sigma-Aldrich (St. Louis, MO). 6-keto prostaglandin $F_{1\alpha}$ ($6KPGF_{1\alpha}$) and deuterated 6-keto prostaglandin $F_{1\alpha}$ ($D4\text{-}6KPGF_{1\alpha}$) were purchased from Cayman Chemical (Ann Arbor, MI). Potassium chloride, hydrochloric acid and methanol (HPLC grade) were purchased from Fischer Scientific (Pittsburgh, PA). Sodium chloride and D-glucose were obtained from BioShop (Burlington, ON), sodium bicarbonate from Anachemia (Lachine, QC), calcium chloride dihydrate ACP Chemicals (Montreal, QC), chloroform (HPLC grade) from JT Baker (Phillipsburg, NJ), and acetonitrile (HPLC grade) from EMD Chemicals (Gibbstown, NJ). Distilled water was purified in a Milli-Q Simplicity 185 and Ultrafree®-0.5 centrifugal filter Units, 10-kDa cut-off ultrafiltration membranes were purchased from Millipore (Billerica, MA). Bondpack C_{18}, 100 mg C_{18} cartridges were obtained from Agilent Technologies (Santa Clara, CA). Nitrogen gas was purchased from Praxair (Danbury, CT).

5.2.2 Preparation of EET standards

Solutions of 0.5 µM EETs were prepared in four different solvents (100% ACN, ACN/H_2O (1:1), 100% MeOH and 100% H_2O) under indirect light and with minimum exposure to air. These stock solutions were maintained at -20 °C at all times during manipulation and stored at -80 °C immediately after use. Transfers were performed in glass gas-tight syringes previously cleaned with ACN and HPLC-grade methanol, and air dried. Dilutions containing 0.25, 0.12, and 0.06 µM EET were prepared in each solvent and aliquoted into 3 batches. The first batch was analyzed on the day of sample preparation. The second and third batches were stored in the dark at -80 °C, and analyzed 24 h and 6 days later.

5.2.3 Preparation of plasma simulator

Tyrode's buffer solution (pH 7.4) was prepared as described in (171). Briefly, an aqueous solution containing 0.13 M NaCl, 5.5 mM glucose, 11 mM $NaHCO_3$, 2.6 mM KCl, 0.5 mM NaH_2PO_4, 2.2 mM $MgCl_2$, and 1.8 mM $CaCl_2 \cdot 2H2O$, and the pH was adjusted to 7.4 with 1 N HCl. A 12% BSA solution was prepared in this buffer and spiked with 0.5 µM 11,12-EET and 0.5 µM 14,15-EET. Where indicated, tridecanoic acid (TA) was added at the same concentration as the internal standard.

5.2.4 EET extraction

EETs were extracted from the plasma simulator as described in (164). Briefly, Millipore ultrafiltration tubes with a 10-kDa cutoff membrane were prewashed twice with 400 µL of water and centrifuged 12,000 rpm for 10 min to remove traces of nitrate. Then, 400 µL of the plasma simulator was loaded into the preconditioned ultrafiltration tube and centrifuged at 12,000 rpm for 20 min to remove BSA. The ultrafiltrate was collected and loaded into a Bondpack C18 cartridge preconditioned with 2 mL of methanol followed by 4 mL of water. EETs were extracted with 1 mL of $CHCl_3/CH_3OH$ (2:1) containing 0.1 mM TPP to quench any free-radical-induced lipid peroxidation (172). The sample was evaporated to dryness under a stream of nitrogen at atmospheric pressure, and the EETs were reconstituted in 300 µL of the solvent of choice.

5.2.5 ESI-MS/MS analysis of EETs

EET analysis was carried out using a Micromass Quattro LC triple quadrupole mass spectrometer equipped with ESI source run by MassLynx software (Water Corp. Milford, MA). ESI-MS was carried out in negative-ion mode by direct infusion at a flow rate of 10 µL/min. A capillary voltage of -3.0 kV, a cone voltage of -40 V, a source block temperature of 90 °C, a nebulizer gas flow of 30 L/h and a desolvation gas flow of 220 L/h were maintained during all analysis. For samples in 100% H_2O a desolvation temperature of 200 °C was used, and for samples in 100% ACN, 100% MeOH and

ACN/H_2O (1:1), the desolvation temperature was set at 150 °C. Mass spectra in MS mode were scanned over the m/z range of 100-500 at a rate of 2 s/scan. In the MS/MS experiments, the deprotonated molecular ions $[M-H]^-$ of the EETs (m/z 319) were selected and fragmented by CID using N_2 gas and a collision energy range between 30 and 50%.

5.2.6 ESI-MS/MS analysis of 6KPGF$_{1\alpha}$

6KPGF$_{1\alpha}$ analysis was carried out as described in (168). Briefly, ESI-MS was performed in negative-ion mode by direct infusion at 10 µL/min into the Quattro LC triple quadrupole mass spectrometer. A capillary voltage of -3.0 kV, a cone voltage of -60 V, a source block temperature of 90 °C, a nebulizer gas flow of 33 L/h, a desolvation gas flow of 253 L/h and a desolvation temperature of 150 °C were maintained during all analysis. In MS mode, spectra were scanned over the m/z range 50-400 at a rate of 2 s/scan. In MS/MS mode, the deprotonated molecular ion $[M-H]^-$ of 6KPGF$_{1\alpha}$ (m/z 369) was selected and fragmented by CID using N_2 gas with a collision energy range between 40 and 60%. Samples were prepared in 10 mM triethylamine:methanol (1:1). A calibration curve was prepared using 6KPGF$_{1\alpha}$ standard solutions ranging from 11 nM to 475 nM.

5.3 Results

5.3.1 ESI-MS and ESI-MS/MS analysis of EETs

EETs were studied by ESI-MS in negative-ion mode by direct infusion into the mass spectrometer. Both 11,12- and 14,15-EET exhibit the same $[M-H]^-$ at m/z 319 (Figure 5.4), but the fragmentation pattern observed by MS/MS was characteristic of each species (Figure 5.4, inserts). A set of common peaks were observed for both molecules at m/z 301, 275 and 257 corresponding to loss of H_2O, CO_2 and both H_2O and CO_2 from the $[M-H]^-$ ion (Figure 5.4) at the optimum collision energy of 40%. In addition, 11,12-EET exhibited fragment ions at m/z 167, 179 and 195. The last two peaks arise from fragmentation *via* opening of the epoxy ring on each side of the oxygen atom. 14,15-EET produced fragments at m/z 113, 205 and 219, with only one fragment related to the opening of the epoxy ring (m/z 219). In an equimolar mixture, the presence of both isomers can be clearly identified by their characteristic fragments (Figure 5.5).

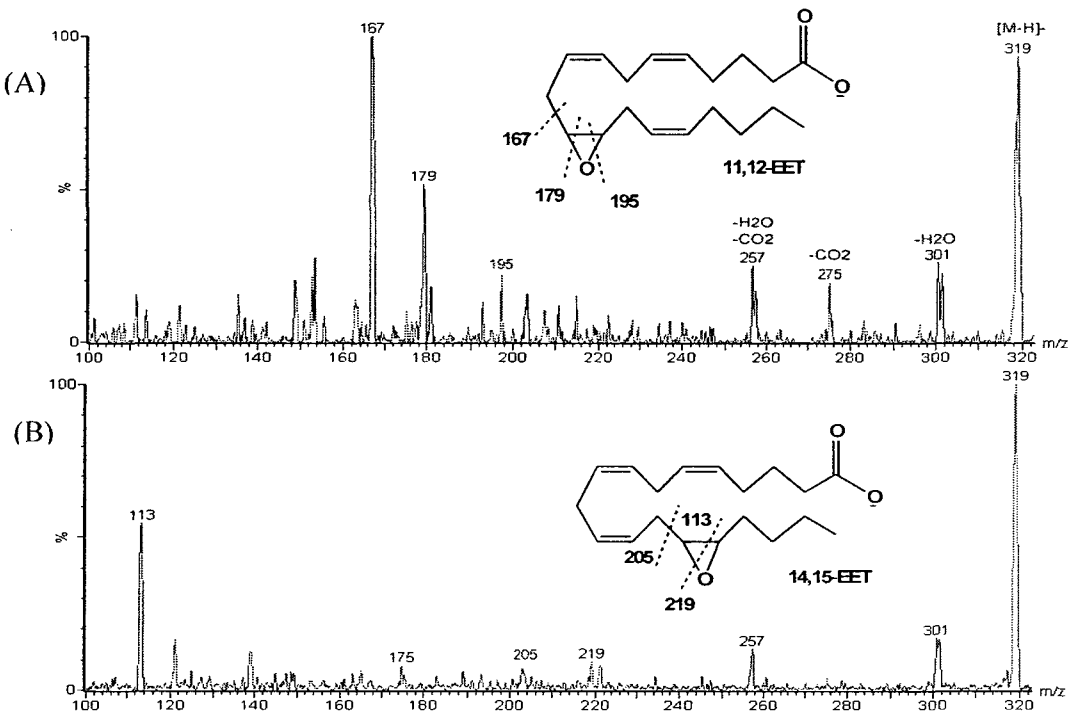

Figure 5.4 Negative-ion ESI tandem mass spectra of EETs. (A) 0.25 μM 11,12-EET, (B) 0.25 μM 14,15-EET. Direct injection at 10 μL/min in ACN. Instrument settings: source block temperature, 90 °C; capillary voltage, -3.0 kV; cone voltage, -40 V, collision gas, N_2, collision energy, 40%. Inserts: fragmentation patterns for 11,12-EET and 14,15-EET.

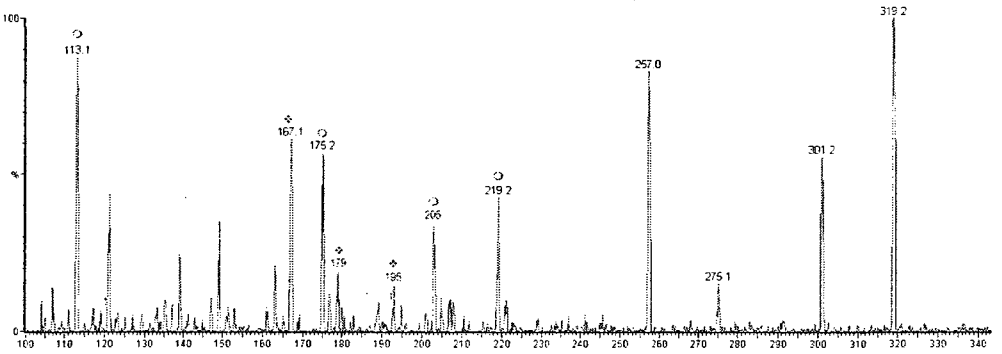

Figure 5.5 Negative-ion ESI tandem mass spectrum of an equimolar EET mixture. Direct injection at 10 μL/min on CAN of a solution of 0.25 μM 11,12-EET and 0.25 μM 14,15-EET was performed. $[M-H]^-$ observed at m/z 319 for both isomers and $[M-H_2O-H]^-$, $[M-CO_2-H]^-$ and $[M-H_2O-CO_2-H]^-$ at m/z 301, 275 and 257, respectively. Peaks labelled O correspond to 14,15-EET fragments, and ❖ correspond to 11,12-EET fragments. Instrument settings: source block temperature, 90 °C; capillary voltage, -3.0 kV; cone voltage, -40 V, collision gas, N_2; collision energy, 40%.

5.3.2 Stability of EETs in different solvents

The effects of solvent and storage on EET stability were assessed. For EET standards prepared in 100% ACN and stored overnight at -80 °C (Figure 5.6), a large decrease in the intensity of the $[M-H]^-$ ion at m/z 319 was observed. New signals not evident in the literature reports (155, 156) appeared at m/z 311, 325, 339, and 343.

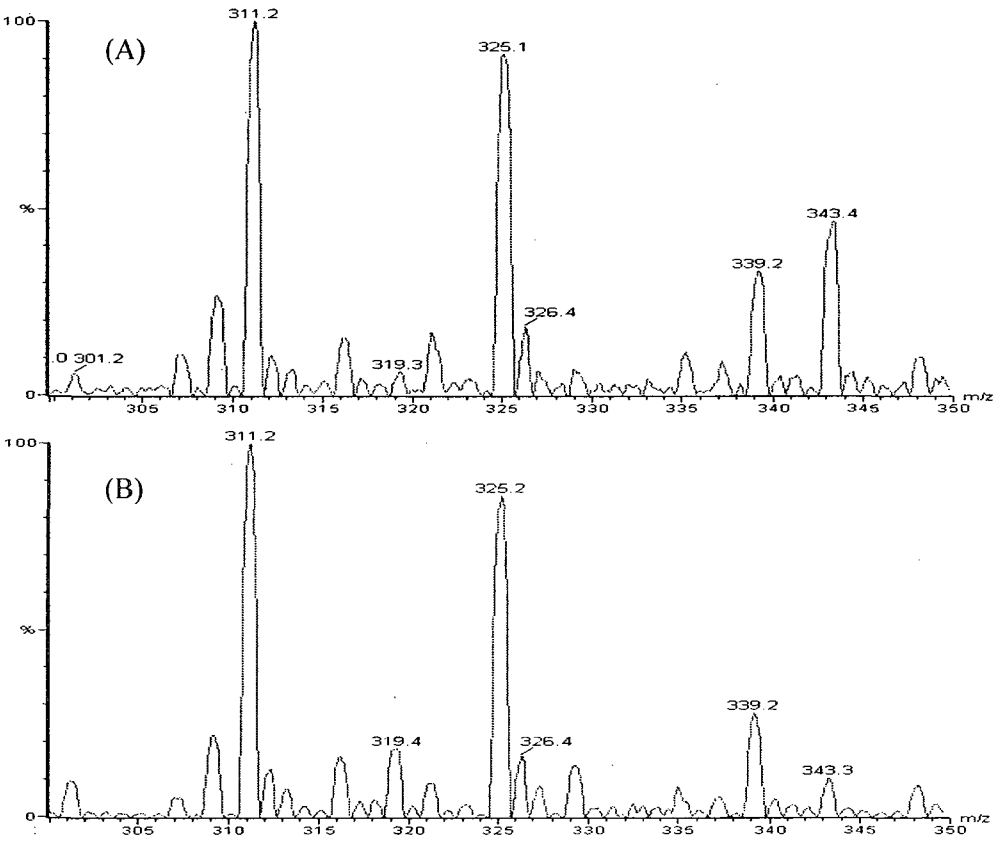

Figure 5.6 Negative-ion ESI mass spectra of EETs in 100% ACN after overnight storage at -80 °C. (A) 11,12-EET and (B) 14,15-EET standards. Direct injection of 0.25 μM EET at 10 μL/min. Instrument settings: source block temperature, 90 °C; capillary voltage, -3.0 kV; cone voltage, -40 V; scan range, 300-350 m/z.

EET standards prepared in ACN:H_2O (1:1) and stored overnight at -80 °C exhibited a strong $[M-H]^-$ peak (Figure 5.7). Weak signals were detected at m/z 311, 312, 316, 320, and 326 with intensities close to the noise.

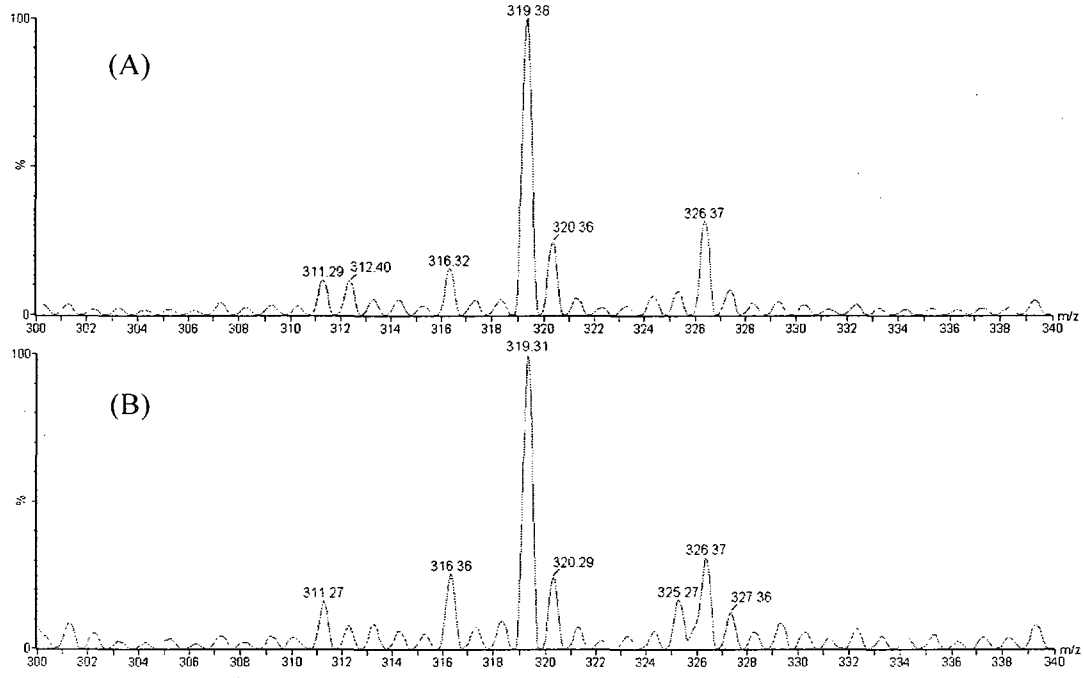

Figure 5.7 Negative-ion ESI mass spectra of EETs in ACN:H_2O (1:1) after overnight storage at -80 °C. (A) 11,12-EET and (B) 14,15-EET standards. Direct injection of 0.25 µM EET at 10 µL/min. Instrument settings: source block temperature, 90 °C; capillary voltage, -3.0 kV; cone voltage, -40 V; scan range, 300-350 m/z.

EET standards prepared in 100% H_2O and stored overnight at -80 °C (Figure 5.8) showed a base peak at m/z 328, with other possible peaks close to the noise level.

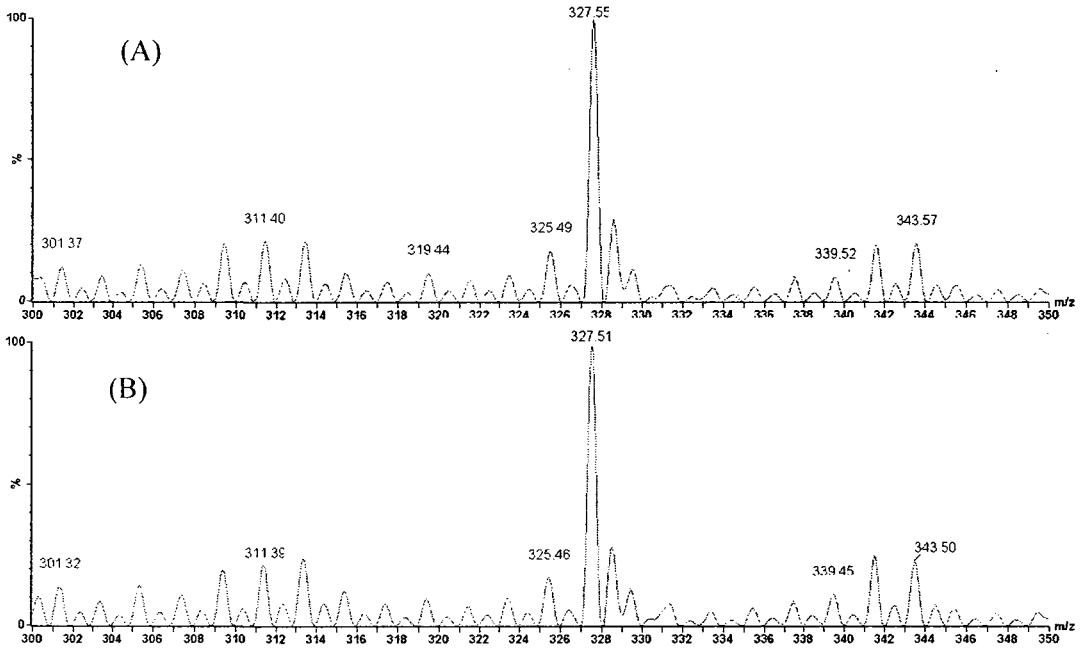

Figure 5.8 Negative-ion ESI mass spectra of EETs in 100% H_2O after overnight storage at -80 °C. (A) 11,12-EET and (B) 14,15-EET standards. Direct injection of 0.25 µM EET at 10 µL/min. Instrument settings: source block temperature, 90 °C; capillary voltage, -3.0 kV; cone voltage, -40 V; scan range, 300-350 m/z.

Freshly prepared EETs in 100% MeOH (Figure 5.9) showed a strong $[M-H]^-$ ion at m/z 319. The peaks observed in ACN, ACN/H_2O, and H_2O (Figures 5.6, 5.7, and 5.8, respectively) with m/z values greater than the $[M-H]^-$ ion are not observed in this case. Fragment ions corresponding to those seen in ACN:H_2O (1:1) (Figure 5.4) are also seen in 100% MeOH (Figure 5.10). The best signal-to-noise ratio for the $[M-H]^-$ ion m/z 319 was obtained for EETs freshly prepared in 100% MeOH.

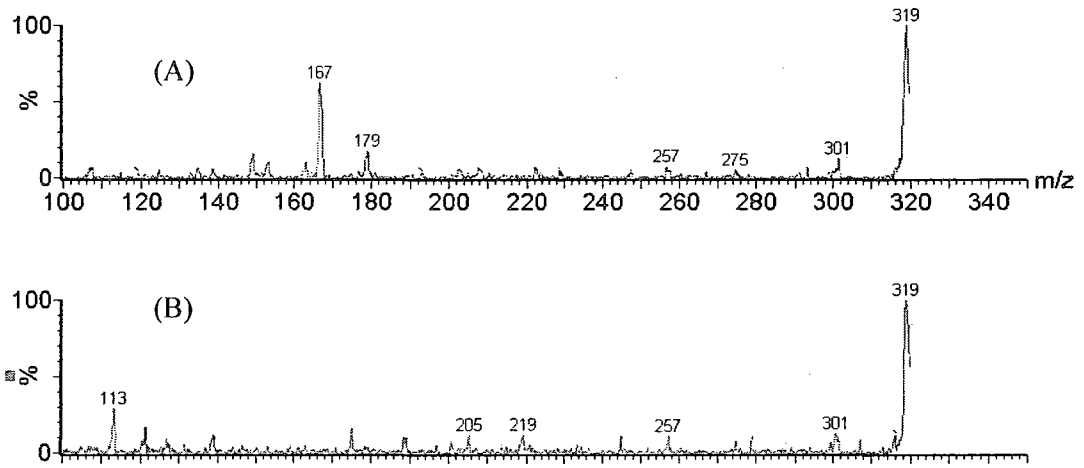

Figure 5.9 Negative-ion ESI mass spectra of EETs freshly prepared in 100% MeOH. (A) 11,12-EET and (B) 14,15-EET standards. Direct injection of 0.25 μM EET at 10 μL/min. Instrument settings: source block temperature, 90 °C; capillary voltage, -3.0 kV; cone voltage, -40 V Note that the scan range for this spectra was m/z 100-320.

Variation in storage time in the solvent systems studied (ACN, ACN/H_2O, H_2O, MeOH) resulted in variation in the intensity of $[M-H]^-$, the signal-to-noise ratio, and the fragmentation patterns. The results are summarized in Table 5.1.

Table 5.1 Effects of solvents and storage conditions on ions observed in the negative-ion ESI mass spectra of EETs

Storage time	Parameter	Solvents			
		ACN	ACN/H_2O (1:1)	H_2O	MeOH
0 min	Signal-to-noise ratio	39.3	675	2.5	725
	Base peak (m/z)	319	319	327	319
	Other peaks (m/z)	311, 325, 339, 343	-	311, 343	-
24 h	Signal-to-noise ratio	46.0	574	2.1	-
	Base peak (m/z)	311	319	327	-
	Other peaks (m/z)	319, 325, 339, 343	311, 325	-	-
6 days	Signal-to-noise ratio	45.3	482	1.8	-
	Base peak (m/z)	325	319	327	-
	Other peaks (m/z)	311, 319, 339, 343	311, 325	-	-

11,12-EET and 14,15-EET (0.25 μM) were directly injected at 10 μL/min into the ESI source. Instrument settings: source block temperature, 90 °C; capillary voltage, -3.0 kV; cone voltage, -40 V; scan range, 300-350 m/z. Data from Figures 5.6, 5.7, 5.8, and 5.9.

The observation of peaks at higher m/z values than $[M-H]^-$ or ions that do not exhibit the fragmentation patterns reported for EETs in the literature suggests the formation of adducts or the evolution of EET degradation products. For identification purposes, MS/MS analysis (Figure 5.11) was performed on the common ions at m/z 339, 325, 311 (Table 5.1). These ions seem to be very stable since they were detected in old samples (stored at -80 °C for about a year, data not shown). The m/z 339 and 325 ions represent mass increases of 20 u and 6 u, respectively, over the EET $[M-H]^-$ ion at m/z

319, while m/z 311 ion represents a reduction of 8 u. After fragmentation with collision energies of 30 to 50%, all of these signals produced a fragment ion at m/z 183 (Figure 5.10).

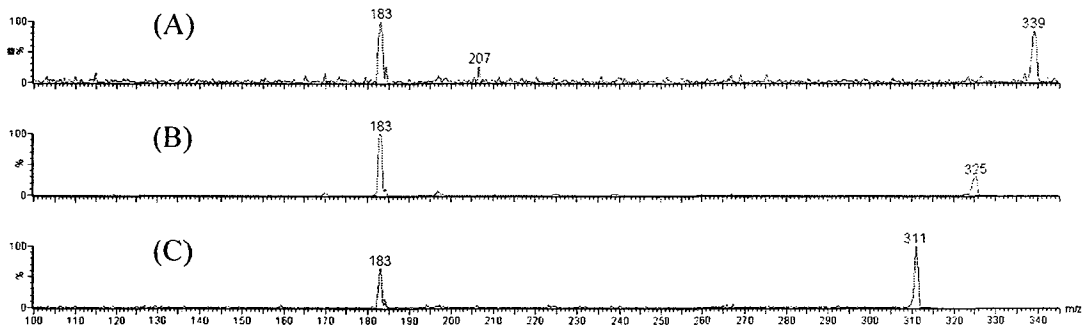

Figure 5.10 Negative-ion ESI mass spectra ions at m/z 339, 325 and 311. (A) m/z 339 ion, (B) m/z 325 ion, and (C) m/z 311 ion.. Direct injection of 0.25 μM EETs in ACN at 10 μL/min. Instrument settings: source block temperature, 90 °C; capillary voltage, -3.0 kV; cone voltage, -40 V, collision gas, N_2; scan range, 100-350 m/z, collision energy 30-50%.

The strong ion at m/z 327 observed for samples prepared in 100% H_2O (Figure 5.8) exhibited a relatively strong peak at m/z 311 on MS/MS analysis (Figure 5.11).

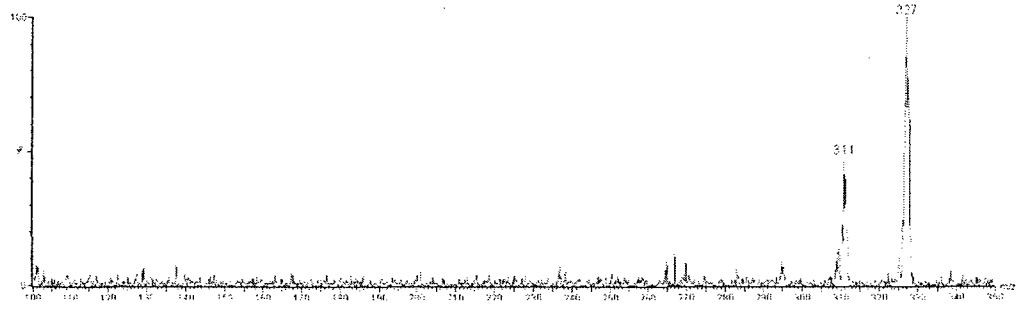

Figure 5.11 Negative-ion ESI tandem mass spectrum of ion at m/z 327. Direct injection of 0.25 μM 11,12-EET and 14,15-EET in H_2O at 10 μL/min. Instrument settings: source block temperature, 90 °C; capillary voltage, -3.0 kV; cone voltage, -40 V, collision gas, N_2; collision energy, 30-50%.

5.3.3 Dynamic range for EET analysis by ESI-MS

Good linearity was observed for the ESI-MS calibration curves using the intensity of the $[M-H]^-$ ion (m/z 319) in equimolar samples of 11,12-EET and 14,15-EET freshly prepared in 100% MeOH and immediately analyzed. A calibration curve was constructed using tridecanoic acid (TA), which exhibits a $[M-H]^-$ ion at m/z 213, at a concentration of 0.16 μM as an internal standard. TA peaks (Figure 5.12) do not interfere with the fragmentation of the analytes, and TA has similar chemical properties to EETs (163). In Figure 5.13 a typical calibration curve for a 0 - 0.5 μM mixture of 11,12-EET and 14,15-EET is presented.

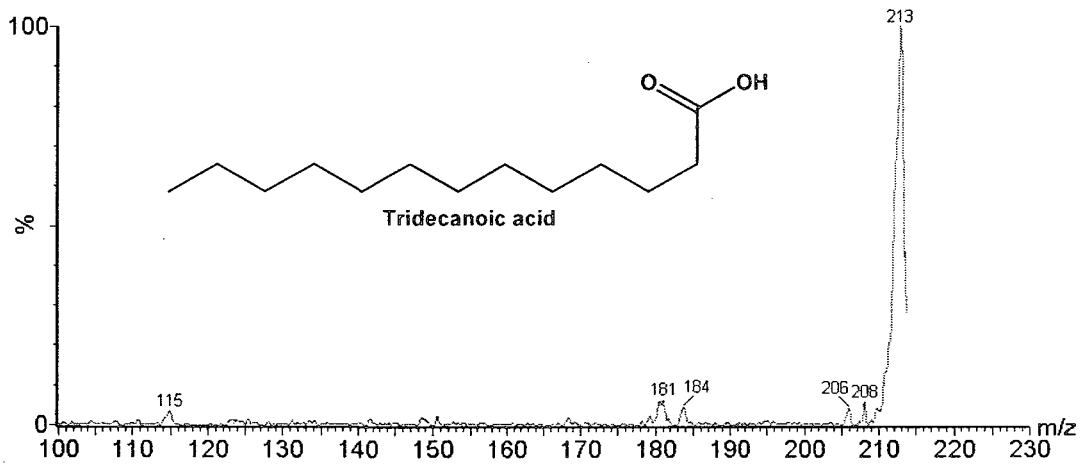

Figure 5.12 Negative-ion ESI mass spectrum of 0.16 μM tridecanoic acid in 100% MeOH. Direct injection at 10 μL/min. Instrument settings: source block temperature, 90 °C; capillary voltage, -3.0 kV; cone voltage, -40 V. $[M-H]^-$ at m/z 213. Insert: TA structure. Note that the scan range used to record this spectra was m/z 100-215.

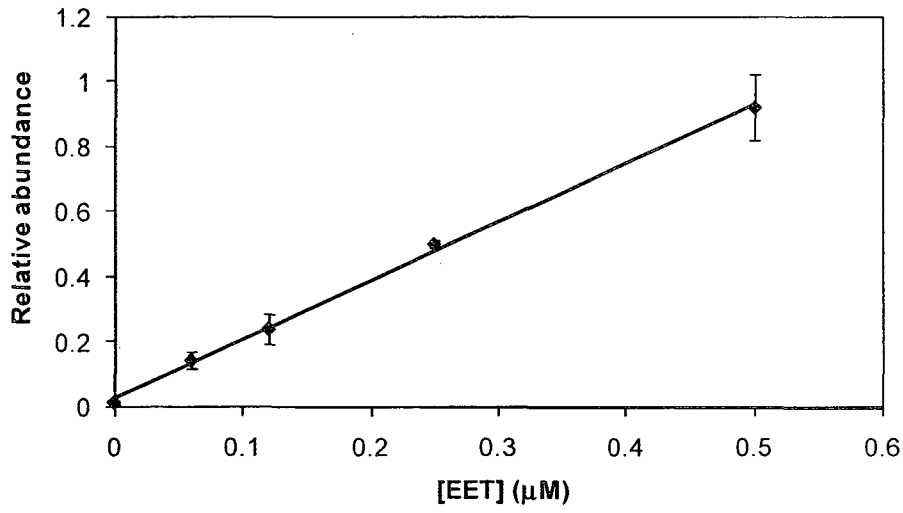

Figure 5.13 EET calibration curve. Relative abundance of $[M-H]^-$ peak at m/z 319 vs total [EET]. Standards containing 0 - 0.5 μM mixtures of 11,12-EET and 14,15-EET with 0.16 μM TA as internal standard in 100% MeOH were directly infused into the ESI source. Experimental details are given in the legend of Figure 5.12. Equation, $y = 1.8 (\pm 0.2) x + 0.03(\pm 0.03)$ and correlation coefficient R^2 is 0.9984 (± 0.0042), n = 2.

5.3.4 Recovery of EETs from artificial plasma

Artificial plasma (Section 5.2.3) was spiked with of 0.5 μM 11,12-EET and 0.5 μM 14,15-EET. After extraction using the procedure described in Section 5.2.4, no EET peaks were detected by ESI-MS. Scans performed between m/z 100-500 yielded spectra very similar to the spectrum of the solvent, 100% MeOH (data not shown). Thus, EETs cannot be recovered from plasma using the solid-phase extraction procedure outlined in Section 5.2.4. It is possible that EETs are retained by interaction with plasma proteins, such as BSA, present in the artificial plasma (Section 5.2.3).

5.3.5 ESI-MS and ESI-MS/MS analysis of $6KPGF_{1\alpha}$

$6KPGF_{1\alpha}$ was studied by ESI-MS in negative-ion mode by direct infusion into the mass spectrometer. The $[M-H]^-$ ion at m/z 369 (Figure 5.14) was fragmented to give the characteristic fragment ions shown in Figure 5.15.

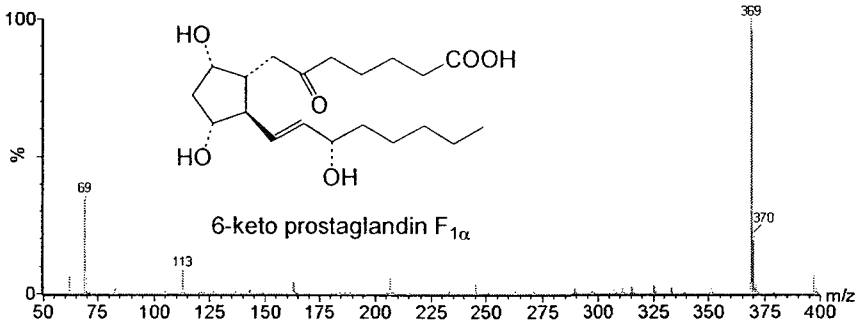

Figure 5.14 Negative-ion ESI mass spectrum of $6KPGF_{1\alpha}$. Direct injection of 475 nM $6KPGF_{1\alpha}$ at 10 µL/min in 10 mM triethylamine:methanol (1:1). Instrument settings: source block temperature, 90 °C; capillary voltage, -3.0 kV; cone voltage, -60 V, scan range, 50-400 m/z. $[M-H]^-$ at m/z 369. Insert: $6KPGF_{1\alpha}$ structure.

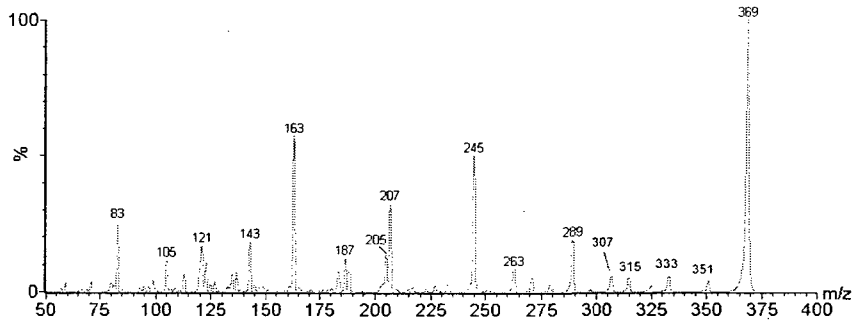

Figure 5.15 Negative-ion ESI tandem mass spectrum of 475 nM $6KPGF_{1\alpha}$. The experimental details are given in Figure 5.14 with the addition of collision gas N_2 at a collision energy of 50%.

A set of weak peaks are observed at m/z 351, 333, 315, and 307 corresponding to the loss of H_2O, $2H_2O$, $3H_2O$ and H_2O+CO_2, respectively. Fragments at m/z 245 ($C_{17}H_{25}O$), 205 ($C_{14}H_{21}O$), and 187 ($C_{14}H_{19}$) have also been reported for PGI_2, and result from the fragmentation of the carbohydrate backbone containing the 5C-ring (168).

In a first attempt at quantitation, D4-6KPGF$_{1\alpha}$ which contains D atoms at the 3, 3', 4, and 4' positions, was used as an internal standard. The structure of D4-6KPGF$_{1\alpha}$ as well as its ESI-MS spectrum is presented in Figure 5.16.

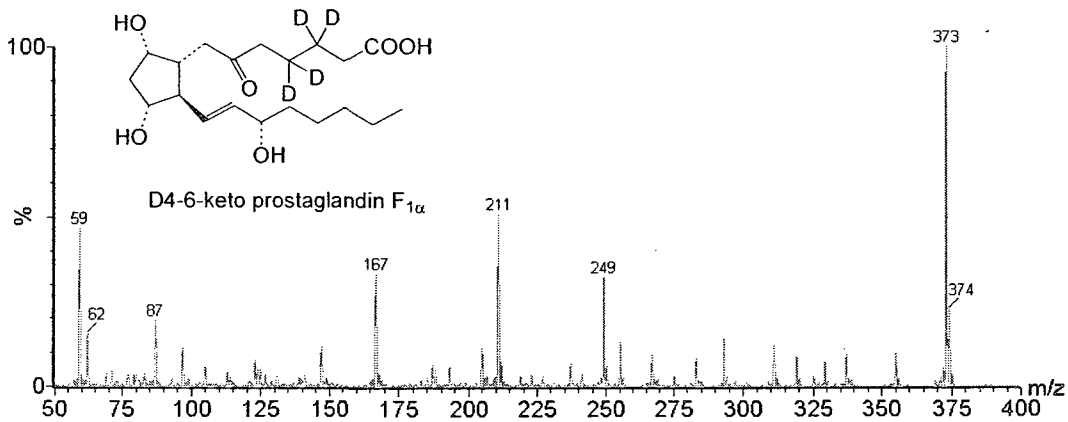

Figure 5.16 Negative-ion ESI mass spectrum of D4-6KPGF$_{1\alpha}$. Direct injection of 107 nM D4-6KPGF$_{1\alpha}$ at 10 µL/min in 10 mM triethylamine:methanol (1:1). Instrument settings: source block temperature, 90 °C; capillary voltage, -3.0 kV; cone voltage, -60 V, scan range, 50-400 m/z. $[M-H]^-$ at m/z 373. Insert: 6KPGF$_{1\alpha}$ structure.

The 6KPGF$_{1\alpha}$ calibration curve (Figure 5.17) exhibited good linearity when the relative abundance of the $[M-H]^-$ ion of 6KPGF$_{1\alpha}$ at m/z 369 was plotted vs [6KPGF$_{1\alpha}$]. The calibration curve was used to confirm the concentration of a D4-6KPGF$_{1\alpha}$ sample,

which was found to be 106.39 nM, deviating from the theoretical value (106.8 nM) by only 0.4% (spectral data not shown).

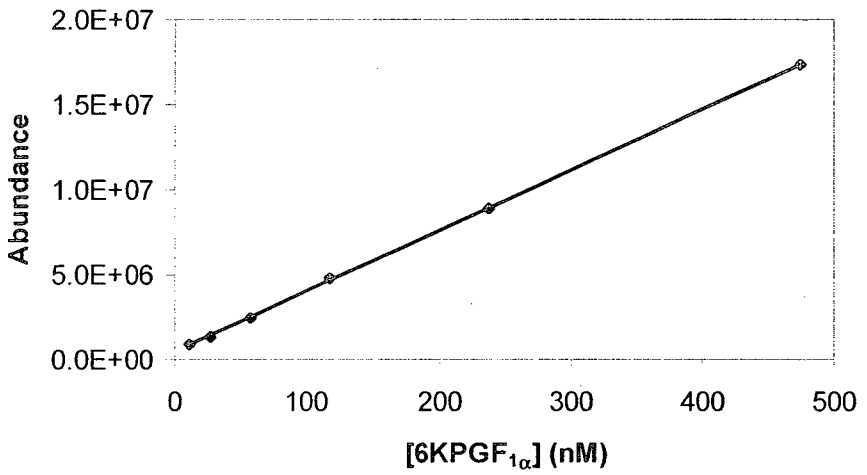

Figure 5.17 6KPGF$_{1\alpha}$ calibration curve of [M-H]$^-$ peak abundance vs [6KPGF$_{1\alpha}$]. Plot represents a typical standard curve from 11 nM to 475 nM 6KPGF$_{1\alpha}$, with equation y = 3.5572 x + 449186 and correlation coefficient R^2 = 0.9999. Standards solutions of 6KPGF$_{1\alpha}$ in 10 mM triethylamine:methanol (1:1) were directly infused into the ESI source. Experimental details are given in the legend of Figure 5.15.

5.4 Discussion

The detection of 11,12-EET and 14,15-EET by ESI-MS is efficient with an LOD of 0.05 μM. Also, these isomers can be easily identified by ESI-MS/MS since characteristic peaks for each EET are clearly distinguishable, as well as typical neutral losses of H_2O and CO_2 (Figures 5.4 and 5.5). EETs are extremely labile, easily air-oxidized and light sensitive. Minimizing light exposure during sample preparation has to be assured. Therefore, working in indirect light as well minimum of contact with air by

the use of glass gas-tight syringes are necessary. Temperature is also an issue during manipulation; the stock solution must be kept below 10 °C at all times and samples are stored at -80 °C immediately after use. Time is also a limiting factor with EETs. Stock solutions degrade after a couple of days, and depending on the type of solvent, detection of the $[M-H]^-$ ion diminishes even during the course of a few hours. From the data in Table 5.1, the occurrence of degradation with time is evident.

Detection of the $[M-H]^-$ ion decreases with time and the evolution of new peaks at higher m/z values was observed. In order to determine whether these peaks were generated from EET degradation or adduct formation, MS/MS analyses were performed. The MS/MS spectra (Figures 5.9 and 5.10) exhibit only weak signals in comparison with the MS/MS spectra obtained for the EET $[M-H]^-$ ion at m/z 319 (Figure 5.5). Also, the fragment ions formed from the unknown high mass ions are not equivalent to those obtained from freshly prepared EETs or to the fragments reported in the literature for EETs analyzed in ACN/water/methanol/acetic acid or ACN/water/methanol/ammonium acetate at a ratio of 60:30:10:0.05 (155, 156).

In an effort to explain the evolution of these new signals, possible mechanisms of EET degradation were considered. Hydrolysis of the epoxy ring (yielding dihydroxyeicosatrienoic acid, DHET) and/or hydrogenation of double bonds (yielding epoxyeicosanoic acid, EEA) represent possibilities (Figure 5.18).

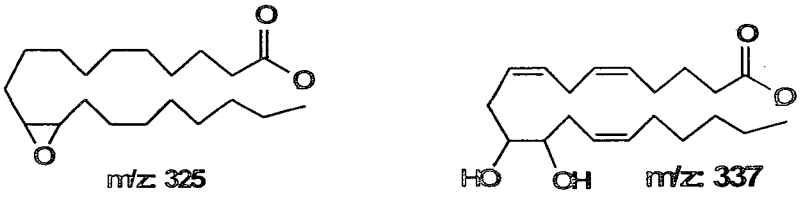

11,12-EEA 11, 12-DHET

Figure 5.18 Degradation products of 11,12-EET. Hydrogenation of double bonds generates 11,12-epoxyeicosanoic acid (11,12-EEA). Hydrolysis of the epoxy ring generates 11,12-dihydroxyeicosatrienoic acid (11,12-DHET)

EEAs and DHETs have been reported in RBCs (154). Since the experimental conditions used here (Sections 5.2.2, 5.2.4 and 4.2.5) are unlikely to convert EETs to EEAs or DHETs, these might have been present as an impurity in the commercial samples.

In summary, $[M-H]^-$ ions dominated the mass spectra of freshly prepared EETs in 100% MeOH. Also, under these conditions, the abundance of the $[M-H]^-$ ion at m/z 319 vs total EET concentration yielded a straight line with a correlation coefficient of 0.9984 for mixtures of 11,12-EET and 14,15-EET. Unfortunately, EET recovery from the plasma simulator was not succesful. Therefore, application of this procedure to biological samples was not attempted.

Detection and quantitation of $6KPGF_{1\alpha}$ was successful. Due to time constrains, application of this method to PGI_2 extracted from plasma could not be performed. Nonetheless, this work is a starting point for future analytical measurements in biological matrices. The use of $6KPGF_{1\alpha}$ as a biomarker for prostaglandins and its deuterated analog D4-$6KPGF_{1\alpha}$ appears to be promising for quantitation of PGI_2 by ESI-MS.

6.0 General conclusions and suggestions for future work

6.1 Conclusions

6.1.1 Chapters 2 and 3

In Chapters 2 and 3, the effects of different stimuli on ATP release from RBCs were determined. Using a chemiluminescent detection method optimized for this study, it was confirmed that deaeration increases ATP release from RBCs (37, 135). It was also demonstrated that the incubation of RBCs with pharmacological concentrations of nitroglycerin results in a similar extracellular profile as nitrite. An initial increase in ATP release is followed by an attenuation of this effect within minutes. While the effects of nitroglycerin are delayed by ~30 s, the effects of nitrite are observed immediately. This difference is attributed to time required for nitroglycerin to release NO_2^- (50, 54). The subsequent attenuation of ATP release observed within 15 min in both cases could be considered as evidence of a negative feedback mechanism in the amplification of the vasodilatory signal. These seminal findings are summarized in Figure 3.5. Our observations constitute the *first* report of vasodilator release (ATP) following RBC stimulation by an endogenous NO donor (NO_2^-) as well as by a pharmacological NO donor, nitroglycerin, and further suggest that RBC-derived ATP is a regulator of NO-mediated vasoactivity in the circulation.

6.1.2 Chapter 4

Activity assays on nitroglycerin-treated human RBCs showed that the drug exerts an inhibitory effect on the activity of GAPDH that is also concentration dependent. This confirms the previous findings in our group (M. Antonic *et al.*, unpublished results), which showed that nitroglycerin is a "suicide substrate" of GAPDH *in vitro*. GAPDH acts as an enzymatic activator of nitroglycerin to generate nitrite, which at the same time causes inactivation of the enzyme. This could partially account for the development of nitrate tolerance upon chronic exposure to the drug.

6.1.3 Chapter 5

Assessment of EET stability in various solvents was performed to establish the optimal conditions for LC-MS analysis. Freshly prepared samples in 100% MeOH proved to be the most stable. LC-MS/MS methods were optimized for the analysis and quantitation of EETs and PGI_2-related metabolites with good sensitivity and selectivity. The method developed has the potential to be applied in the detection and quantitation of these vasodilators in human plasma.

6.2 Suggestions for future work

I. The HPLC/UV methodology presented in Chapter 2 for the detection of extracellular ribonucleotides could be used to study the role of nucleases in the regulation of amplification of ATP-derived vasodilation signals, as well as for analyzing extracellular AMP/ATP and ADP/ATP levels related to stimulation by nitroglycerin, NO_2^-, and other vasodilators. Synergistic or antagonistic effects of ATP and its related ribonucleoside adenosine, a known endogenous vasodilator, could also be assessed using this method.

II. The development of an online/flow-through chemiluminescent detection system (8, 37, 173) to study instantaneous or short-term changes in the RBC ATP-release profile would provide more precise time resolution of ATP variation during and after stimulation with pharmacological agents or endogenous vasodilators. Such information would help to better understand the role of extracellular ATP in the propagation of vasodilatation and how this purinergic signaling pathway is controlled.

III. The optimization of LC-UV/MS methodology for the detection and quantitation of nitroglycerin, 1,2- and 1,3-glyceryl dinitrates, and glyceryl mononitrate present in drug-treated RBCs, plasma, and intact blood vessels would help confirm the mechanisms by which the drug is activated in the vascular system. These

measurements, accompanied by the monitoring of NO_2^- levels, would also shed light on the mechanisms by which nitroglycerin exerts vasodilation. This still remains a mystery after more than 100 years of its use as a pharmacological treatment for ischemic diseases.

IV. Isolation of GAPDH from human RBCs is of interest. The study of RBC GAPDH from healthy individuals and patients chronically exposed to nitroglycerin would help elucidate the role of this enzyme in the activation of nitroglycerin, and its possible involvement in the evolution of nitrate tolerance.

V. The detection of EETs and PGI_2 in plasma by LC-MS/MS should be further developed. Sensitive methods like ELISA are already available and these could be applied directly to plasma extracts to provide detection limits in the pg/mL range.

7. References

1. Whittam, R, *Transport and diffusion in red blood cells*. The Williams and Wilkins Company: Baltimore, **1964;** p 1-5.

2. Boushel, R, *Metabolic control of muscle blood flow during exercise in humans*. Can. J. Appl. Phys. **2003,** 25 (5), 754-773.

3. Gladwin, MT; Raat, NJH; Shiva, S; Dezfulian, C; Hogg, N; Kim-Shapiro, DB; Patel, RP, *Nitrite as a vascular endocrine nitric oxide reservoir that contributes to hypoxic signaling, cytoprotection, and vasodilation*. Am. J. Physiol. Heart. Circ. Physiol. **2006,** 291 (5), H2026-2035.

4. Stein, JC; Ellis, CG; Ellsworth, ML, *Relationship between capillary and systemic venous PO_2 during nonhypoxic and hypoxic ventilation*. Am. J. Physiol. Heart Circ. Physiol. **1993,** 265 (2), H537-542.

5. Ellsworth, ML; Forrester, T; Ellis, CG; Dietrich, HH, *The erythrocyte as a regulator of vascular tone*. Am. J. Physiol. Heart Circ. Physiol. **1995,** 269 (6), H2155-2161.

6. Gonzalez-Alonso, J; Mortensen, SP; Dawson, EA; Secher, NH; Damsgaard, R, *Erythrocytes and the regulation of human skeletal muscle blood flow and oxygen delivery: role of erythrocyte count and oxygenation state of haemoglobin*. J. Physiol. **2006,** 572 (1), 295-305.

7. Sprague, RS; Stephenson, AH; Dimmitt, RA; Weintraub, NL; Branch, CA; McMurdo, L; Lonigro, AJ; Weintraub, NA, *Effect of L-NAME on pressure-flow relationships in isolated rabbit lungs: role of red blood cells*. Am. J. Physiol. Heart. Circ. Physiol. **1995,** 269 (6), H1941-1948.

8. Price, AK; Fischer, DJ; Martin, RS; Spence, DM, *Deformation-induced release of ATP from erythrocytes in a poly(dimethylsiloxane)-based microchip with channels that mimic resistance vessels*. Anal. Chem. **2004,** 76 (16), 4849-4855.

9. Hester, R; Choi, J, *Blood flow control during exercise: role for the venular endothelium?* Exerc. Sport. Sci. Rev. **2002,** 30 (4), 147-151.

10. Sprague, RS; Stephenson, AH; Ellsworth, ML, *Red not dead: signaling in and from erythrocytes*. Trensd. Endocrin. Met. **2007,** 18 (9), 350-355.

11. Crawford, JH; Isbell, TS; Huang, Z; Shiva, S; Chacko, BK; Schechter, AN; Darley-Usmar, VM; Kerby, JD; Lang, JD, Jr; Kraus, D; Ho, C; Gladwin, MT; Patel, RP, *Hypoxia, red blood cells, and nitrite regulate NO-dependent hypoxic vasodilation*. Blood. **2006,** 107 (2), 566-574.

12. Gladwin, MT, *Hemoglobin as a nitrite reductase regulating red cell-dependent hypoxic vasodilation*. Am. J. Respir. Cell Mol. Biol. **2005,** 32 (5), 363-a-366.

13. Cosby, K; Partovi, KS; Crawford, JH; Patel, RP; Reiter, CD; Martyr, S; Yang, BK; Waclawiw, MA; Zalos, G; Xu, X; Huang, KT; Shields, H; Kim-Shapiro, DB; Schechter, AN; Cannon, RO; Gladwin, MT, *Nitrite reduction to nitric oxide by*

deoxyhemoglobin vasodilates the human circulation. Nat. Med. **2003,** 9 (12), 1498-1505.

14. Gonzalez-Alonso, J; Olsen, DB; Saltin, B, *Erythrocyte and the regulation of human skeletal muscle blood flow and oxygen delivery: role of circulating ATP.* Circ. Res. **2002,** 91 (11), 1046-1055.

15. The Nobel Foundation The Nobel Prize in physiology or medicine 1998, (Online). http://nobelprize.org/nobel_prizes/medicine/laureates/1998/index.html (accessed June 25, 2008).

16. Lehninger, AL, *Principles of biochemistry.* Worth Publishers: New York, N. Y., **1986;** p 1011.

17. Hakim, TS; Sugimori, K; Camporesi, EM; Anderson, G, *Half-life of nitric oxide in aqueous solutions with and without haemoglobin.* Physiol. Meas. **1996,** 17 (4), 267-277.

18. Shiva, S; Wang, X; Ringwood, LA; Xu, X; Yuditskaya, S; Annavajjhala, V; Miyajima, H; Hogg, N; Harris, ZL; Gladwin, MT, *Ceruloplasmin is a NO oxidase and nitrite synthase that determines endocrine NO homeostasis.* Nature Chemical Biology **2006,** 2 (9), 486-493.

19. Chiodi, H; Collier, CR; Mohler, JG, *In vitro methemoglobin formation in human blood exposed to NO_2.* Environ. Res. **1983,** 30 (1), 9-15.

20. Huang, Z; Shiva, S; Kim-Shapiro, DB; Patel, RP; Ringwood, LA; Irby, CE; Huang, KT; Ho, C; Hogg, N; Schechter, AN; Gladwin, MT, *Enzymatic function of hemoglobin as a nitrite reductase that produces NO under allosteric control.* J. Clin. Invest. **2005,** 115 (8), 2099-107.

21. Stamler, JS; Jia, L; Eu, JP; McMahon, TJ; Demchenko, IT; Bonaventura, J; Gernert, K; Piantadosi, CA, *Blood flow regulation by S-nitrosohemoglobin in the physiological oxygen gradient.* Science. **1997,** 276 (5321), 2034-2037.

22. Singel, DJ; Stamler, JS, *Chemical physiology of blood flow regulation by red blood cells:The role of nitric oxide and S-nitrosohemoglobin.* Annu. Rev. Physiol. **2005,** 67 (1), 99-145.

23. Gladwin, M; Schechter, A; Kim-Shapiro, D; Patel, R; Hogg, N; Shiva, S; Cannon III, R; Kelm, M; Wink, D; Espey, M; Oldfield, E; Pluta, R; Freeman, B; Lancaster Jr, J; Feelisch, M; Lundberg, J, *The emerging biology of the nitrite anion.* Nature Chemical Biology **2005,** 1 (6), 308-314.

24. Hermann, L, *Ueber die wirkungen des stickoxydulgases auf das blut.* Arch. Anat. Physiol. Lpz. **1865,** 469–481.

25. Bryan, NS; Fernandez, BO; Bauer, SM; Garcia-Saura, MF; Milsom, AB; Rassaf, T; Maloney, RE; Bharti, A; Rodriguez, J; Feelisch, M, *Nitrite is a signaling molecule and regulator of gene expression in mammalian tissues.* Nature Chemical Biology **2005,** 1 (5), 290-297.

26. Li, H; Cui, H; Kundu, TK; Alzawahra, W; Zweier, JL, *Nitric oxide production from nitrite occurs primarily in tissues not in the blood: critical role of xanthine oxidase and aldehyde oxidase*. J. Biol. Chem. **2008,** 283 (26), 17855-17863.

27. Quilley, J; McGiff, JC, *Is EDHF an epoxyeicosatrienoic acid?* Trends Pharmacol. Sci. **2000,** 21 (4), 121-124.

28. Michaelis, UR; Fleming, I, *From endothelium-derived hyperpolarizing factor (EDHF) to angiogenesis: Epoxyeicosatrienoic acids (EETs) and cell signaling.* Pharmacology & Therapautics **2006,** 111 (3), 584-595.

29. Archer, SL; Gragasin, FS; Wu, X; Wang, S; McMurtry, S; Kim, DH; Platonov, M; Koshal, A; Hashimoto, K; Campbell, WB; Falck, JR; Michelakis, ED, *Endothelium-derived hyperpolarizing factor in human internal mammary artery is 11,12-epoxyeicosatrienoic acid and causes relaxation by activating smooth muscle BKCa channels*. Circulation. **2003,** 107 (5), 769-776.

30. Larsen, BT; Campbell, WB; Gutterman, DD, *Beyond vasodilatation: non-vasomotor roles of epoxyeicosatrienoic acids in the cardiovascular system.* Trends in Pharmacological Sciences **2007,** 28 (1), 32-38.

31. Jiang, H, *Erythrocyte-derived epoxyeicosatrienoic acids*. Prostag. Oth. Lipid M. **2007,** 82 (1-4), 4-10.

32. Falck, JR; Krishna, UM; Reddy, YK; Kumar, PS; Reddy, KM; Hittner, SB; Deeter, C; Sharma, KK; Gauthier, KM; Campbell, WB, *Comparison of*

vasodilatory properties of 14,15-EET analogs: structural requirements for dilation. Am. J. Physiol. Heart. Circ. Physiol. **2003,** 284 (1), H337-349.

33. Yue, H; Jansen, SA; Strauss, KI; Borenstein, MR; Barbe, MF; Rossi, LJ; Murphy, E, *A liquid chromatography/mass spectrometric method for simultaneous analysis of arachidonic acid and its endogenous eicosanoid metabolites prostaglandins, dihydroxyeicosatrienoic acids, hydroxyeicosatetraenoic acids, and epoxyeicosatrienoic acids in rat brain tissue.* J. Pharmaceut. Biomed. **2007,** 43 (3), 1122-1134.

34. Parkington, HC; Coleman, HA; Tare, M, *Prostacyclin and endothelium-dependent hyperpolarization*. Pharmacol. Res. **2004,** 49 (6), 509-514.

35. Voet, D; Voet, J, *Biochemistry*. 2nd ed.; Wiley & Sons Inc.: New York, **1995;** p 425.

36. Erlinge, D; Burnstock, G, *P2 receptors in cardiovascular regulation and disease.* Purinergic Signal. **2008,** 4 (1), 1-20.

37. Faris, A; Spence, DM, *Measuring the simultaneous effects of hypoxia and deformation on ATP release from erythrocytes.* Analyst. **2008,** 133 (5), 678-682.

38. Dietrich, HH; Ellsworth, ML; Sprague, RS; Dacey, RG, Jr., *Red blood cell regulation of microvascular tone through adenosine triphosphate.* Am. J. Physiol. Heart. Circ. Physiol. **2000,** 278 (4), H1294-1298.

39. Duff, F; Patterson, GC; Shepherd, JT, *A quantitative study of the response to adenosine triphosphate of the blood vessels of the human hand and forearm.* J. Physiol. **1954,** 125 (3), 581-589.

40. van Ginneken, EEM; Meijer, P; Verkaik, N; Smits, P; Rongen, GA, *ATP-induced vasodilation in human skeletal muscle.* Br. J. Pharmacol. **2004,** 141 (5), 842-850.

41. Rongen, G; Smits, P; Thien, T, *Characterization of ATP-induced vasodilation in the human forearm vascular bed.* Circulation. **1994,** 90 (4), 1891-1898.

42. Korchazhkina, O; Wright, G; Exley, C, *Intravascular ATP and coronary vasodilation in the isolated working rat heart.* Br. J. Pharmacol. **1999,** 127 (3), 701-708.

43. Sprague, RS; Ellsworth, ML; Stephenson, AH; Lonigro, AJ, *ATP: the red blood cell link to NO and local control of the pulmonary circulation.* Am. J. Physiol. Heart. Circ. Physiol. **1996,** 271 (6), H2717-2722.

44. Min, J; Kyung Kim, Y; Cipriani, PG; Kang, M; Khersonsky, SM; Walsh, DP; Lee, J-Y; Niessen, S; Yates, JR; Gunsalus, K; Piano, F; Chang, Y-T, *Forward chemical genetic approach identifies new role for GAPDH in insulin signaling.* Nature Chemical Biology **2007,** 3 (1), 55-59.

45. Hara, MR; Agrawal, N; Kim, SF; Cascio, MB; Fujimuro, M; Ozeki, Y; Takahashi, M; Cheah, JH; Tankou, SK; Hester, LD; Ferris, CD; Hayward, SD; Snyder, SH; Sawa, A, *S-nitrosylated GAPDH initiates apoptotic cell death by nuclear translocation following Siah1 binding.* 665 - 674 **2005,** 7, 665-674.

46. Ismail, SA; Park, HW, *Structural analysis of human liver glyceraldehyde-3-phosphate dehydrogenase*. Acta Crystallogr. D. **2005,** 61 (11), 1508-1513.

47. Heard, K; Diguette, M; Heard, A; Carruthers, A, *Membrane-bound glyceraldehyde-3-phosphate dehydrogenase and multiphasic erythrocyte sugar transport*. Exp. Physiol. **1998,** 83 (2), 195-202.

48. Mercer, R; Dunham, P, *Membrane-bound ATP fuels the Na/K pump. Studies on membrane-bound glycolytic enzymes on inside-out vesicles from human red cell membranes*. J. Gen. Physiol. **1981,** 78 (5), 547-568.

49. *Heart disease and stroke 2008 update at-a-glance statistics*; American Heart Association: Dallas, Texas, 2008.

50. O'Rourke, ST, *Nitro vasodilators: Pharmacology and use in the treatment of myocardial ischemia*. Am. J. Pharm. Educ. **2002,** 66, 177-180.

51. Ignarro, L; Lippton, H; Edwards, J; Baricos, W; Hyman, A; Kadowitz, P; Gruetter, C, *Mechanism of vascular smooth muscle relaxation by organic nitrates, nitrites, nitroprusside and nitric oxide: evidence for the involvement of S-nitrosothiols as active intermediates*. J. Pharmacol. Exp. Ther. **1981,** 218 (3), 739-749.

52. Cossum, PA; Roberts, MS, *Nitroglycerin disposition in human blood*. Eur. J. Clin. Pharmacol. **1985,** 29 (2), 169-175.

53. Malta, E, *Studies on the biphasic relaxant curve of glyceryltrinitrate in rat aorta: role of GTN metabolites*. Clin. Exp. Pharmacol. P. **1989,** 16 (11), 829-835.

54. Ignarro, LJ; Gruetter, CS, *Requirement of thiols for activation of coronary arterial guanylate cyclase by glyceryl trinitrate and sodium nitrite possible involvement of S-nitrosothiols*. BBA-Gen. Subjects. **1980,** 631 (2), 221-231.

55. Keen, JH; Habig, WH; Jakoby, WB, *Mechanism for the several activities of the glutathione S-transferases*. J. Biol. Chem. **1976,** 251 (20), 6183-6188.

56. Lau, D; Benet, L, *Nitroglycerin metabolism in subcellular fractions of rabbit liver. Dose dependency of glyceryl dinitrate formation and possible involvement of multiple isozymes of glutathione S-transferases*. Drug Metab. Dispos. **1990,** 18 (3), 292-297.

57. Butler, AR; Ridd, JH, *Formation of nitric oxide from nitrous acid in ischemic tissue and skin*. Nitric Oxide. **2004,** 10 (1), 20-24.

58. Kurz, MA; Boyer, TD; Whalen, R; Peterson, TE; Harrison, DG, *Nitroglycerin metabolism in vascular tissue: role of glutathione S-transferases and relationship between NO and NO_2^- formation.* Biochem. J. **1993,** 292 (2), 545-550.

59. Chen, Z; Stamler, JS, *Bioactivation of nitroglycerin by the mitochondrial aldehyde dehydrogenase*. Trends. Cardiovas. Med. **2006,** 16 (8), 259-265.

60. Chong, S; Fung, H, *Thiol-mediated catalysis of nitroglycerin degradation by serum proteins. Increase in metabolism was not accompanied by S-nitrosothiol production*. Drug. Metab. Dispos. **1990,** 18 (1), 61-67.

61. Bennett, B; Kobus, S; Brien, J; Nakatsu, K; Marks, G, *Requirement for reduced, unliganded hemoprotein for the hemoglobin- and myoglobin-mediated biotransformation of glyceryl trinitrate*. J. Pharmacol. Exp. Ther. **1986,** 237 (2), 629-635.

62. Nordberg, M; Duffus, J; Templeton, D, *Glossary of terms used in toxicokinetics (IUPAC Recommendations 2003)*. Pure Appl. Chem. **2004,** 76 (5), 1033–1082.

63. Servent, D; Delaforge, M; Ducrocq, C; Mansuy, D; Lenfant, M, *Nitric oxide formation during microsomal hepatic denitration of glyceryl trinitrate: Involvement of cytochrome P-450*. Biochem. Biophys. Res. Co. **1989,** 163 (3), 1210-1216.

64. McDonald, BJ; Bennett, BM, *Cytochrome P-450 mediated biotransformation of organic nitrates*. Can. J. Physiol. Pharmacol. **1990,** 68 (12), 1552-7.

65. Minamiyama, Y; Takemura, S; Akiyama, T; Imaoka, S; Inoue, M; Funae, Y; Okada, S, *Isoforms of cytochrome P450 on organic nitrate-derived nitric oxide release in human heart vessels*. FEBS Lett. **1999,** 452 (3), 165-169.

66. Li, H; Liu, X; Cui, H; Chen, Y-R; Cardounel, AJ; Zweier, JL, *Characterization of the mechanism of cytochrome P450 reductase-cytochrome P450-mediated nitric*

oxide and nitrosothiol generation from organic nitrates. J. Biol. Chem. **2006,** 281 (18), 12546-12554.

67. Li, H; Samouilov, A; Liu, X; Zweier, JL, *Characterization of the magnitude and kinetics of xanthine oxidase-catalyzed nitrate reduction: evaluation of its role in nitrite and nitric oxide generation in anoxic tissues*. Biochemistry. **2003,** 42 (4), 1150-1159.

68. Li, H; Samouilov, A; Liu, X; Zweier, JL, *Characterization of the effects of oxygen on xanthine oxidase-mediated nitric oxide formation*. J. Biol. Chem. **2004,** 279 (17), 16939-16946.

69. Millar, TM; Stevens, CR; Benjamin, N; Eisenthal, R; Harrison, R; Blake, DR, *Xanthine oxidoreductase catalyses the reduction of nitrates and nitrite to nitric oxide under hypoxic conditions*. FEBS Lett. **1998,** 427 (2), 225-228.

70. Doel, JJ; Godber, BLJ; Eisenthal, R; Harrison, R, *Reduction of organic nitrates catalysed by xanthine oxidoreductase under anaerobic conditions*. BBA-Gen. Subjects. **2001,** 1527 (1-2), 81-87.

71. Li, H; Cui, H; Liu, X; Zweier, JL, *Xanthine oxidase catalyzes anaerobic transformation of organic nitrates to nitric oxide and nitrosothiols: Characterization of this mechanism and the link between organic nitrate and guanylyl cyclase activation*. J. Biol. Chem. **2005,** 280 (17), 16594-16600.

72. National Center for Biotechnology Information Aldehyde dehydrogenase 2 family (mitochondrial) ALDH2 [Homo sapiens].

http://www.ncbi.nlm.nih.gov/sites/entrez?Db=gene&Cmd=ShowDetailView&TermToSearch=217 (accessed July 2, 2008).

73. Chen, Z; Zhang, J; Stamler, JS, *Identification of the enzymatic mechanism of nitroglycerin bioactivation*. Proc. Natl. Acad. Sci. USA. **2002,** 99 (12), 8306-8311.

74. Shen, ML; Lipsky, JJ; Naylor, S, *Role of disulfiram in the in vitro inhibition of rat liver mitochondrial aldehyde dehydrogenase*. Biochem. Pharmacol. **2000,** 60 (7), 947-953.

75. Tsuchida, S; Maki, T; Sato, K, *Purification and characterization of glutathione transferases with an activity toward nitroglycerin from human aorta and heart. Multiplicity of the human class Mu forms*. J. Biol. Chem. **1990,** 265 (13), 7150-7157.

76. Katz, RJ, *Mechanisms of nitrate tolerance: A review*. Cardiovasc. Drug. Ther. **1990,** 4 (1), 247-252.

77. Needleman, P; Johnson, EM, JR., *Mechanism of tolerance development to organic nitrates*. J. Pharmacol. Exp. Ther. **1973,** 184 (3), 709-715.

78. Arnér, ESJ; Holmgren, A, *Physiological functions of thioredoxin and thioredoxin reductase*. Eur. J. Biochem. **2000,** 267 (20), 6102-6109.

79. Hirai, N; Kawano, H; Yasue, H; Shimomura, H; Miyamoto, S; Soejima, H; Kajiwara, I; Sakamoto, T; Yoshimura, M; Nakamura, H; Yodoi, J; Ogawa, H,

Attenuation of nitrate tolerance and oxidative stress by an angiotensin II receptor blocker in patients with coronary spastic angina. Circulation. **2003**, 108 (12), 1446-1450.

80. Daiber, A; Wenzel, P; Oelze, M; Münzel, T, *New insights into bioactivation of organic nitrates, nitrate tolerance and cross-tolerance.* Clin. Res. Cardiol. **2008**, 97 (1), 12-20.

81. Wenzel, P; Hink, U; Oelze, M; Schuppan, S; Schaeuble, K; Schildknecht, S; Ho, KK; Weiner, H; Bachschmid, M; Münzel, T; Daiber, A, *Role of reduced lipoic acid in the redox regulation of mitochondrial aldehyde dehydrogenase (ALDH-2) activity: Implications for mitochondrial oxidative stress and nitrate tolerance.* J. Biol. Chem. **2007**, 282 (1), 792-799.

82. Fung, H-L, *Biochemical mechanism of nitroglycerin action and tolerance: Is this old mystery solved?* Annu. Rev. Pharmacol. **2004**, 44 (1), 67-85.

83. Parker, J; Farrell, B; Lahey, K; Moe, G, *Effect of intervals between doses on the development of tolerance to isosorbide dinitrate.* N. Engl. J. Med. **1987**, 316 (23), 1440-1444.

84. Münzel, T; Sayegh, H; Freeman, BA; Tarpey, MM; Harrison, DG, *Evidence for enhanced vascular superoxide anion production in nitrate tolerance. A novel mechanism underlying tolerance and cross-tolerance.* J. Clin. Invest. **1995**, 95 (1), 187-94.

85. Lange, RL; Reid, MS; Tresch, DD; Keelan, MH; Bernhard, VM; Coolidge, G, *Nonatheromatous ischemic heart disease following withdrawal from chronic industrial nitroglycerin exposure*. Circulation. **1972,** 46 (4), 666-678.

86. Dalal, JJ; Parker, JO, *Nitrate cross-tolerance: Effect of sublingual isosorbide dinitrate and nitroglycerin during sustained nitrate therapy*. he American Journal of Cardiology Nitric Oxide-Enhancing Therapy: An Evolving Approach in the Management of Heart Failure **1984,** 54 (3), 286-288.

87. Wang, EQ; Lee, WI; Brazeau, D; Fung, HL, *cDNA microarray analysis of vascular gene expression after nitric oxide donor infusions in rats: implications for nitrate tolerance mechanisms*. AAPS Pharm. Sci. **2002,** 4 (2), E10.

88. Abraham, EH; Salikhova, AY; Hug, EB, *Critical ATP parameters associated with blood and mammalian cells: Relevant measurement techniques*. Drug Develop. Res. **2003**, 59 (1), 152-160.

89. Harvey, EN, *The Mechanism of Light Production in Animals*. Science. **1916**, 44 (1128), 208-209.

90. Dubois, R, *Note sur la physiologie des Pyrophores*. Comptes Rendus des Seances de la Societe de Biologie, Paris **1885**, 2, 559.

91. Harvey, EN, *Studies on bioluminescence: V. The chemistry of light production by the fire-fly*. Am. J. Physiol. **1917**, 42 (2), 342-348.

92. McElroy, WD, *The energy source for bioluminescence in an isolated system.* Proc. Natl. Acad. Sci. USA. **1947,** 33 (11), 342-345.

93. McElroy, WD; Strehler, BL, *Factors influencing the response of the bioluminescent reaction to adenosine triphosphate.* Arch. Biochem. **1949,** 22 (3), 420-33.

94. Shimomura, O, *Bioluminescence: Chemical principles and methods.* 1st ed.; World Scientific Publising: Singapore, **2006;** p 470.

95. McElroy, WD; DeLuca, M, Firefly luminescence. In *Chemi- and bioluminescence,* Burr, JG, Ed. CRC press: New York, 1985; Vol. 16, pp 387-399.

96. Gould, SJ; Subramani, S, *Firefly luciferase as a tool in molecular and cell biology.* Anal. Biochem. **1988,** 175 (1), 5-13.

97. Green, AA; McElroy, WD, *Crystalline firefly luciferase.* Biochim. Biophys. Acta. **1956,** 20, 170-176.

98. Conti, E; Franks, NP; Brick, P, *Crystal structure of firefly luciferase throws light on a superfamily of adenylate-forming enzymes.* Structure. **1996,** 4 (3), 287-298.

99. Seliger, HH; McElroy, WD, *Chemiluminescence of firefly luciferin without enzyme.* Science. **1962,** 138 (3541), 683-685.

100. McElroy, WD; Seliger, HH, Mechanisms of bioluminescent reactions. In *A Symposium on Light and Life,* Johns Hopkins Press: 1961.

101. Drew, B; Leeuwenburgh, C, *Method for measuring ATP production in isolated mitochondria: ATP production in brain and liver mitochondria of Fischer-344 rats with age and caloric restriction.* Am. J. Physiol. Regul. Integr. Comp. Physiol. **2003,** 285 (5), R1259-1267.

102. Darby, M; Kuzmiski, JB; Panenka, W; Feighan, D; MacVicar, BA, *ATP released from astrocytes during swelling activates chloride channels.* J. Neurophysiol. **2003,** 89 (4), 1870-1877.

103. Olearczyk, JJ; Ellsworth, ML; Stephenson, AH; Lonigro, AJ; Sprague, RS, *Nitric oxide inhibits ATP release from erythrocytes.* J. Pharmacol. Exp. Ther. **2004,** 309 (3), 1079-1084.

104. Coolen, EJCM; Arts, ICW; Swennen, ELR; Bast, A; Stuart, MAC; Dagnelie, PC, *Simultaneous determination of adenosine triphosphate and its metabolites in human whole blood by RP-HPLC and UV-detection.* J. Chromatogr. B. **2008,** 864 (1-2), 43-51.

105. Meyer, J; Froelich, J; Reid, G; Karunarathne, W; Spence, D, *Metal-activated C-peptide facilitates glucose clearance and the release of a nitric oxide stimulus via the GLUT1 transporter.* Diabetologia. **2008,** 51 (1), 175-182.

106. Holmsen, H; Holmsen, I; Bernhardsen, A, *Microdetermination of adenosine diphosphate and adenosine triphosphate in plasma with the firefly luciferase system.* Anal. Biochem. **1966,** 17 (3), 456-473.

107. Bencic, David C; Yates, Todd J; Ingermann, Rolf L, *Ecto-ATPase activity of vertebrate blood cells*. Physiol. Biochem. Zool. **1997,** 70 (6), 621-630.

108. Yegutkin, GG, *Nucleotide- and nucleoside-converting ectoenzymes: Important modulators of purinergic signalling cascade.* BBA - Mol. Cell Res. **2008,** 1783 (5), 673-694.

109. Xu, H-L; Pelligrino, DA, *ATP release and hydrolysis contribute to rat pial arteriolar dilatation elicited by neuronal activation.* Exp Physiol **2007,** 92 (4), 647-651.

110. Braun, N; Sévigny, J; Robson, SC; Enjyoji, K; Guckelberger, O; Hammer, K; Di Virgilio, F; Zimmermann, H, *Assignment of ecto-nucleoside triphosphate diphosphohydrolase-1/cd39 expression to microglia and vasculature of the brain.* Eur. J. Neurosci. **2000,** 12 (12), 4357-4366.

111. Dranoff, JA; Kruglov, EA; Robson, SC; Braun, N; Zimmermann, H; Sévigny, J, *The ecto-nucleoside triphosphate diphosphohydrolase NTPDase2/CD39L1 is expressed in a novel functional compartment within the liver.* Hepatology **2002,** 36 (5), 1135-1144.

112. Ignarro, LJ; Ross, G; Tillisch, J, *Pharmacology of endothelium-derived nitric oxide and nitrovasodilators*. West. J. Med. **1991,** 154 (1), 51-62.

113. Furchgott, RF, *Endothelium-derived relaxing factor: discovery, early studies, and identification as nitric oxide*. Bioscience Rep. **1999,** 19 (4), 235-251.

114. Ignarro, LJ, *Nitric oxide: a unique endogenous signaling molecule in vascular biology*. Bioscience Rep. **1999,** 19 (2), 51-71.

115. Boushel, R, *Metabolic control of muscle blood flow during exercise in humans*. Can. J. Appl. Physiol. **2003,** 28, 754-773.

116. Kamper, AM; Blauw, GJ, *Acethylcholine and serotonin induced vasodilation in the human forearm: interaction between nitric oxide and prostaglandin pathways*. Atherosclerosis Supplements. **2001,** 2 (2), 144.

117. Denninger, JW; Marletta, MA, *Guanylate cyclase and the NO/cGMP signaling pathway*. BBA - Bioenergetics. **1999,** 1411 (2-3), 334-350.

118. Arnold, WP; Chandra, KM; Shoji, K; Ferid, M, *Nitric oxide activates guanylate cyclase and increases guanosine 3':5'-cyclic monophosphate levels in various tissue preparations*. Proc. Natl. Acad. Sci. USA. **1977,** 74 (8), 3203-3207.

119. Smith, JJ; Kampine, JP, *Circulatory physiology: the essentials*. 3rd ed.; Williams & Wilkins: Baltimore, **1990**.

120. Singel, DJ; Stamler, JS, *Chemical physiology of blood flow regulation by red blood cells: The role of nitric oxide and S-nitrosohemoglobin*. Annu. Rev. Physiol. **2005,** 67, 99-145.

121. Jia, L; Bonaventura, C; Bonaventura, J; Stamler, JS, *S-nitrosohaemoglobin: a dynamic activity of blood involved in vascular control*. Nature. **1996,** 380 (6571), 221-226.

122. Cosby, K; Partovi, KS; Crawford, JH; Patel, RP; Reiter, CD; Martyr, S; Yang, BK; Waclawiw, MA; Zalos, G; Xu, X; Huang, KT; Shields, H; Kim-Shapiro, DB; Schechter, AN; Cannon, RO, 3rd; Gladwin, MT, *Nitrite reduction to nitric oxide by deoxyhemoglobin vasodilates the human circulation*. Nature Medicine **2003,** 9 (12), 1498-505.

123. Gladwin, MT; Crawford, JH; Patel, RP, *The biochemistry of nitric oxide, nitrite, and hemoglobin: role in blood flow regulation*. Free Radical Bio. Med. **2004,** 36 (6), 707-717.

124. Rassaf, T; Flogel, U; Drexhage, C; Hendgen-Cotta, U; Kelm, M; Schrader, J, *Nitrite reductase function of deoxymyoglobin: oxygen sensor and regulator of cardiac energetics and function*. Circ. Res. **2007,** 100 (12), 1749-1754.

125. Huang, KT; Keszler, A; Patel, N; Patel, RP; Gladwin, MT; Kim-Shapiro, DB; Hogg, N, *The reaction between nitrite and deoxyhemoglobin: reassessment of reaction kinetics and stoichiometry*. J. Biol. Chem. **2005,** 280 (35), 31126-31131.

126. Robinson, JM; Lancaster, JR, Jr., *Hemoglobin-mediated, hypoxia-induced vasodilation via nitric oxide: mechanism(s) and physiologic versus pathophysiologic relevance*. Am. J. Respir. Cell Mol. Biol. **2005,** 32 (4), 257-261.

127. Kim-Shapiro, DB; Gladwin, MT; Patel, RP; Hogg, N, *The reaction between nitrite and hemoglobin: the role of nitrite in hemoglobin-mediated hypoxic vasodilation*. Journal of Inorganic Biochemistry - Special Issue in Memory of Edward I. Stiefel **2005,** 99 (1), 237-246.

128. Palmer, RMJ; Ferrige, AG; Moncada, S, *Nitric oxide release accounts for the biological activity of endothelium-derived relaxing factor*. Nature. **1987**, 327 (6122), 524-526.

129. Arnal, JF; Münzel, T; Venema, RC; James, NL; Bai, CL; Mitch, WE; Harrison, DG, *Interactions between L-arginine and L-glutamine change endothelial NO production. An effect independent of NO synthase substrate availability*. J. Clin. Invest. **1995**, 95 (6), 2565-72.

130. Guo, JP; Murohara, T; Buerke, M; Scalia, R; Lefer, AM, *Direct measurement of nitric oxide release from vascular endothelial cells*. J. Appl. Physiol. **1996**, 81 (2), 774-779.

131. Thatcher, GJR; Weldon, H, *NO problem for nitroglycerin: organic nitrate chemistry and therapy*. Chemical Sociery Reviews **1998**, 27, 331-337.

132. Mayer, B, *Bioactivation of nitroglycerin - A new piece in the puzzle*. Angew. Chem. Int. Edit. **2003**, 42 (4), 388-391.

133. Dejam, A; Hunter, CJ; Schechter, AN; Gladwin, MT, *Emerging role of nitrite in human biology*. Blood Cell. Mol. Dis. **2004**, 32 (3), 423-429.

134. Dejam, A; Hunter, CJ; Tremonti, C; Pluta, RM; Hon, YY; Grimes, G; Partovi, K; Pelletier, MM; Oldfield, EH; Cannon, RO, III; Schechter, AN; Gladwin, MT, *Nitrite infusion in humans and nonhuman primates: endocrine effects, pharmacokinetics, and tolerance formation*. Circulation. **2007**, 116 (16), 1821-1831.

135. Bergfeld, GR; Forrester, T, *Release of ATP from human erythrocytes in response to a brief period of hypoxia and hypercapnia.* Cardiovasc. Res. **1992,** 26 (1), 40-47.

136. Hess, JR; Hill, HR; Oliver, CK; Lippert, LE; Rugg, N; Joines, AD; Gormas, JF; Pratt, PG; Silverstein, EB; Greenwalt, TJ, *Twelve-week RBC storage.* Transfusion. **2003,** 43 (7), 867-872.

137. Henretig, FM; Gribetz, B; Kearney, T; Lacouture, P; Lovejoy, FH, *Interpretation of color change in blood with varying degree of methemoglobinemia.* J. Toxicol. Clin. Toxicol. **1988,** 26 (5-6), 293-301.

138. Dejam, A; Hunter, CJ; Pelletier, MM; Hsu, LL; Machado, RF; Shiva, S; Power, GG; Kelm, M; Gladwin, MT; Schechter, AN, *Erythrocytes are the major intravascular storage sites of nitrite in human blood.* Blood **2005,** 106 (2), 734-739.

139. Kadowitz, PJ; Nandiwada, P; Gruetter, CA; Ignarro, LJ; Hyman, AL, *Pulmonary vasodilator responses to nitroprusside and nitroglycerin in the dog.* J. Clin. Invest. **1981,** 67 (3), 893-902.

140. Silva, G; Beierwaltes, WH; Garvin, JL, *Extracellular ATP stimulates NO production in rat thick ascending limb.* Hypertension. **2006,** 47 (3), 563-567.

141. Lauer, T; Michael, P; Tienush, R; Bodo, ES; Andreas, D; Martin, F; Malte, K, *Plasma nitrite rather than nitrate reflects regional endothelial nitric oxide*

synthase activity but lacks intrinsic vasodilator action. Proc. Natl. Acad. Sci. USA. **2001,** 98 (22), 12814-12819.

142. Olearczyk, JJ; Stephenson, AH; Lonigro, AJ; Sprague, RS, *Heterotrimeric G protein Gi is involved in a signal transduction pathway for ATP release from erythrocytes.* Am. J. Physiol. Heart. Circ. Physiol. **2004,** 286 (3), H940-945.

143. Bogle, RG; Coade, SB; Moncada, S; Pearson, JD; Mann, GE, *Bradykinin and ATP stimulate L-arginine uptake and nitric oxide release in vascular endothelial cells.* Biochem. Biophys. Res. Co. **1991,** 180 (2), 926-932.

144. Rubbo, H; Tarpey, M; Freeman, BA, *Nitric oxide and reactive oxygen species in vascular injury.* Biochem. Soc. Symp. **1995,** 61, 33-45.

145. Liu, X; Mark, JSM; Mahesh, SJ; Douglas, DT; Jack, RL, Jr., *Accelerated reaction of nitric oxide with O_2 within the hydrophobic interior of biological membranes.* Proc. Natl. Acad. Sci. USA. **1998,** 95 (5), 2175-2179.

146. Münzel, T; Daiber, A; Mulsch, A, *Explaining the phenomenon of nitrate tolerance.* Circ. Res. **2005,** 97 (7), 618-628.

147. Olearczyk, JJ; Stephenson, AH; Lonigro, AJ; Sprague, RS, *NO inhibits signal transduction pathway for ATP release from erythrocytes via its action on heterotrimeric G protein Gi.* Am. J. Physiol. Heart. Circ. Physiol. **2004,** 287 (2), H748-754.

148. Buehner, M; Ford, GC; Moras, D; Olsen, KW; Rossmann, MG, *D-Glyceraldehyde-3-phosphate dehydrogenase: three-dimensional structure and evolutionary significance*. Proc. Natl. Acad. Sci. USA. **1973,** 70 (11), 3052-3054.

149. Price, NC; Radda, GK, *A fluorescent probe for the coenzyme-induced structural changes in glyceraldehyde-3-phosphate dehydrogenase from rabbit muscle*. BBA - Protein Structure **1974,** 371 (1), 102-116.

150. *Worthington Enzyme Manual: Enzymes and related biochemicals.* Worthington Biochemical Corp.: Freehold, NJ, **1993**.

151. Gregus, Z; Nemeti, B, *The glycolytic enzyme glyceraldehyde-3-phosphate dehydrogenase works as an arsenate reductase in human red blood cells and rat liver cytosol*. Toxicol. Sci. **2005,** 85 (2), 859-869.

152. Lai, MW; Boyer, EW; Kleinman, ME; Rodig, NM; Ewald, MB, *Acute arsenic poisoning in two siblings*. Pediatrics **2005,** 116 (1), 249-257.

153. Fleming, I, *Epoxyeicosatrienoic acids, cell signaling and angiogenesis*. Prost. Oth. Lipid M. **2007,** 82 (1-4), 60-67.

154. Jiang, H; McGiff, JC; Quilley, J; Sacerdoti, D; Reddy, LM; Falck, JR; Zhang, F; Lerea, KM; Wong, PY-K, *Identification of 5,6-trans-epoxyeicosatrienoic acid in the phospholipids of red blood cells*. J. Biol. Chem. **2004,** 279 (35), 36412-36418.

155. Jiang, H; Quilley, J; Reddy, LM; Falck, JR; Wong, PY-K; McGiff, JC, *Red blood cells: reservoirs of cis- and trans-epoxyeicosatrienoic acids*. Prostag. Oth. Lipid. M. **2005,** 75 (1-4), 65-78.

156. Nakamura, T; Bratton, DL; Murphy, RC, *Analysis of epoxyeicosatrienoic and monohydroxyeicosatetraenoic acids esterified to phospholipids in human red blood cells by electrospray tandem mass spectrometry*. J. Mass Spectrom. **1997,** 32 (8), 888-896.

157. Webb, DJ; Vallance , P, *Vascular endothelium in human physiology and pathophysiology*. CRC Press, Inc.: Amsterdam, **2000.**

158. Lüscher, TF; Vanhoutte, PM, *The endothelium: Modulator of cardiovascular function*. CRC Press, Inc.: Boca Raton, **1990.**

159. Proctor, K; Falck, J; Capdevila, J, *Intestinal vasodilation by epoxyeicosatrienoic acids: arachidonic acid metabolites produced by a cytochrome P450 monooxygenase*. Circ. Res. **1987,** 60 (1), 50-59.

160. Liclican, EL; McGiff, JC; Pedraza, PL; Ferreri, NR; Falck, JR; Carroll, MA, *Exaggerated response to adenosine in kidneys from high salt-fed rats: role of epoxyeicosatrienoic acids*. Am. J. Physiol. Renal Physiol. **2005,** 289 (2), F386-392.

161. Li, P-L; Zhang, DX; Ge, Z-D; Campbell, WB, *Role of ADP-ribose in 11,12-EET-induced activation of KCa channels in coronary arterial smooth muscle cells*. Am. J. Physiol. Heart. Circ. Physiol. **2002,** 282 (4), H1229-1236.

162. Tune, JD; Richmond, KN; Gorman, MW; Feigl, EO, *Control of coronary blood flow during exercise.* Exp. Biol. Med. **2002,** 227 (4), 238-250.

163. Nithipatikom, K; Pratt, PF; Campbell, WB, *Determination of EETs using microbore liquid chromatography with fluorescence detection.* Am. J. Physiol. Heart. Circ. Physiol. **2000,** 279 (2), H857-862.

164. Laterreur, J. Role of nitrite and endothelium-derived vasodilators in blood flow. Concordia University, Montreal, 2007.

165. Guay, J; Bateman, K; Gordon, R; Mancini, J; Riendeau, D, *Carrageenan-induced paw edema in rat elicits a predominant prostaglandin E2 (PGE2) response in the central nervous system associated with the induction of microsomal PGE2 synthase-1.* J. Biol. Chem. **2004,** 279 (23), 24866-24872.

166. Gelpí, E; Ramis, I; Hotter, G; Bioque, G; Bulbena, O; Roselló, J, *Modern high-performance liquid chromatographic-radioimmunoassay strategies for the study of eicosanoids in biological samples.* J. Chrom. B. **1989,** 492, 223-250.

167. Daret, D; Blin, P; Dorian, B; Rigaud, M; Larrue, J, *Synthesis of monohydroxylated fatty acids from linoleic acid by rat aortic smooth muscle cells and tissues: influence on prostacyclin production.* J. Lipid Res. **1993,** 34 (9), 1473-1482.

168. Dickinson, JS; Murphy, RC, *Mass spectrometric analysis of leukotriene A4 and other chemically reactive metabolites of arachidonic acid.* J. Am. Soc. Mass Spectr. **2002,** 13 (10), 1227-1234.

169. Whittaker, N; Bunting, S; Salmon, J; Moncada, S; Vane, JR; Johnson, RA; Morton, DR; Kinner, JH; Gorman, RR; McGuire, JC; Sun, FF, *The chemical structure of prostaglandin X (prostacyclin)*. Prostaglandins. **1976,** 12 (6), 915-28.

170. Brash, A; Jackson, E; Saggese, C; Lawson, J; Oates, J; FitzGerald, G, *Metabolic disposition of prostacyclin in humans*. J. Pharmacol. Exp. Ther. **1983,** 226 (1), 78-87.

171. Basham, C; Hart, L *Design of a carbon based plasma purification system to augment haemodialysis*; Department of Chemical Engineering, Loughborough University: Loughborough, Leicestershire, UK.

172. Karara, A; Wei, S; Spady, D; Swift, L; Capdevila, JH; Falck, JR, *Arachidonic acid epoxygenase: Structural characterization and quantification of epoxyeicosatrienoates in plasma*. Biochem. Bioph. Res. Co. **1992,** 182 (3), 1320-1325.

173. Kotsis, DH; Spence, DM, *Detection of ATP-induced nitric oxide in a biomimetic circulatory vessel containing an immobilized endothelium*. Anal. Chem. **2003,** 75 (1), 145-151.